A STUDY OF THE SEISMIC WAVES SKS AND SKKS

Thesis by

Robert Leslie Nelson

In Partial Fulfillment of the Requirements
for the Degree of
Doctor of Philosophy

California Institute of Technology
Pasadena, California

1952

ACKNOWLEDGMENTS

The writer is indebted to Professor Beno Gutenberg for suggestion of the problem and for many helpful criticisms during the course of the investigation and preparation of the manuscript. The suggestions and comments of Professor Charles F. Richter and Dr. Hugo Benioff on many phases of the problem have been helpful and inspiring.

This study has been materially aided by the Stanolind Oil and Gas Company Fellowship held by the writer during the school years 1950-51 and 1951-52.

ABSTRACT

Arrival times, amplitudes, and periods of the seismic phases SKS and SKKS have been investigated for normal, intermediate, and deep earthquakes recorded at Pasadena and Huancayo, Peru. New observed time-distance curves are constructed for depths of <60, 100, 200, and 600 kilometers. Travel-times for the core have been calculated from normal shock time data. Slight modification of wave velocity just inside the core and of travel times within the core are suggested. Calculated travel times of SKS, SKKS, and SKKKS are in good agreement with observations.

Energy parameters determined from observed amplitude/period ratios are found in only fair agreement with those calculated from theory. Observed energies are too large for most of the phase components and depths considered. The horizontal components of SKKS over the whole distance range, and of SKS at $\Delta < 100^\circ$ for all depths, yield observed energies less than those predicted by theory. Both discrepancies are at least qualitatively explained by a proposed non-spherical distribution of shear strain about the fault source, and by abnormal absorption in the outer 700 kilometers of the core. A period increase with epicentral distance for

SKS and SKKS is best explained by selective absorption in this same zone.

Anomalous observed energies, as a function of epicentral location, can also be accounted for by the proposed non-spherical distribution of energy. A similar regional phase-period dependence is considered in terms of finite faulting velocities. Times, energies, and periods of multiple SKS phases for the depths studied are presented. No single hypothesis commensurate with all observed conditions is found, but the phases pSKS and sSKS for normal shocks are probably represented.

TABLE OF CONTENTS

Table of Contents (cont.)

ILLUSTRATIONS

Illustrations (cont.)

PLATES

TABLES

INTRODUCTION

Purpose and Scope of Investigation.

Since the latter part of the last century, seismologists have been engaged in investigations of the earth's internal constitution through the study of elastic waves instrumentally recorded from distant earthquakes. Studies of this type have contributed data from which logical deduction and inference are continually presenting a better hypothetical earth model. It is the purpose of this report to add to this body of data, and to perhaps add to or further clarify previous inference and extrapolation, particularly in regard to the core of the earth.

Elastic body waves utilized in this study are those which have traversed the mantle as distortional vibrations and have travelled a variable number of core paths as dilatational waves. These waves are commonly referred to as SKS, SKKS, and SKKKS - indicating none, one, and two internal reflections within the core, respectively. Such impulses have been observed at epicentral distances whose central angles are between 75° and 180°. Figure 1 contains a schematic ray path plot of these phases and their observed time-distance relations.

Materials for Study.

Records of 313 station-shocks have been examined. Of these, 57 are from the Geophysical Institute of Huancayo, Peru. A list of the earthquakes studied, as a function of epicentral distance and depth, is found in the Appendix. A total of 1227 readings have been made of the phases within the SKS family on these seismograms. A breakdown of the readings by station and focal depth follows:

	Normal	Intermediate	Deep
Pasadena	667	225	44
Huancayo	291	-	-

The observations may be divided into two groups on the basis of the recording instruments involved. One thousand and seven readings were made on the records of instruments whose absolute magnifications have been recently determined, while 220 are from seismograms written by older instruments whose relative magnifications only are known. Amplitudes and periods of waves in both groups were measured, but values from the latter can serve only in the comparison of phases on the same seismogram. Readings from the older records, however, in addition to approximately two hundred others from similar instruments for the later years not totalled above, are confidently utilized in travel time determinations.

Instrumental constants of the seismographs whose absolute magnifications are known are shown in the following table. T_o refers to the free period, in seconds, of the seismometer and T_g to that of the recording galvanometer.

Comp.	Type of Instrument	Design T_o	Design T_g	Normal Static Magnif.
Z	Benioff Electromagnetic	1	90	
N-S	" "	1	90	
E-W	" "	1	90	
N-S	Wood-Anderson Torsion	6		800
E-W	" " "	6		800
Z	Benioff Electromagnetic	1	0.23	
N-S	" "	1	0.23	
E-W	" "	1	0.23	

Few readings were made on the Benioff short-period (T_g) instruments because of the reduced magnification for periods like those in the SKS group. First arrivals and periods are difficult to determine definitely, except for the larger shocks.

<u>Methods of Study.</u>

To facilitate use of the data in other seismological studies, the time, amplitude and period measurements from the above readings, and parameters derived mathematically from them, are presented in the following sections in two parts. The first is a presentation and discussion of the data with a minimum of inference and interpretation. It is difficult to divorce time-distance, amplitude, and period relations one from another, but an effort has been made to do so for clarity of presentation.

The latter part of the text is devoted to implications of the results obtained concerning indicated modifications of the classical theory and earth model. This is followed by an overall summary of the data and its interpretation.

PRESENTATION AND DISCUSSION OF THE DATA

OBSERVED TRAVEL TIMES

General Statement.

Because of the considerable effect of the slope of the time-distance curve upon calculations of expected energy for a particular phase, a complete restudy and determination of the travel times of the SKS group has been carried out. A large number of data are particularly necessary in this study because of the longer periods and indefinite beginnings characteristic of distortional waves recorded from teleseisms. An additional masking factor for these emergent phases is microseismic background motion of similar frequency. Amplitudes of microseisms are frequently of the same magnitude as those of SKS phases from relatively small shocks at large distances.

The result of both effects is a tendency to read times which are somewhat later than the actual arrivals. This inherent difficulty can be partly minimized by a weighting of time readings in proportion to the earthquake magnitude. Larger earthquakes, though usually exhibiting bothersome complexities in the wave train, record with much sharper initial impulses.

New Observed Travel-Time Data for the SKS Group.

The following two tables contain the time-distance relations for the phases and depths studied, upon which calculations and analyses to follow are based. "Normal" depth is here considered to include shocks down to sixty kilometers below the surface. To simplify comparison with other published travel times, the observed values for normal shocks have been corrected to a hypothetical surface focus. Observed times for intermediate and deep shocks have been corrected to the nearest one hundred kilometer level shown. Observations embrace only the epicentral distances indicated. Bracketed figures reflect doubtful values.

TABLE I. NORMAL SHOCKS

Times for Surface Focus in min:sec.

Dist. (deg.)	SKS	SKKS	SKKKS	Dist. (deg.)	SKS	SKKS	SKKKS
76	(22:00)	-	-	130	26:27	28:15	28:43
78	(14)	-	-	132	31	27	57
				134	36	38	29:10
80	(27)	-	-	136	40	49	23
82	(41)	-	-	138	44	29:00	36
84	54	-	-				
86	23:06	23:25	-	140	47	11	49
88	19	39	-	142	50	22	30:05
				144	53	34	18
90	31	54	-	146	56	45	31
92	42	24:08	-	148	58	56	44
94	54	22	-				
96	24:04	37	-	150	27:00	30:07	57
98	14	51	(24:53)	152	02	18	31:09
				154	04	29	22

TABLE I. (cont.)

100	24:25	25:06	(25:08)
102	34	20	(23)
104	43	34	37
106	53	47	52
108	25:02	26:01	26:07
110	11	14	21
112	20	27	35
114	28	40	50
116	36	52	27:04
118	44	27:03	18
120	52	17	33
122	26:00	29	47
124	07	40	28:01
126	14	52	15
128	21	28:04	29

156	27:06	30:40	31:34
158	07	51	47
160	08	31:01	59
162	09	12	32:12
164	10	23	24
166	11	34	36
168	12	44	48
170	13	54	33:01
172	14	32:04	-
174	14	14	-
176	15	-	-
178	15	-	-
180	16	-	-

TABLE II. INTERMEDIATE AND DEEP SHOCKS

Travel times for depths in kilometers shown at head of appropriate column.

Dist. (deg.)	SKS			SKKS		
	100	200	600	100	200	600
80	22:22	21:52	20:46	-	-	-
85	49	22:22	21:16	-	-	-
90	23:15	51	43	23:27	23:00	21:52
95	41	23:19	22:08	58	34	22:24
100	24:06	45	32	24:28	24:06	54
105	30	24:09	55	58	37	23:23
110	52	32	23:17	25:28	25:07	53
115	25:14	52	37	58	36	24:22
120	33	25:12	54	26:28	26:05	52
125	50	31	24:09	57	33	25:20
130	26:04	48	-	27:25	27:00	(49)
135	17	-	-	53	-	-
140	27	-	-	28:19	-	-

Comparison of these times with previously determined curves is hampered by the fact that few tabulations by different workers are completely observational. This is particularly true of intermediate and deep shock tables. The table below contains residuals between published times of Gutenberg and Richter (1939, pp. 118 and 129) and those of the author for SKS and SKKS of normal shocks. Plus values indicate earlier times for the new data; negative ones later times.

	80°	90°	100°	110°	120°	130°	140°	150°	160°
SKS	0	0	+1	+1	+2	-7	-4	-3	-
SKKS	-	-	+6	+1	+1	+5	+12	+17	+21

It is seen that the new SKS data require a somewhat steeper travel time curve at the shorter epicentral distances, but that the agreement in general is good. Large residuals near 130° and 140° coincide with the point of intersection of the theoretically expected branches of this phase, and indicate that the new curve more clearly reflects the break in slope resulting from this intersection. This relation is illustrated in figure 2. The observed SKS times are plotted with those calculated in a later section.

Agreement between the SKKS curves is fair up to 130° and poor at larger distances. This may in part be due to a reduced number of observations for this phase, and is certainly a function of its characteristically less definite beginning. Better agreement is found between the new times and those calculated for this phase from core data. For convenience of comparison, the observational times of all phases will be included in the tables of calculated values in a later section.

Observations of SKS at epicentral distances less than that of its point of intersection with the S curve are few. Approximately 25 station-shocks were studied in the distance range $75^{\circ} - 83^{\circ}$, and in only eight cases were phases found which are definitely thought to be SKS. At the lower end of the range SKS is easily confused with a strong late branch of ScS, and with PS; while near 82° and 83° the two strong S phases make identification uncertain. Some of the clearly identified observations are illustrated in Plate I.

While the intersection of the two principal branches of SKS is reflected in a slope change of the observed travel-time curve, delineation of the later segments of these branches has not been made. Time intervals involved are small, and multiple phases of the earlier branch mask arrivals of the later segment.

Multiplicity of SKS Phases.

Because of the inevitable scatter of points on the time-distance plot - due principally to uncertainties in origin time and epicenter, and to slight variations in depth of the "normal" shocks - the multiple phases of SKS are not as clearly defined as the study of a single seismogram would suggest. To obviate this difficulty, a separate plot of SKS-P versus distance was constructed to 120°. The diffracted P curve was used beyond 105°. Such a plot confirms, with only slight modification, the identification of four phases in the SKS group made by Gutenberg and Richter (1934, p. 113). Phase multiplicity on seismograms from normal and intermediate shocks is illustrated in Plate I.

The second curve, or SKS_2, is observed with very nearly the same continuity as SKS_1 from 86° to 175°. Amplitude ratios differ considerably with distance but the time interval between these two phases varys only between nine and eleven seconds. The slight existing variation seems to stem from the unsmoothed nature of the curves rather than an epicentral distance dependence.

Although the data are fewer and conclusions less definite, the third and fourth curves (SKS_3 and SKS_4) appear to exhibit this same parallelism, but independently of the former two curves. Observations of SKS_3

extend from 88° to approximately 112°; while those of SKS_4 continue from just beyond its intersection with SKKS at 94° to approximately 123°. The time interval throughout their overlapping portions is between six and eight seconds. A measure of the independence of parallelism of the two pairs of multiple phases is given by variation of the time interval SKS_4-SKS_1 with distance. At 95° it is 27^s; at 100°, 26^s; 105°, 25^s; 110°, 23^s; 115°, 21^s; and at 120°, 19^s. These compare with values found by Gutenberg and Richter (ibid.) of 26^s at 95° and 22^s at 120°.

Multiplicity of SKS is also apparent in intermediate and deep earthquakes. It is perhaps noteworthy, however, that only the first and second phases have been observed, even in the intermediate shocks where data at Pasadena are plentiful. The curves for 100, 200, and 600 kilometers all show SKS_2 paralleling SKS_1 with time intervals near eight seconds. It is to be noted that these SKS_2-SKS_1 time intervals are in fair agreement with that of earthquakes at normal depth.

Component Relations.

It is characteristic of most of the shocks studied that arrival times differ on seismograms recording different components of the earth's motion. This is no doubt partly due to difficulties in determining the exact arrival time, forreasons discussed previously, but many instances of sharp impulses exhibiting this time variation have been noted. The arrival time differences between components are normally of the order of one to three seconds, but five seconds is not uncommon. An analysis of all the data for normal shocks has disclosed no system to this variation. It does not seem possible to predict early or late arrival of a component on the basis of either direction or distance to the epicenter, or the theoretical polarization (SV) of the incident SKS wave.

AMPLITUDES AND ENERGY

General Statement.

On the basis of time-distance considerations alone, an hypothetical earth model has evolved which fairly well allows prediction of the arrival time of most wave types to an accuracy within the limits of observational error and those imposed by variable and unknown near surface effects. Recent studies of the energy content of several phases (Martner, 1950; Mooney, 1951; Gutenberg, 1951; Denson, in press; Ergin, in press), however, indicate that many of our assumptions concerning this model, known to be oversimplifications when made, are in need of revision. For this reason, energy of waves in the SKS group are considered in the sections to follow.

The Observed Energy Parameter A_o .

A comparison of observed and theoretical energies requires the use of a parameter which can be determined both from seismograms and theoretical ground displacements. Gutenberg (1945a) has set up such a parameter, A, which may be defined for the observational case (A_o) as

$$A_o = M - \log \frac{u,w}{T} - G(M - 7); \qquad (1)$$

where M is the magnitude of the shock (Richter, 1935; Gutenberg, 1945a, b) u and w the horizontal and vertical ground displacements, respectively (u is the vector sum of horizontal displacements in two mutually perpendicular directions), and T the period of the disturbance. The last term is a consequence of limitations on simplifying assumptions made in the original derivation. It was assumed that the duration of a phase increases with distance proportionally to T. However, this relation is also found to be influenced by the magnitude of the particular shock under consideration and an empirical corrective term is required. As a first approximation, G is assumed to be 0.25 for shocks with magnitudes greater than 7.

Further adjustment of the A_o values calculated from seismograms is necessary because of ground and crustal variations from station to station. Empirical station correction factors have been determined by Gutenberg (1945b), and those for Pasadena and Huancayo have been used in this study.

The quantity M in equation (1) has been taken from Gutenberg and Richter (1949) where possible. For the later years, magnitudes have been taken from the station bulletins and files of the Seismological Laboratory in Pasadena.

Errors involved in the determination of A_o are those in the quantity M, identification of phases, measurements on the seismograms, and the determination of instrumental constants. The maximum displacement of a phase on the records is not always coincident with the first motion. In general, amplitudes have been measured within a few seconds of the phase arrival but the selection involved is a source of error. The period of the wave is also difficult to determine in some instances because of background noise, particularly microseisms, and natural complexities of the phase which are a reflection of its nonsinusoidal form.

Figures 3 through 10 are plots of A_w and A_u (vertical and horizontal components of A_o) as a function of epicentral distance. The data are rather scanty in figures 5, 9, and 10, but even a few points in a narrow distance range can serve as a rough check on the theory. Figure 5 was included because this phase (SKS_3) is occasionally the strongest phase in the SKS group at particular distances. The points in figures 9 and 10, though fragmental with respect to distance, do indicate a change in A_o with depth at particular distances.

It is noticed that the data for A_w are fewer than for A_u for each phase. This results from the fact that no suitable long period vertical instrument is available at Huancayo, and that records from torsion instruments were available at Pasadena before those from long period vertical instruments with known absolute magnification. Inasmuch as this study is concerned with distortional vibrations, which yield larger horizontal displacements, the incompleteness of the vertical data is not as serious as it otherwise might be.

Properties of A_o for the SKS Group.

Aside from its value in comparison with expected energies from theoretical considerations, some generalization of the properties of A_o itself, as a function of phase and distance, are informative. It is seen that, in accord with theory, vertical displacements are in general less strong than horizontal ones for SKS. (One must keep in mind that the magnitude of the A_o parameter has an inverse relation to the energy in the phase.) This seems notably not true for SKS_1 between 85° and 110°, and for SKS_2 from 115° to 130°.

Further data in regard to the problem of multiplicity are offered by the relative energies contained in the various phases of SKS as a function of distance. For horizontal components, the principal energy is carried by phases three and four from 85° to 112°. SKS_1 then becomes the stronger phase out to the limit of observation. For vertical components, SKS_2 and SKS_3 are the larger to approximately 125°, where SKS_1 becomes the largest.

The magnitude of an earthquake may be calculated from Pasadena seismograms using equation (1) and the A_o values determined above, if the distance is known. Inasmuch as it is common routine station practice to measure the largest amplitudes in a given train of body waves for this purpose, the data from figures 3 through 6 have been combined in such a way as to give the largest of the multiple SKS phases (SKS^*) for each seismogram. Figure 11 is a plot of these A_o values for both horizontal and vertical components. The mean values of $A_u{}^*$ and $A_w{}^*$ from this plot are given in Table III as a function of distance. These values have been corrected for the last term in equation (1) but do not include the Pasadena station correction. They are therefore applicable to magnitude determination from SKS phases at any station.

TABLE III

Distance	A_w*	A_u*	Distance	A_w*	A_u*
86	7.8	7.8	130	7.8	7.9
88	7.8	7.9	132	7.8	7.9
			134	7.8	7.9
90	7.9	7.9	136	7.8	7.9
92	7.9	7.8	138	7.7	7.9
94	7.9	7.8			
96	7.9	7.8	140	7.7	7.9
98	7.9	7.7	142	-	7.9
			144	-	7.8
100	7.9	7.7	146	-	7.8
102	7.9	7.7	148	-	7.8
104	7.9	7.6			
106	7.8	7.6	150	-	7.8
108	7.8	7.6	152	-	7.8
			154	-	7.8
110	7.8	7.6	156	-	7.9
112	7.8	7.7	158	-	7.9
114	7.8	7.7			
116	7.8	7.7	160	-	7.9
118	7.8	7.7	162	-	7.9
			164	-	8.0
120	7.8	7.8	166	-	8.0
122	7.8	7.8	168	-	8.0
124	7.8	7.8			
126	7.8	7.9	170	-	8.1
128	7.8	7.9			

The scatter of A_u and A_w values seems in excess of that expected from the errors involved. An analysis of this scatter was made by taking residuals, point by point, with respect to a mean curve. A_u for SKS_1 (figure 3) was selected for preliminary study because of the greater number of observations involved in its determination. Figure 12a is a plot of A_u from 80 normal shocks recorded at Pasadena from distances between 85° (where identification of phase first becomes reliable) and 150°.

Only readings from Pasadena were used to better isolate causative factors, thereby reducing the epicentral distance range somewhat.

The residuals of each observation were first examined with respect to the magnitude to determine if G in equation (1), which was determined by Gutenberg largely from a study of longitudinal waves, was equally applicable in considerations involving shear waves. This comparison showed no consistent deviation with magnitude and serves to confirm the factor given by Gutenberg for both shallow and deep shocks (Gutenberg 1945a, 1945b), and to extend its use to energy studies involving shear wave phases.

It was apparent, however, that the residuals are definitely a function of azimuth and also of the epicentral distance along one azimuth. This means, then, that the predominant effect upon the magnitude and sign of any particular residual is the geographic location of the earthquake involved. This hypothesis, resulting from the investigation of SKS_1 residuals, was tested first by a study of other phases in the SKS group, and then by considering all the intermediate shock data for similar geographic regions. The agreement in both instances is in general very good, with inconsistencies (usually residuals of opposite sign but small magnitudes) occurring mostly in the deeper intermediate data.

Tables IV and V contain the residuals for normal and intermediate shocks, respectively, as a function of geographic location of the epicenter. Intermediate shocks are grouped as being nearest 100 kilometers or 200 kilometers. Serial numbers in the table are those of the shock list in the Appendix. The residuals are taken as the mean A_u value minus the individually calculated values, thus a plus residual indicates a smaller A_u value (greater energy) than the mean.

TABLE IV

Residuals (A_u (mean) - A_u (obs.)) for SKS_1 as a function of epicentral location. Pasadena Normal Shocks.

No.	Residual	Location	No.	Residual	Location.
89	+.5	37½N-58E	61	+.1	4S-142E
			60	+.1	3½S-141¾E
65	+.2	40½N-36½E	66	+.4	1½S-138E
59	+.2	41N-34E	67	+.6	2½S-139E
58	+.5	41½N-32½E	93	+.5	2S-128½E
62	+.2	31½N-15¼E	90	0.0	6S-134½E
			81	+.5	4½S-135E
64	0.0	1S-14½W			
			97	-.2	½N-126E
118	+.4	49½S-32E			
			87	+.3	3½N-127½E
104	0.0	57S-26W	85	+.2	4½N-127½E
106	+.1	59½S-25W	76	+.2	7½N-128E
105	+.2	60S-27W	78	-.1	7¾N-127E
83	+.1	61S-38W	86	+.3	5¾N-126¼E
			72	+.2	12½N-125½E
52	+.1	54S-71W	91	0.0	8½N-122½E
53	+.2	54S-71W	88	+.3	10½N-122E
			82	-.2	13½N-121E
			70	+.5	18N-121E
38	-.3	57S-122W	71	+.2	18½N-119E

TABLE IV (cont.)

98	-.4	53S-159E			
			112	+.2	6½S-105½E
50	0.0	40½S-175½E	110	0.0	5½S-104¾E
45	-.4	39½S-177E	114	0.0	5S-102¾E
42	-.2	38½S-178½E	109	-.2	0-98¼E
			111	+.1	0-99½E
77	-.1	46½S-165½E			
			40	-.3	27½N-129½E
30	+.2	22S-167½E	51	-.3	25½N-125E
29	+.2	22S-169½E	23	-.5	32N-132E
			20	-.3	32½N-134½E
18	-.4	12½S-167E			
28	-.2	10½S-161¾E	84	+.1	29½N-100½E
26	0.0	10S-161½E	69	-.3	31¾N-103½E
27	-.5	10S-161E			
32	-.1	10½S-159E	95	-.6	23½N-96E
			100	-.2	23½N-94¼E
34	+.3	6½S-155½E	94	0.0	28½N-94E
36	+.3	6S-155E	99	0.0	26N-93E
39	+.1	5S-153E			
37	+.3	4½S-153½E			
			116	+.3	½N-76E
44	+.2	6S-151E			
41	+.5	4½S-152½E	56	-.5	44N-84E
47	0.0	6½S-151E	63	-.1	41N-83½E
49	-.3	6S-150E			
48	+.2	5¾S-152¼E			
54	+.2	6½S-148½E	101	-.2	29½N-66¾E
35	+.4	2½S-152¾E	107	+.3	26½N-63E
			108	-.5	24½N-63E

TABLE V

Residuals (A_u (mean) - A_u (obs.)) for SKS_1 as a function of epicentral location. Pasadena Intermediate Shocks.

100 Kilometers Depth

No.	Residual	Location	No.	Residual	Location
303	+.6	37S-74W	332	0.0	6½S-152E
311	+.1	40S-72½W	330	-.1	4½S-153½E
			331	+.3	5S-153½E
307	-.1	29S-177W			

TABLE V (cont.)

310	0.0	30S-178W	335	+.1	5S-145E
322	+.5	32S-180	336	-.2	6S-145E
306	+.3	28S-177½W	337	+.2	4¾S-144E
			338	+.1	4½S-143½E
301	-.3	24S-177W			
			349	+.4	9S-123E
326	+.6	24S-171E			
317	+.2	22½S-172E	327	+.6	13N-143½E
321	+.3	22S-171E	305	-.2	18N-147½E
325	0.0	22½S-171E	309	+.1	17½N-146½E
323	+.5	19½S-168E			
314	-.2	15¾S-167¾E			
313	0.0	14¾S-168E	343	-.3	0-124E
315	+.2	15½S-167E	345	-.3	0-124E
312	+.2	14S-167¾E			
324	-.2	10½S-161½E	342	+.1	5N-126E
			341	+1.0	6½N-125E
			334	+.5	24¾N-123E
329	+.2	6½S-155E			
328	-.3	4¾S-154E			

200 Kilometers Depth

365	-.1	32½S-178½W	373	+.1	½S-121½E
355	+.1	28½S-178½W	371	+.2	0-123E
354	+.5	28S-178½W			
			364	+.5	19N-145½E
361	-.2	19S-169E	353	+.1	19N-146E
362	-.2	19S-169E	358	+.2	22N-142½E
363	+.1	19S-169E			
366	-.3	20S-170E			
360	+.1	18½S-170E	368	+.1	36½N-70½E
359	-.1	16¼S-168½E	370	-.1	36½N-70½E
357	-.2	13½S-167E	369	+.1	36N-70½E

In determining an average regional residual, or corrective factor, complexities arise in the delineation of the boundaries of adjacent regions. This is particularly true for the island arcs of the southwest Pacific.

Maps and descriptive data from Gutenberg and Richter (1949) have been used extensively in this determination. The adopted average residuals for the indicated regions are summarized in Table VI. The residual from each area can be taken, with opposite sign, as a corrective factor for the A_u values given in Table III in determining earthquake magnitude from amplitudes and periods of SKS. In actual practice it would be more convenient to retain one set of A_o values and apply the correction factors by subtracting them from the second term in equation (1) as read from the seismograms.

TABLE VI

Regional correction factors to be subtracted from the logarithm of the amplitude/period ratio in equation (1) for magnitude determination using SKS at Pasadena.

Region	Correction	Region	Correction
NORMAL DEPTH			
North Iran and Turkey	+.4	Aroe Isl	+.25
		Celebes	-.2
No. Africa	+.2	Sumatra	0.0
Mid-Atlantic Ridge	0.0	Philippines	+.2
Atlantic, off Capetown	+.4	Formosa-Japan	-.35
S. Antilles and Tierra del Fuego	+.15	Szechwan (China)	-.1
		Burma	-.4

TABLE VI (cont.)

New Zealand	-.3	E. India	0.0
New Hebrides	+.2	Indian Ocean	+.3
Santa Cruz Isl.	-.25	Sinkiang (China)	-.3
Solomon Isl.	+.3	Pakistan	-.1
New Britain	+.25		
New Guinea	+.3		

DEPTH = 100 KILOMETERS

So. America	+.3	New Britain	0.0
Kermadec Isl.	+.2	New Guinea	+.1
Tonga Isl.	-.3	Sunda Arc	+.25
New Hebrides	+.2	Marianas Isl.	+.25
Santa Cruz Isl.	-.2	Celebes	-.3
Solomon Isl.	0.0	Philippines	+.5

DEPTH = 200 KILOMETERS

Kermadec Isl.	+.2	Celebes	+.15
New Hebrides	-.05	Marianas Isl.	+.3
Sunda Arc	-.1	Hindu Kush	0.0

To illustrate the effectiveness of the average residuals found, they have been applied to the observed A_u values in figure 12a. The new A_u values are plotted in figure 12b. It is noted that the scatter is reduced about sixty per-cent by this regional correction.

Inasmuch as the known magnitudes from which the A_o values in Table III were originally calculated are an average over many stations of the world, the above geographic correction factors should bring individual determinations of magnitude, using SKS at Pasadena, into much closer agreement with the eventual averaged value. Occasionally, readings from a few well recorded shocks which fall at an interesting and significant epicentral distance are given special weight in energy studies of a particular phase. If the apparent energy variation with epicentral location is real and of a magnitude which the residuals seem to indicate, errors of interpretation could obtain in such cases.

How much of the disagreement in residuals with depth of focus in a single region is real and an indication of very complex local structures in the areas involved is not known. Coincidence of all the anomalies with zones of sharply flexed structural trends in the major and minor arc units of the general circum-Pacific belt suggests that the anomalies are not wholly due to errors and statistical inconsistencies of the method. Because of the incomplete nature of the data available from this one phase for many of the geographic regions listed, one sees here only a beginning for this type of analysis. Limitations on shock distance and magnitude, imposed by characteristics of the SKS group, require the omission of many active seismic areas and incomplete coverage of others. It is hoped that such studies can be extended in the future to other phases and station.

The Theoretical Energy Parameter A_t.

The basic equation of total ground displacement for a given body wave is based on the theory by Zoeppritz (Zoeppritz, Geiger, and Gutenberg, 1912) and is expressed as

$$u, w = KTN\sqrt{E} , \tag{2}$$

where

$$N(U,W) = Q_{H,Z}\sqrt{(F_1 F_2 \ldots F_n)e^{-kD} \frac{\sin i_h}{\sin\Delta \cos i_o} \cdot \frac{di_h}{d\Delta}} \cdot \tag{3}$$

In equation (2): u and w are the horizontal and vertical components of ground displacement, respectively; K is the fraction of the energy E going into a particular phase; and T is the period of the wave type in question. N has horizontal and vertical components which are designated as U and W. The above quantities and those in the expression for N have been discussed by Gutenberg (1944, 1945a). It is sufficient here to enumerate the sources of quantities in (3).

Q_H, Q_Z - These quantities are the ratios of true ground displacement, horizontal and vertical components, respectively, to incident wave amplitude. Values are taken from Gutenberg (1944, p. 99).

F - This factor is the ratio of refracted or reflected energy to the energy incident at a discontinuity. For the SKS group we need only the values for refraction of energy into and out of the core and reflection within the core. Values, plotted as a function of angle of incidence, are taken from Dana (1944, p. 194, 196).

k - k is the absorption coefficient. It is assumed to be constant throughout the earth and has been found by Gutenberg to have the value 0.12 if the path length, D, is expressed in megameters (Gutenberg, 1945a, p. 58).

i_o - i_o is the surface angle of incidence of the ray. It is calculated from the apparent velocity determined from the phase travel time curve.

Δ - Δ is the central angle, expressed in degrees, of the complete ray path.

i_h - i_h is the angle of incidence of the outgoing ray at a source at depth h.

From a consideration of energy and magnitude, Gutenberg (1945a) has defined the constant C as

$$C = M - \log u,w + \log U,W - 0.1\ (M-7) + \log T \quad . \qquad (4)$$

C depends on the fractions of energy distributed among the fundamental types of vibrations. Theoretically it has three values; one for P, one for SV, and one for SH waves. Calculation by Gutenberg from measured trace amplitudes and periods has shown that to the limits of accuracy desired, C = 6.3 for all wave types.

Combining equations (1) and (4) yields

$$C = A + \log U,V \; , \tag{5}$$

from which

$$A = C - \log U,V \; . \tag{6}$$

Then from (3)

$$A = C - \log Q_{H,Z} \sqrt{(F_1 \; F_2 \ldots F_n) \; e^{-kD} \; \frac{\sin \; i_h}{\sin\Delta \cos \; i_o} \; \frac{di_h}{d\Delta}} \; . \tag{7}$$

It is this quantity which we designate as A_t in the discussion to follow. A more useful form of (7) is obtained by taking the individual logarithms of quantities in the last term, yielding finally

$$A_t = 6.3 - \log Q_H, Q_Z - 0.5 \log F + 0.217 \; kD$$
$$- 0.5 \log \frac{\sin \; i_h}{\sin\Delta \cos \; i_o} \; \frac{di_h}{d\Delta} \; . \tag{8}$$

Because only core waves are involved in this study, a further simplification of (8) is possible. Angles of incidence at the surface (i_o) for phases in the SKS group range from 0^o to less than 15^o. For this reason, angles of incidence at the source at depth h (i_h) cannot differ appreciably from i_o even for deep shocks. When it is considered that only the logarithms of these quantities are actually involved, we may safely substitute i_o for i_h and the last term in (8) reduces to

$$-0.5 \log \frac{\tan i_o}{\sin\Delta} \frac{di_o}{d\Delta} .$$

Horizontal and vertical components of A_t, calculated from (8), are presented in figures 13 through 17 for SKKS and for SKS from normal, intermediate, and deep shocks.

Comparison of Observed and Calculated Energies.

Residuals of the relation (A_o-A_t) for a particular phase and focal depth are a measure of the ratio of energy expected to that observed at a particular epicentral distance Δ. These residuals were calculated for the same wave types and depths given above. Horizontal and vertical components are plotted against Δ in figures 18 through 21. A plus residual indicates that the observed energy is less than that calculated from theory and a minus residual has the converse relation. Because of errors and uncertainties in calculating both A_t and A_o, residuals, either plus or minus, are considered to indicate agreement of theory with observation unless they exceed .25. This represents a factor of 1.8 (antilog of .25) between observed and theoretical energies.

A more ordered discussion will obtain by considering the phases one by one in the following sections. This is followed by sections devoted to overall implications of the data.

<u>SKS at normal depth.</u> As seen in figure 18, the vertical component of motion of this phase agrees fairly well with theory from 85° to about 130°. At that point the observations indicate energies in excess of those calculated by factors up to about 3. From 85° to 100° observed energies are slightly smaller than expected, while from 100° to 125° they are slightly larger than those calculated.

The horizontal component shows little agreement over the whole range of observation. Observed energies are too small by factors up to 10 from 85° to 110°. From 110° to 120° the agreement is fair but the observed energies become again too small from 120° to 138°. At this point the ratio assumed negative residuals and observed energies are too large by factors of 3 or 4 at about 150° to 160°, up to 10 at 170°. Figure 18 also shows residuals of theoretical horizontal values with respect to the largest of the multiple phases of SKS at each epicentral distance (SKS*). In general the agreement is better at the shorter distances where multiplicity is best developed, but energy ratios still indicate factors of 5 or more between observed and calculated values.

<u>SKS for intermediate and deep shocks.</u> In general, the agreement in the vertical components of the three depths studied (100, 200, and 600 kilometers) is good from 80° to 94°. (See figures 20 and 21). All three depths show energies slightly larger than the predictions of theory in this range. From 95° to the limit of observations at 120° the observed vertical component energies are larger than those expected by factors up to 5.

From 80° to 120°, observed energies in the horizontal component for shocks of 100 kilometers depth are in good agreement with theory. Data for shocks of 200 and 600 kilometer depth, though less complete, have similar horizontal residual relations at distances where comparison can be effected. From 80° to 95° the residuals are of like sign and degree, but near 120° the observed energies for 200 kilometer shocks are too small, rather than too large as in the other cases. It is to be emphasized that none of the horizontal component residuals in the intermediate and deep shocks are comparable in magnitude to those for normal depth. Energy ratios never exceed 2.5 and are usually closer to 1.5 or less.

<u>SKKS for normal depth.</u> Figure 19 illustrates that observed energies for the vertical component of this phase are larger than those expected from theory throughout the whole range of observation. The agreement is fair from 100° to 120°, where energy ratios are two or less, but is poor from 120° to 135°. The observed energies are too high by factors of from 2 to 4 in this latter range.

Horizontal components of SKKS, on the other hand, reflect small observed amplitude/period ratios for the whole distance range 90° to 170°. Peak positive values for the residuals, indicating smaller observed than theoretical energies, occur at 100°, 120°, and 170°. From 90° to 105°, and from 130° to 155° the agreement between observation and theory is fairly good.

<u>General Discussion of Results.</u>

Any complete theory of the physical properties of the earth medium must be capable of predicting energy variations as functions of epicentral distance in addition to time-distance relations. Previous wave energy studies have given results similar in complexity to those of the SKS group. The enormousness of the problem is evident. It is believed that less drastic adjustments of the classical hypotheses are necessary after a critical evaluation of the observed energy parameter derived in this study.

A striking feature of the $(A_o - A_t)$ residual plot for

SKS, figure 18, is that the largest positive residuals (deficient observed energy) coincide with the range of epicentral distance where multiplicity is best observed. In this range the later phases often show larger amplitude to period ratios than the principal phase. Using the largest of these phases at a particular distance (SKS*) reduced these positive residuals only slightly. The next step is to add the energies of multiple SKS phases on each seismogram and to compare this quantity with the theory. SKS for normal shocks was again investigated because it represents the greatest number of observations and seems in poorest agreement with theory.

Figure 22a is a plot of A_u, determined in this manner, as a function of epicentral distance. The energies were combined by adding directly the ground amplitude/period ratios for the four phases in the SKS group. In general, all four phases could not be identified on each seismogram, especially at shorter distances where other phases such as S, PS, and ScS follow SKS closely and obscure the "picks." Single phase readings occasionally had to be utilized and they serve to increase the scatter in figure 22a. It is not to be inferred that the other multiples are missing in other instances, but rather that definite beginnings were hard to determine because of disturbance of the trace by earlier arrivals.

Figure 22b is a new residual plot based on the mean combined energy parameter determined from figure 22a. Comparison with the similar plot where only SKS_1 was used in computing the residuals (figure 18) discloses two main features. The maximum energy ratio is reduced from a factor of 10 to a factor of 2 at short distances; and the observed energy is now generally greater than that expected from theory. The latter feature demands an entirely different causal hypothesis from that which might have been deduced for the residuals shown in figure 18. It is to be noted, however, that the relative variation from zone to zone on the distance axis is still in the same direction in all cases from either approach.

Figure 23 is a similar plot for the vertical component of SKS. It is noticed that the new curve (compare with figure 18) now shows predominantly greater energy than expected for almost all of the range of distance. It cannot be said that such a treatment of all the data would produce such striking results. The general effect is to lower the A_0 values and in some instances this would force the energy ratios further from agreement (i.e., the vertical component of SKS for shocks at depths near 100 kilometers). In the illustration given, however, the effect would not be large because only SKS_2 could be identified at depths greater than normal, and it is usually a weak phase. No certain multiple phases were identified in association with SKKS, so they must also contain very little energy. Inasmuch as SKS exhibits the greatest multiplicity, the new residuals (figures 22b and 23b) will be used in comparisons of phases and depths. The other residuals are used unchanged.

Having eliminated effects on the residuals of A_o calculated from (1), the remaining energy discrepancies can be explained only on the basis of variations in A_t from its calculated values. This, of course, necessitates a departure from the simplified theory which is the basis for equation (8). The quantities in this equation which appreciably affect A_t have been examined to see if their variation could resolve the remaining energy residuals.

Inasmuch as it represents the fitting of a line to more or less scattered points, the slope of the assumed travel-time curve comes first into consideration. Because it directly affects i_o, slight changes in the slope will vary every term on the right side of equation (8) except that for absorption. In a study of longitudinal core waves, $di_o/d\Delta$ is the term most affected. For SKS, however, external and internal angles of incidence at the core boundary are often near critical values, and the energy ratios F are subject to large variation. Frequently, variations in this term are of opposite sign and offset any improvement in A_t values due to variation of $di_o/d\Delta$. Several minor changes of slope at critical ranges of distance were tried, within limits set by observation, but only second decimal place improvements resulted.

Distortional and dilatational wave velocity assumptions at the surface and at the core boundary are involved in the determination of core angles of incidence and hence in the quantity F. It was found by trial and error that the following values give the best agreement between A_t and A_o:

Velocity of S waves near the surface - 3.75 km./sec.

Velocity of S waves just outside the core - 7.25 km./sec.

Velocity of P waves just inside the core - 7.9 km./sec.

Dana's F factors were computed on somewhat different velocity assumptions and slight modifications of his curves were necessary.

A study of the (A_o-A_t) residual curves shows that the vertical components of all phases usually have higher energy ratios than the corresponding horizontal components over much of the distance range. This might seem to cast doubt on the Q_H and Q_Z values used, inasmuch as these terms alone differentiate the horizontal and vertical components of A_t. The theory of these factors is oversimplified but unassailable. In addition, Q_H and Q_Z for SKS and SKKS are determined by surface angles of incidence always less than 15^o, well away from zones of rapid change in Q near critical values of i_o. The fact that vertical and horizontal components of the residuals are frequently of different magnitude and sign may also be attributable to inaccuracies in instrumental constants. The effects are difficult to evaluate for the older instruments but must be kept in mind as a source of error.

The remaining variable term in equation (8) is concerned with absorption over the ray path. The coefficient k was found by Gutenberg (1945a) to have closely similar values for mantle as well as combined mantle and core paths. Only longitudinal phases were considered in the evaluation of k, and therefore no core paths were included which closely follow the core boundary. This, then, leaves a zone where absorption might well be appreciably different from that used in calculations of A_t. Possible effects of this zone will presently be discussed.

Finally, the constant term C in equation (8) must be examined. C was originally evaluated by Gutenberg (1945a) for the phases P, PP, and S. From its derivation, it can depend only on the fractions of the given energy going into the fundamental types of waves. Several assumptions were made, but none with reference to wave path except for the requirement of spherical symmetry of energy propagation about the source. If this assumption is valid, C should have the same value for core phases as for those with paths wholly in the mantle. Discussion of this assumption in the light of energy residuals is reserved for a later section.

PHASE PERIODS

Because of their possible effect on the problems of phase multiplicity and wave energy content, a study has been made of phase periods in the SKS group. Median periods, averaged over all the Pasadena readings, are as follows:

	SKS_1		SKS_2	SKS_3	SKS_4	SKKS	
	Horiz.	Vert.	(Horizontal)			Horiz.	Vert.
Normal	5.3	5.3	4.7	5.1	5.2	5.4	5.7
Intermediate	5.1	4.8	-	-	-	4.5	5.0
Deep	4.1	3.6	-	-	-	-	-

From these data it may be concluded that: (1), the later SKS phases are generally of shorter period than the principal one, particularly SKS_2; (2), SKKS in both components is generally of longer period than SKS; and (3), the median period of a phase decreases as the depth of focus increases. This latter point is in accord with findings by Mooney (1951) for the phases P and pP.

If, however, we now add the periods of readings from seismograms of Huancayo, Peru, we find that the median period for horizontal components of SKS_1 and SKKS increase to 5.7 and 6.2, respectively. This is disturbing inasmuch as most of the data for SKS and SKKS beyond 140° in this study are derived from this source. It thus is difficult to evaluate whether the increase in period is due to the increasing epicentral distance, or to response characteristics of the instruments at Huancayo. It is also possible that near-station structural variations can account for the differences in wave frequencies recorded by the two laboratories. Figures 24 and 25 show periods of SKS and SKKS as a function of epicentral distance.

Records from Huancayo used in this study were written by long-period N-S and E-W Wenner seismographs. The response curves (Wenner, 1929) have been examined and are similar to those of the long-period Benioff instruments at Pasadena. If the Huancayo instruments were operated with the design characteristics, no distortion of the impulse to a longer period response should have occured. Both figures 24 and 25 illustrate a somewhat discontinuous jump in period beyond 130°, however, and the uncertainty is not completely resolved. Evidence for the reality of this period increase is contributed by findings of Denson (1950) that the phase P'' exhibits a similar period increase near 125°.

The above period considerations introduced an additional uncertainty in observed energy parameters calculated from Huancayo readings and absolute magnifications. Factors used in this study to convert Huancayo seismogram trace amplitudes, measured in millimeters, to ground motion amplitudes in microns are contained in the following table. It is seen that for both components, the magnification curves are relatively insensitive to inaccuracies in period determination over the range in which we are interested (5 to 8 seconds).

TABLE VII

Factors for converting Huancayo trace amplitudes in millimeters to ground displacements in microns. (T is the period of the wave.)

T	N-S	E-W
1	2.50	2.80
2	1.30	1.50
3	0.99	1.02
4	0.80	0.92
5	0.75	0.85
6	0.72	0.78
7	0.70	0.84
8	0.72	0.88
9	0.72	0.90
10	0.80	1.00

Figures 24 and 25 also illustrate an interesting difference in Pasadena horizontal and vertical period data. There is a tendency for periods of SKS and SKKS, recorded on horizontal instruments, to increase with epicentral distance. The median period increases one to two seconds in the distance range $90^{\circ} - 150^{\circ}$. Periods in the vertical component for both phases, however, exhibit a tendency to decrease with distance. Again the decrease is not marked but is apparently real.

The scattering of period values in figures 24 and 25 warrants analysis. Wave periods were first investigated for a magnitude dependence. Including the Huancayo data, the mean periods for various magnitude intervals are as follows:

$6\frac{3}{4}$-7	7-$7\frac{1}{4}$	$7\frac{1}{4}$-$7\frac{1}{2}$	$7\frac{1}{2}$-$7\frac{3}{4}$	$7\frac{3}{4}$-8
5.5	5.7	5.7	5.7	5.5

The periods are thus clearly not a function of earthquake magnitude.

As with the observed energy parameters, phase periods are found to depend upon the geographic location of the epicenter. Regions considered were those of Table VI and, in general, those areas in the table with a plus corrective factor (abnormally high energy) have periods shorter than the mean values. Inasmuch as equation (1) contains the ratio $\frac{u}{T}$, this period relation may well be a partial cause for the anomolous energy parameters calculated for the particular regions. It is probable that the period of motion of phases on a seismogram is a function of the mechanics of rupture of particular faults or fault systems.

MULTIPLICITY

Arrival time relations of the four observed SKS phases were outlined in an early section. Later sections devoted to energy and period considerations have added to this data and it is intended here to collect and summarize the observed facts. The earlier, principal phase (SKS_1) has been adequately treated elsewhere.

The second phase (SKS_2) is observed following SKS_1 at a uniform time interval of about 10 seconds throughout the whole range of distance. From 85° to 110°, SKS_2 is often found to have larger amplitude/period ratios, in both horizontal and vertical components, than the principal phase. This relation is due both to larger absolute amplitudes and to shorter average periods.

Unlike the second phase, the third and forth multiples do not seem to follow SKS_1 at a fixed time interval. On the time-distance plot these two phases are parallel, with a 6 to 8 second time interval, but approach the earlier two phases at increasing distances. They have slightly shorter periods than the principal phase and are occasionally stronger than SKS_1, especially on the horizontal components at short epicentral distances. Observations of SKS_3 appear to end at approximately 112°, either because the phase is too small at greater distances or because the mechanism producing it is no longer effective. SKS_4 continues somewhat further - to about 123°.

Multiple phases following SKKS were never confidently identified. This is the more striking when it is considered that SKKS is sometimes the largest phase in the SKS group on a particular seismogram. Gutenberg and Richter (1934, p. 119) give times for only the principal phase but mention weak indications of a second phase 15 to 20 seconds later at a few distances. Beyond 120°, such readings have in this study been attributed to SKKKS.

The identification of SKS phases on seismograms of intermediate and deep shocks is usually less of a problem than with shallow earthquakes. A less complex source mechanism seems indicated by a reduction of the apparently random background "noise" associated with each phase arrival. This should result in clear later phases for SKS so it is perhaps of interest that only observations of SKS_2 are sufficiently numerous to warrant inclusion as a separate travel time curve, for both intermediate and deep shocks.

POLARIZATION

All transverse waves having a partial core path must, according to theory, vibrate in a vertical plane containing the ray. Transformation from dilatational to distortional vibration upon exit from the core cannot give rise to an SH component in the transverse wave. Therefore, the polarization of phases within the SKS group should be simply defined by the directions of motion of the arriving wave.

Thirty-five large shocks evenly distributed over the distance range 85° to 155° were selected for special studies relating to polarization, and the direction of first motion of SKS_1 was determined independently of knowledge of the epicentral location. It is generally recognized from experience in reading seismograms that a particular relation which is "sought" can very often be "found." This is especially true in the case of obscure beginnings of long period waves.

When compared with the actual direction of approach of the ray, the observations are divisible into three groups. The first consists of those instances where the vertical and both horizontals give the correct relation for SV vibration from the quadrant of incidence involved. Twenty-three of the 35 shocks studied gave this expected relation. The second group contains those cases where the horizontal components give the correct relation but which have the vertical component reversed from that of an incident SV vibration. As an illustration, a pure SV vibration approaching from the third quadrant (180° to 270°) should give a ground motion up and to the southwest or down and to the northeast, depending on the phase. Three of the cases studied had this vertical motion reversed, indicating vibration along the ray instead of perpendicular to it.

The third group consists of nine cases where neither of the two types of vibration discussed above seemsto apply. One horizontal component is opposite to that which would obtain for either pure P or SV motion. Four of the nine instances are from shocks very near quadrant boundaries (within 15°), where a small SH component could account for the inconsistencies.

To determine whether the incident wave contained appreciable SH vibration, a study was made of the amplitudes in the two horizontal components for shocks nearly due west of Pasadena. The active south Pacific area is admirably suited to this purpose and 17 shallow earthquakes at azimuths between 263° and 278° were studied. All were recorded on horizontal long-period Benioff instruments, the two components of which have similar characteristics, so that direct comparison is possible.

At 260° and 280° the N-S amplitudes should be approximately one-fifth those on the E-W component if the motion is pure SV. At azimuths only 5° from due west this fraction is reduced to one-tenth. Of the 17 shocks studied, only five had amplitudes in the two components which could be compared within these limits. The remaining twelve had N-S components up to one-third or one-half of the E-W amplitudes and therefore indicate appreciable SH motion in the transverse vibrations.

A much better evaluation of SKS polarization could be effected by a study involving the time. A vectorial plot of the total ground displacement at uniform time intervals over the complete pulse would be far more accurate and informative. Such a study is outside the scope of this paper.

CALCULATED TRAVEL TIMES

Core Travel Times.

Travel times between points on the surface of the core have been calculated by the well-known method of Wadati and Masuda (1934). SKS-ScS and (SKKS-ScS)/2 clearly yield the core Δ and t desired if the ScS segments used have the same surface angles of incidence as the corresponding SKS and SKKS. In these calculations the observed travel times for SKS and SKKS in Table I were combined with data for ScS given by Gutenberg and Richter (1939, p. 106).

Because only the first arriving segments of the two main branches of SKS have been observed, only the corresponding parts of the time-distance curve within the core may be calculated. Data from SKS yield time-distance relations from about 23° to 180° in the core, but at distances larger than 120° a different branch is involved. SKKS, because of its larger internal angles of incidence in the core, furnishes travel times for core distances of 13° to 74°. Results from the two sets of data agree very well, being usually within three seconds at any particular distance.

Values for the overlapping range in Table VIII below are a combination of the SKS and SKKS curves. Columns two and three contain the most recent data from other sources. It is difficult to combine such times in one table because of differences in the location of the cusps of the later segments by different workers. Data from Gutenberg (1951) are shown in column two, with cusps at 130° and 100°. The third column contains necessarily incomplete data from Jeffreys (1939). His cusps are at 120° and 88°, and therefore the beginning of his second segment cannot be shown in this table.

TABLE VIII

Calculated travel times between points on the surface of the core. (Nelson - N; Gutenberg - G; Jeffreys - J)

Δ_K	$t_K(N)$	$t_K(G)$	$t_K(J)$	Δ_K	$t_K(N)$	$t_K(G)$	$t_K(J)$
5	0:40	0:37	0:37	125	-	10:55	-
10	1:19	1:15	1;15	130	-	11:06	-
15	57	52	52	125	-	10:55	-
20	2:34	2:29	2:28	120	-	44	-
25	3:10	3:06	3:04	115	-	33	-

TABLE VIII (cont.)

30	3:44	3:42	3:39	110	-	10:22	-
35	4:18	4:17	4:13	105	-	13	-
40	48	51	46	100	-	03	-
45	5:19	5:23	5:18	105	-	10:13	10:10
50	48	53	48	110	-	22	19
55	6:16	6:21	6:17	115	-	30	28
60	42	47	45	120	10:40	39	38
65	7:07	7:11	7:11	125	50	47	46
70	32	34	36	130	59	55	55
75	55	56	8:00	135	11:07	11:03	11:03
80	8:18	8:19	22	140	14	10	10
85	39	40	43	145	20	16	16
90	9:01	9:01	9:03	150	25	22	22
95	21	21	22	155	29	27	27
100	40	40	40	160	32	32	31
105	59	59	56	165	34	35	34
110	10:15	10:14	10:11	170	36	37	36
115	28	28	24	175	38	39	38
120	42	42	37	180	39	40	38

It is seen that the Nelson and Gutenberg curves are most divergent at 50° to 55° where the SKS and SKKS data require times five seconds later than those given by Gutenberg. The two curves are practically identical from 75° to 120°. The times again diverge near 140° where those here proposed are again later. This is a result of SKS times just past the branch intersection at 130°. Although SKS times were seen to reflect this change of slope (figure 2), they cannot be completely accurate and the times of Gutenberg in this range of distance are to be preferred.

The times calculated in this study agree with those of Jeffreys erratically but in general quite well. A maximum of five seconds difference is reached at 75° with Jeffreys' times being later. His values are up to four seconds earlier from 120° to 180°.

Calculated Times of the SKS Group.

Using combined time-distance values for the core from Table VIII and the ScS data noted above, travel times of SKS, SKKS, and SKKKS for surface foci have been calculated. The times here proposed for the core have been used up to 120°. For the branches, the times of Gutenberg were used because his data seem in better agreement with K times here determined near this distance range. From 120° outward on the third branch, the Gutenberg and Jeffreys times, which agree within one second, were favored.

The resulting travel times are shown in the second columns of Tables IX and X. The first column contains observed times from Table I for ease of comparison. The third and fourth columns show residuals from published data by Gutenberg and Richter (1939) and Jeffreys (1939), respectively. The same designation by initials is used. The residuals are taken in respect to the times in column two, therefore plus residuals indicate earlier times than those here calculated and minus residuals later times. No calculated times for SKKKS have been given by Gutenberg and Richter.

TABLE IX

Calculated travel times for SKS for surface focus in min:sec. (For last two columns see text.)

Δ	t observ. (N)	t calc. (N)	Residuals (G)	Residuals (J)
80	22:27	22:28	-1	-2
85	23:00	23:01	0	0
90	31	31	-1	-2
95	59	59	-1	-2
100	24:24	24:24	-2	-3
105	48	48	-3	-3
110	25:11	25:10	-4	-2
115	31	31	-4	-1
120	52	52	-2	+2
125	26:11	26:10	-1	+4
130	26	25	-2	+5
135		39	-3	
140		50	-6	
130		26:28	(-6)	
125		17	-	
120		07	(-5)	
115		25:58	-	
110		48	(-3)	
115		58	-3	+4
120		26:07	-3	+3
125		16	-4	+3
130	26:26	25	-4	+3
135	32	34	-4	+3
140	47	42	-5	+3
145	54	50	-5	+3
150	27:00	56	-7	+2
155	05	27:02	-	+2
160	08	06	-9	+1
165	11	09	-	0
170	13	12	-	0
175	14	14	-	+1
180	15	15	-5	+1

TABLE X

Calculated travel times for SKKS and SKKKS for surface focus in min:sec.

Δ	SKKS t obs. (N)	SKKS t calc. (N)	SKKS Resid. (G)	SKKS Resid. (J)	SKKKS t obs. (N)	SKKKS t calc. (N)	SKKKS Resid. (J)
80	-	22:33	-	-	-	22:34	-
85	-	23:12	-	+7	-	23:14	-
90	23:54	49	-	+7	-	52	+ 9
95	24:29	24:25	-4	+7	-	24:30	+10
100	25:06	25:02	-1	+8	25:08	25:08	+11
105	41	37	+1	+7	45	46	+13
110	26:14	26:10	+2	+5	26:21	26:22	+12
115	46	44	+4	+4	57	58	+12
120	27:17	27:16	+4	+2	27:33	27:34	+12
125	46	48	+5	+1	28:08	28:10	+12
130	28:15	28:19	+5	-1	43	46	+12
135	44	49	+4	-2	29:18	29:21	+12
140	29:11	29:18	+3	-3	52	55	+11
145	40	46	+2	-4	30:25	30:28	+ 9
150	30:07	30:14	+2	-4	57	31:01	+ 8
155	34	40	+1	-6	31:28	33	+ 6
160	31:01	31:06	+1	-6	59	32:05	+ 5
165	29	31	0	-7	32:30	36	+ 3
170	55	56	-1	-7	33:01	33:07	+ 1
175	32:19	32:19	-	-8	-	37	- 1
180	43	42	-4	-8	-	34:06	- 3

Observed and calculated times for SKS agree very well except just following the branch intersection near 130°. This difference has a maximum of five seconds at 140°. Calculated SKS travel times of Jeffreys seem in better agreement than those of Gutenberg with those here calculated, especially at the larger distances.

Greater divergences occur in SKKS and SKKKS times because of amplification of core time-differences. The observed and calculated times of this report are at most seven seconds apart at 140° for SKKS, and six seconds at 170° for SKKKS. The calculated curve for SKKS is clearly in closer agreement with the times calculated by Gutenberg than those by Jeffreys, the maximum divergence being five seconds. The agreement of observed and calculated times is not all that one might wish, but is better than most published comparisons. Calculated values for the SKKKS phase are up to thirteen seconds larger than those of Jeffreys.

INTERPRETATION OF THE DATA

Statement of the Problem.

It is the purpose of the following paragraphs to study those facets of the observations which are not in accord with present theory and assumption and to suggest, where possible, modifications of the theory which seem necessary to a more complete agreement. In many instances it is not possible to suggest hypotheses which will account for all observational variations. However, the data are often of use in eliminating certain possibilities and evaluating others which have been advanced in the past.

Anomalies in time, amplitude, and period relations requiring study and explanation may be summarized from the sections above as follows:

(1) Variation of phase energy with epicentral location.

(2) Variation of phase period with epicentral location.

(3) Variation of period with epicentral distance and phase.

(4) Anomalous energy relations.

(5) Multiplicity of phases.

Because it is believed that some of these problems are interrelated, individual discussion would entail considerable repetition of causative factors. For this reason, the effects of variations from some of the basic assumptions of seismology are first considered. The resulting concepts are then applied in considerations of several of the numbered problems.

Spherical symmetry of energy propagation. In the derivation of equation (8), many broad simplifying assumptions are made. The earth is considered to be an homogeneous, isotropic, perfectly elastic medium. Gradual or sudden change of velocity with depth is introduced and refraction phenomena obtained using Snell's Law. Plane waves are assumed in problems concerning layer boundaries. These simplifications of earth structure have withstood the test of many years of seismological research, except perhaps for the layers very near the surface. The further common assumption, however, that energy is radiated equally in all directions from the hypocenter seems no longer tenable.

As pointed out by Byerly (1938, p. 11; 1942, p. 239) in his studies relating fault plane attitudes and the direction of first motion of seismic waves, the energy arriving at any one station in a particular longitudinal or transverse wave should also be a function of orientation of the fault plane with respect to the station. This idea was apparently first noted by Nakano (1923) but has received little attention in the literature.

Extension and application of this amplitude and energy concept is presented here.

Shear stress near a linear earthquake source is believed to be distributed about the point of origin prior to fracture somewhat as shown in figure 26a. The actual stress distribution is not known, but the use of tangent circles fulfills the requirement that the shear be a maximum perpendicular to the fault strike and zero along it. The dashed lines indicate vibration 180° out of phase with that of the solid lines. Figure 26b is the type of rosette which gives the corresponding compressional stress distribution about the source. Four minima and maxima are required in this case.

In evaluating the effects of these proposed distributions, it is necessary to consider the actual types of faulting involved. To facilitate discussion, coordinate axes are taken as follows: the y- and z-axes are in the fault plane with y in the direction of strike; z is positive upwards; and x is perpendicular to both the strike and dip directions.

Thus figure 26a can be considerd a two-dimensional figure for strike-slip movement on a vertical fault plane. In three dimensions the curve is rotated about the y-axis and the figure becomes a toroid of revolution. The axis of revolution is also the axis of zero shear and always lies in the direction of fault displacement. All radii in the x-z plane are directions of maximum shear for this case. Inasmuch as all phases in the SKS group have surface angles of incidence less than 15°, all the rays lie near the z axis and hence should contain energies near the maximum. We may represent this relation by a cone of incidence with a central angle of 30°, axis vertical, and apex at the point source.

Strike-slip motion along nearly vertical faults is locally of considerable importance, for example in California, but does not appear to be a large factor in the major fault systems of the world as a whole. A second case, dip-slip motion along a vertical fault, has the same qualifications. Block faulting is most commonly associated with fault planes at angles less than 90° with the horizontal. However, the energy distribution figure for this special case is of value in visualizing transitions to the more common fault orientations and motions.

In this second case, the z-axis is the direction of zero shear and all directions from the origin (0) in the x-y plane are those of maximum shear. Our still vertical cone of incidence cuts little of the solid of revolution and transverse waves with partial core paths should contain very little energy from such displacements.

A third case for vertical fault planes is introduced by oblique-slip displacement. Such a consideration requires rotation of the energy distribution figure about the x-axis and all variations between the above limiting cases are possible. Again, nearly vertical faults are probably not typical and these examples have been treated primarily as transitions to faults with dip angles less than 90°.

The permutations of many directions of motion on fault planes with different angles of inclination are too numerous for discussion. Instead, a simplification is made by assuming two predominant dip angles and one predominant direction of displacement. The basis for the choice involved is found in recent studies by Benioff involving many of the major fault systems of the world (Benioff, 1949; and personal communications). He has found from a detailed study of the seismicity of several of the circum-Pacific arc structures that the hypocenters of shallow, intermediate, and deep shocks, where associated, fall on two surfaces which dip at angles near 30° and 60°, respectively. Transition between the two planes apparently takes place between 175 and 400 kilometers indepth in areas having continental type rocks on one side of the fault. Where this condition is not met, only the steeper angle is determined. The hypothesis deduced by Benioff to explain the origin of these great fault zones requires predominantly dip-slip displacement.

At both these angles, the axis of revolution of the toroidal figure (z for dip-slip movement) is inclined at the dip angle. For the 30° plane, the x-axis of maximum shear is inclined 60° from the horizontal and the cone of incidence cuts out a surface on the solid giving more energy in certain azimuths about the origin than in others, but a fairly high level for all. Figure 27a is a two-dimensional illustration of this case for a vertical section through the origin and perpendicular to the strike. Figure 27b is a similar example for the steeply dipping fault plane. In this case the variation of energy with azimuth is more pronounced and all values are smaller than for the more gently dipping fault. Small strike-slip components of displacement will not greatly alter the orientation of the figures. The chief characteristics of the energy distribution figure for dipping faults, then, are that: (1) considerable variation in energy with azimuth from the point of origin, at equal angles of incidence, is possible; (2) there is a variation of energy with varying angle of incidence of the rays; and (3) both the above variations are increased, although absolute values are decreased, by increasing angles of dip of the fault plane.

A similar development is possible for the distribution of dilatational energy. The three-dimensional figure in this instance consists of two mutually perpendicular, intersecting toroids each similar to that for shear. The general properties of this figure can be summed up as being similar to those already developed, except that much more uniform relations obtain. The zones of zero energy are greatly reduced and the cone of incidence cuts out surfaces yielding much less extreme variations at all angles of incidence and fault plane attitudes. In other words, the energy distribution solid is a much better approximation to a sphere.

Progressive faulting. In the preceding analysis the unrealistic concept of a point source was retained. The writer is indebted to Dr. Benioff of the Seismological Laboratory at Pasadena for the suggestion to consider the effect of a finite faulting velocity on the derived figures. During an earthquake, the strain adjustment by faulting can be propagated up to several hundred kilometers at speeds somewhat less than those of seismic waves (Benioff, 1949, p. 1856). One of the pulse-front diagrams derived by Benioff (discussed at the 1951 meeting of the Seismological Society of America) for various faulting velocities is shown in figure 28 of this paper. An illustration of the condition that the faulting velocity is less than that of shear waves in the medium has been adapted to the example of a gently dipping fault having predominantly dip-slip displacement. The direction of fracture movement is up-dip as shown by the arrow at F.

Inasmuch as time relations are here of interest, we consider circular wave fronts. Variation of energy along the wave fronts is not shown. The numbered dots represent equal units of time and we may, for simplicity in this two-dimensional case, consider a moving point source. The Huygens wavelets associated with each point are then seen to exhibit the Doppler effect; that is, there is a crowding of wavefronts in the direction of motion and attenuation behind. Thus the frequency of vibration, and hence the energy spectrum, is different in different azimuths from the fault plane.

If we now superpose the cone of incidence on this figure at some instant (here instant #4), it is seen that different rays within the cone will exhibit different periods of wave vibration. Ray a will have a lower frequency than ray b. If we were to further superpose figure 27a on this diagram at instant #4, it is obvious that the rays having the shorter periods also have the larger energies.

Actually, the cone of incidence should be moved with the source, but frequency variations remain the same for this more complex condition. Faulting motion with the same speed but opposite sense yields a converse relation. Minimum periods are then associated with minimum amplitudes or energy. From a study of the maximum energy generated by earthquakes at varying depths, Gutenberg and Richter (1949, p. 101) deduce that the breaking strength of rocks decreases with depth. Thus the direction of progressive rupture first illustrated above may possibly be the usual case at any particular depth where stresses have accumulated.

Variation of Wave Energy with Epicentral Location.

By application of the concept of non-spherical distribution of energy about the source, the residuals of observed energy over the mean are explained by variations in strike of the major faults involved with respect to azimuths from Pasadena. Figure 27 indicates that the mechanism is competent to account for the magnitude of the residuals involved in those areas where sufficient observations exist to yield a good average value.

Variation in energy with azimuth might also be attributed to anisotropy of the earth medium. However, it is difficult to imagine directional properties so sharply defined as to yield residuals of opposite sign at Pasadena from areas less than one thousand kilometers apart (e.g., the New Hebrides and Santa Cruz Islands). The perhaps erratic effect of crustal layers on energy propagation near the source as an explanation of the residuals is refuted by the agreement between normal and intermediate shock data. Inequalities in shape of the core which could alter incident to refracted energy ratios have also been considered. Calculations using equation (8) show that a five degree change in slope is required to produce a .1 unit change in A, even with the coincidental doubled effect of an equally unfavorable slope relation at the point of emergence of the ray. Surface inequalities of the core large enough to account for the residuals seem excessive.

<u>Variation of Wave Period with Distance and Phase.</u>

Figures 24 and 25 illustrate, at least for the horizontal components, a slight increase in period for SKS and SKKS with the distance of wave travel. The relation holds even without inclusion of the Huancayo data. No explanation for the opposite effect in the vertical components is forthcoming. It is possible that the number of data for this component is too small for a truly representative distance function.

This property of seismic waves has been reported by many workers (Macelwane, 1923; Byerly, 1926; Gutenberg and Richter, 1936; Munk, 1947; Wilson, 1948) but discussion has largely been confined to surface waves. Richter (1943) mentions similar relations for body waves. The period increase has been attributed to two major factors by different students of the problem. The effect of "internal friction" on wave periods is uncertain and has not been worked out for body waves. Selective absorption due to viscosity of the medium has been treated by Jeffreys (1926, 1931), and by Sezawa and Kanai (1938). Richter (ibid., p. 487) states that some type of viscosity is indicated and that normal dispersion does not offer a solution. Munk (1947, 1949), and Wilson (1948) offer theory and illustrations to show that dispersion may well "stretch" wave groups in which the crests are conserved, although Wilson does not rule out selective absorption.

The data from this study are believed to favor the selective absorption hypothesis, especially if the outermost regions of the core are effective in producing such absorption. The wave lengths of both SKS and SKKS are considerably less than those of either Love or Rayleigh waves - the wave types for which period increase by dispersion is advocated - and only layers less than about twenty kilometers in thickness could be effective in their dispersion.

Also, under the dispersion hypothesis, one would expect little difference in the period increase of SKS and SKKS inasmuch as their near surface paths are very similar. Actually, the increase for SKKS is on the order of twice that for SKS (see figures 24 and 25) and an explanation must be sought which takes into account the parts of their paths which are dissimilar, e.g., the proportion of path in the outermost parts of the core to the total path length. Further evidence regarding special absorptive properties of this hypothetical zone is given below in the discussion of anomalous energy relations between phases.

Finally, if the dispersion is considered to originate in near surface velocity variations in thin layers, the very steep paths of both SKS and SKKS near the surface seem unfavorable to appreciable dispersive action.

It could of course be argued that the dispersion for these body waves may take place in the outer regions of the core. This would explain the observed period relations between SKS and SKKS. However, the latest published velocity data of both Jeffreys (1939) and Gutenberg (1951) for the core show no discontinuous jumps or rapid increase with depth but rather a uniform gradual rise (1.2 km./sec/1000 km.) near its surface. Such a condition is not favorable to dispersion.

Thus it is seen, largely through negation, that for transverse body waves with partial core paths a period increase with distance is probably not attributable to the processes of dispersion. The data are more in accord with selective absorption due to viscosity of the medium, probably in effect over the whole core path but possibly a maximum in the outer layers of the core.

The decrease of period with increasing depth of focus is not contradictory to such a hypothesis. Periods characteristic of intermediate earthquakes are shorter but have a rate of increase with epicentral distance similar to that for normal shocks. The shorter periods are probably a function of faulting mechanisms under different conditions of temperature and pressure, or to changes in elastic constants of the rocks at depth.

Anomalous Energy Relations.

The principal discrepancies between observed energies and those expected from the theory may be summarized from figures 19 to 23 as follows:

(a) observed energies of the horizontal component of SKS from normal shocks are smaller than expected for $\Delta < 100^{\circ}$, and larger than expected at greater distances;

(b) observed energies in the horizontal component of SKS from intermediate and deep shocks also change from too small to too large near $\Delta = 100^{\circ}$, but are in much closer accord with theory over similar ranges of distance;

(c) observed energies of the horizontal component of SKKS from normal shocks are smaller than expected over the whole distance range to 180°;

(d) observed energies in the vertical components of all phases are too large at all distances and all depths of focus, although those for SKKS are closest to those predicted by theory.

Conditions (a), (b), and (c) above can all be at least qualitatively explained by considerations of the energy distribution diagrams in figure 27, and the constants C and k in equation (8). In calculating the constant C in equation (2), Gutenberg (1945a) used equation (4) with values of U and W obtained from (3). u and w were taken from bulletins of stations in a world-wide net, and a great range of distances and azimuths from the major seismic areas of the earth are thus involved. For this reason, it is proposed that the numerical value determined for C from the transverse mantle phase used is not applicable to calculations involving the core phases SKS or SKKS. A study of figure 27 shows that if the rays can have incident angles from 15° to, say, 75° (true for the S phase), and all possible azimuths from the source, the average amplitudes observed at the wide net of stations will be <u>lower</u> than that which would be determined from a study of SKS or SKKS alone.

The difference is obviously greater for shallow shocks (gently dipping plane) than for deeper foci (steeply dipping plane). The lowering of averaged amplitudes is due to a greater effect of the zones of small shear energy at larger angles of incidence and tends to give a higher value of C in (4). If C is too large for study of waves within the cone of incidence here considered, A_t in equation (8) is too large and the residuals ($A_o - A_t$) thus are too small. This effect at Pasadena increases with distance because shocks approaching the antipodes (Indian Ocean) are apparently along faults so oriented as to give larger than average amplitudes (see Tables IV and VI) which cannot be averaged out in other azimuths. Therefore values of C still further below that determined from S are required.

Thus we might expect negative residuals for the whole range of distance of SKS and SKKS, but with better accord shown by the deeper shocks. This explanation removes the second parts of discrepancies (a) and (b) above.

SKS for all depths has positive residuals at distances less than 100°. Assuming for a moment that this is due to increased absorption in the outer regions of the core, what interrelation could we expect with residuals of SKKS? An SKS ray emerging at 100° has 70° of this path in the core. Thus the equivalent SKKS ray will emerge at 170°. If observed energies are too small for SKS in the distance range considered because of the abnormal absorption assumed, energies of SKKS, because of its doubled core path, should be roughly twice as small over the whole range to 170°. Figure 19 shows this to be approximately the case. Such an argument, coupled with evidence given above for the period increase of both phases, suggests the existence of such a zone. A thickness of seven hundred kilometers has been determined by calculating the deepest point on a ray having a central angle in the core of 70° by the method of Herglotz and Wiechert. Calculation of probable values of k in the outer core are not possible until adjusted values of C have been determined and the required variation in A_t defined. The use of P' offers no help since it has no core paths following the core boundary this closely.

Mooney (1951, p. 26) tabulated energy residuals as a function of epicentral region for the phases P and pP. His residuals are taken with respect to theoretical values rather than mean observational values as in Table VI, and the sign is reversed because he makes use of the residual ($A_t - A_o$) rather than the converse here employed. It is of interest, however, that with a reversed sign for one set of data, all the residuals for regions common to both investigations are of similar sign (Marianas Islands, New Guinea, New Hebrides Islands, and Kermadec Islands). Furthermore, all of the residuals based on longitudinal phases are of smaller magnitude, as is predicted by comparison of the energy distribution patterns in figure 26 for distortional and dilatational vibration.

No hypothesis for the explanation of discrepancy (d) above (abnormally large vertical amplitudes) is suggested by either the shear stress distribution diagram or the abnormal absorption hypothesized above. Similar results were obtained by Ergin (in press,a) for the phases PcS and ScS. He also found that the supposedly minor horizontal components of PcP and ScP are too large. On the basis of energy distribution about fault sources formulated above, we might expect that at least two of these four phases, those starting from the source as S waves with angles of incidence similar to those for SKS, should exhibit larger observed A values than those calculated from theory. This effect is borne out by the data presented by Ergin.

In a later paper, Ergin (in press,b) attempts to explain the discrepancy between energies calculated from horizontal and vertical instruments for the two phases arriving at the station as shear waves (PcS, ScS). It is proposed as being due to P motion, refracted from the wave at some near surface layer, which immediately precedes the S motion. Ground displacement vector studies with time were utilized and the minor P phase detected. Such an explanation is preferable to hypotheses that energy gradients across wave fronts are appreciable or that true S or P motion does not actually exist (Stoneley, 1949), but it is not completely borne out by the data for SKS. Of the thirty-five shocks studied for polarization relations, only three gave directions of first motion commensurate with vibration along the ray instead of perpendicular to it. Ergin's method of analysis is superior to considerations of first motion only, but directions of motion must be correlated with it.

Inasmuch as fairly strong components of SH motion are inexplicably present in the total ground displacement due to SKS waves, it is not improbable that the alternate hypotheses noted above may share in the discrepancies for vertical motion.

Multiplicity of SKS Phases.

Data have been presented for four SKS phases from normal shocks, two SKS phases for intermediate and deep shocks, and a single SKKS phase for all depths. It is possible that additional phases in the latter two categories are present. If so, they must contain very little energy. The properties of the multiple phases which must be considered in the development of a causal mechanism or hypothesis are summarized below.

(1) Phases one and two are separated by approximately the same time interval for all epicentral distances (nine to eleven seconds).

(2) Phases three and four, where present, exhibit somewhat the same parallelism at approximately a six to eight second interval, but both approach the first and second curves at increasing distance (an eight second decrease in the time SKS_4-SKS_1, from 95° to 120°).

(3) Median periods in the late phases are equal to or less than that of the principal phase.

(4) At particular distances within the common range, any one of the SKS phases may carry the largest proportion of energy. Figure 11 illustrates the randomness of this relation.

The problem of multiplicity has been observed and studied by many workers. A summary is found in Gutenberg and Richter (1934, pp. 80-81, 129-130). Several causal hypotheses have been deduced and discussed. Although the final theory will ultimately come from a study of all the seismic waves exhibiting the phenomenon, the data here presented may perhaps evaluate some of the proposed causal factors.

The older concept of origination in terms of variable source phenomena is refuted by observations of the same phases in a particular wave type from many different foci, and by the dissimilar nature of multiple phases in different wave groups from the same focus. The concept of anomalous dispersion as a cause for multiplicity, with group velocities less than the phase velocity, has been investigated by Sommer (1931). She concludes (ibid., p. 121) that it is not supported by the appearance of the seismograms. The mean periods of this study for late SKS phases are in accord with such a conclusion.

SKS phases of normal shocks with initial paths leaving the source nearly vertically toward the surface (pSKS and sSKS) could offer an explanation for the third and fourth multiples if the time relations were correct. Gutenberg and Richter (ibid., p. 80) allow such a possibility for the early multiple phases of P. A decreasing time interval after the principal phase with increasing distance is predicted, but the observed decrease is too high. The observed time intervals at $\Delta = 100^\circ$ are within two seconds of those predictable under this hypothesis (for a depth of focus of fifty kilometers and with average velocities of seven and four km./sec. for P and S in the layers above, respectively). SKS_2 is not explained by such an hypothesis, nor are energy anomalies between phases clear. The quite different median period for SKS_2 suggests that it has a different origin than SKS_3 or SKS_4. This hypothesis does, however, explain the difference in number of multiples for SKS at normal and deeper depths, the phases pSKS and sSKS having been observed for intermediate and deep shocks but not counted as multiples.

The data favor such an explanation more than any other. The fact that the two phases disappear at increasing epicentral distance is perhaps consistent with the greater loss of energy for surface reflections at larger angles of incidence. Also, $(A_o - A_t)$ residuals for SKS would be brought into closer accord with theory if the later two phases were not combined in the A_o term.

Transformation of waves from S to P, or vice-versa, at boundaries in the upper earth layers has frequently been suggested as a possible cause of multiplicity. Gutenberg (1949) has advanced such an hypothesis for certain late P phases recorded at Huancayo, Peru. The depths of refraction involved are roughly 40, 80, and 150 kilometers. An analogous relation for S phases is of course impossible unless the SKS multiples are considered in reverse order. If SKS_2 were really the principal phase, SKS_1 should have been refracted to P at a boundary roughly 95 kilometers in depth to account for the time difference. Such a possibility is doubtful in view of the first motion studies for SKS_1 reported above, and the fact that SKS_2 has a smaller median period than SKS_1. In addition, SKS_2 shows higher than expected vertical component amplitudes like those of SKS_1.

A remaining possibility concerns multiple reflections between boundaries of layers near, or including, the surface. Transformation from transverse to longitudinal vibration is not required but is possible. As in a straight transformation process, no appreciable dependence of the time interval on epicentral distance is inferred. A layer approximately 19 kilometers thick would account for the time interval SKS_2-SKS_1 if the incident SKS wave is reflected downward from the surface to the boundary and then up again with no change in mode of vibration. Transformation to longitudinal vibration occurring at any of the reflections would require a deeper boundary. Again, the observed energy variations are poorly accounted for.

In summary, no single hypothesis here advanced can satisfactorily explain the time relations of multiple phases of SKS, and observed energy differences in the phases are far from predictable. The phases pSKS and sSKS for shocks of normal depth apparently offer the best explanation for the multiples SKS_3 and SKS_4. Time and energy relations are not perfect but are at least of the right order of magnitude. SKS_2 might conceivably be the principal pure SKS phase, with SKS_1 its counterpart which was transformed to longitudinal vibration near a depth of 95 kilometers on its upward path. Detailed calculations are hampered by poorly known, and highly variable, crustal velocities.

SUMMARY AND CONCLUSIONS

A study of wave periods, amplitudes, and arrival times for the seismic phases SKS and SKKS has been made on over one thousand seismograms of normal, intermediate, and deep earthquakes with epicentral distances from Pasadena or Huancayo, Peru between 75° and 175°. Selected large shocks over a similar distance range were examined for direction and component relations of the first SKS motion recorded.

The constructed travel time curves of SKS, SKKS, and SKKKS are believed to be an improvement over previous observed curves as they are in better agreement with calculated arrival times. Observation of the later branched segments has not been possible, but the new SKS curve reflects rather closely the abrupt slope change near 130° at the theoretical branch intersection. Late arrivals of SKS clearly delineate three multiple phases for normal earthquakes, in addition to the principal phase, and at least one for intermediate and deep shocks. Only one phase has been observed for SKKS.

It is felt that the observed times for SKS are now within the limits of error set by the determination of epicenters and origin times, and by variable crustal effects. Additional time-distance data for SKKS and SKKKS would be of value.

Travel times between points on the surface of the core have been calculated by the method of Wadati and Masuda using SKS and SKKS times from this study, and the ScS curve of Gutenberg and Richter (1939). Times from both calculations are in very good agreement over the common range and require a steeper curve slope, and hence slightly lower velocity, just inside the core than the latest published data of both Gutenberg and Jeffreys. Up to about 120° the times are in excellent agreement with those of Gutenberg. From 120° to 180° they are up to four seconds later than those of both Gutenberg and Jeffreys.

Using an averaged core travel time curve, and times for the later branches not derivable from SKS from Gutenberg (1951), times were calculated for SKS, SKKS, and SKKKS. Agreement with observed times is best for SKS, but the residuals for the other two phases never exceed seven seconds.

Observed periods have been analyzed as functions of phase and component, magnitude, depth of focus, epicentral distance, and epicentral location. Periods of all phases decrease with increasing hypocentral depth but exhibit no magnitude dependence. SKKS periods are longer than those of SKS in both components (except for intermediate depths), but both show a gradual increase with epicentral distance for horizontal components.

The increase for SKKS is roughly double that for SKS. Consideration of wavelengths, ray paths, relations between periods of SKS and SKKS, and wave velocity data favors the causal hypothesis of selective absorption by viscosity of the medium for the observed period increase. Such absorption doubtless is effective over the whole path length, but is possibly intensified in the outermost seven hundred kilometers of the core.

There is apparently a dependence of phase period on geographic location of the epicenter. The phenomenon is explained on the basis of a form of the Doppler effect produced by progressive rupture propagated along the fault plane with velocities somewhat less than that of the shear wave velocity. The periods of all multiple phases are found to be equal to, or less than, that of the principal phase.

Parameters which are measures of wave energy have been determined from observed amplitudes and calculated from elastic wave theory. Agreement between observation and theory for all phases is in general only fair or even poor. The observed energies are too large for all phases, components, and distances except for the horizontal component of SKKS over the whole range of distance, and of SKS at epicentral distance less than 100°. These anomalies have led to the consideration of a non-spherical energy distribution about the source. A completely quantitative treatment is not possible at this time, but the proposed variations of energy as a function of ray azimuth and angle of incidence from the fault source can remove most of the observed discrepancies. Remaining residuals of opposite sign are explained on the basis of a highly absorptive zone within the core from its surface down to an approximate depth of seven hundred kilometers.

The energies calculated from records of vertical instruments are too large for all phases studied. Analysis of the directions of first ground motion and relative component amplitudes, with respect to those expected from the ray azimuth and angle of incidence, is not conclusive. The frequent presence of an appreciable component of SH motion in the theoretically pure SV vibration is disclosed but only a few instances of longitudinal vibration, which could account for the abnormal vertical amplitudes, are indicated. It is probable that a combination of factors is involved.

Observed energy parameters show a definite epicentral location dependence. Residuals from mean values are tabulated for several regions as correction factors which can be used at Pasadena in calculations of magnitude from SKS amplitudes for earthquakes of normal and intermediate depths. These energy variations with azimuth and epicentral distance are also qualitatively explained by the non-spherical energy distribution noted above.

Energies, periods, and times of multiple SKS phases have not been explained by any of the prevailing hypotheses suggested for the solution of the multiplicity problem. An extensive study of the theoretical possibilities is required. The data of this investigation exclude an explanation involving anomalous dispersion in the wave spectrum, and suggest that the phases pSKS and sSKS for shocks of normal depth may possibly be a factor.

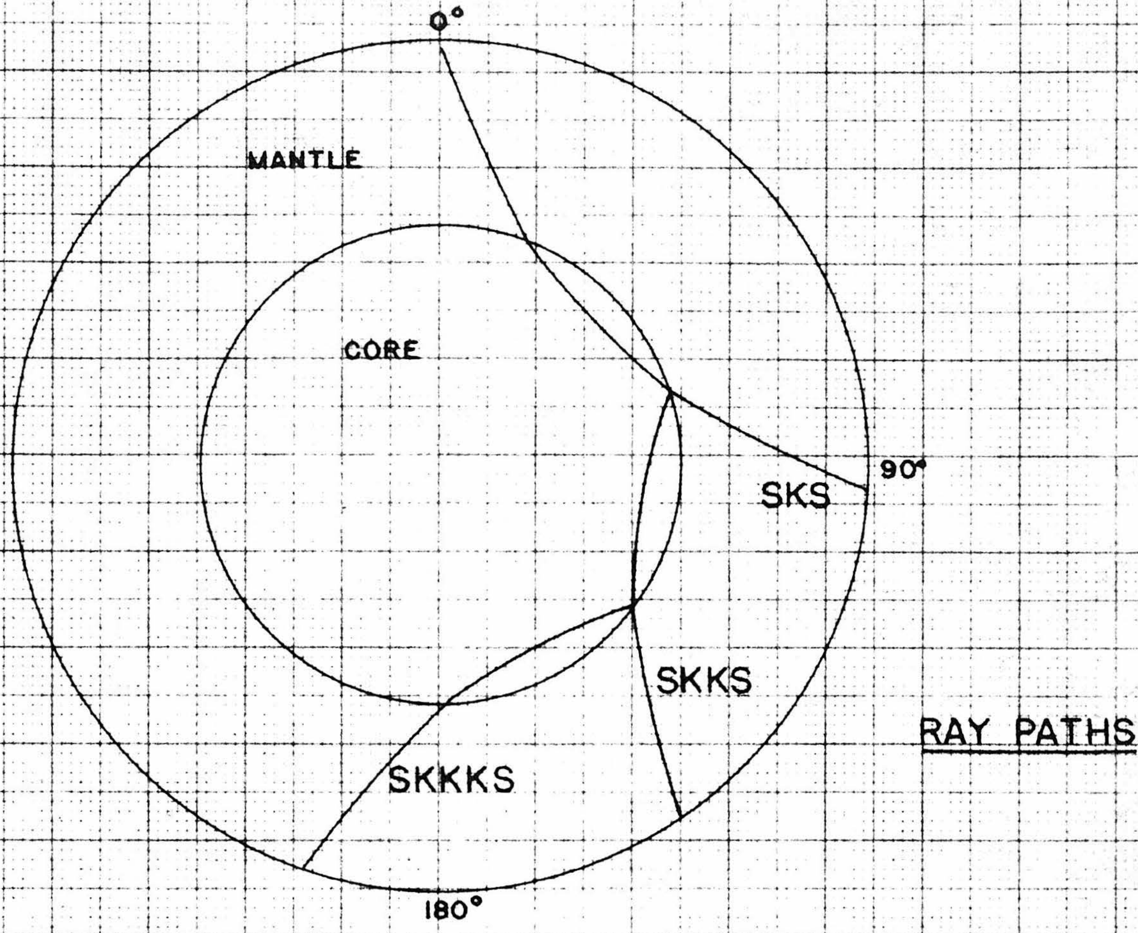

0°
MANTLE
CORE
90°
SKS
SKKS
SKKKS
180°
RAY PATHS

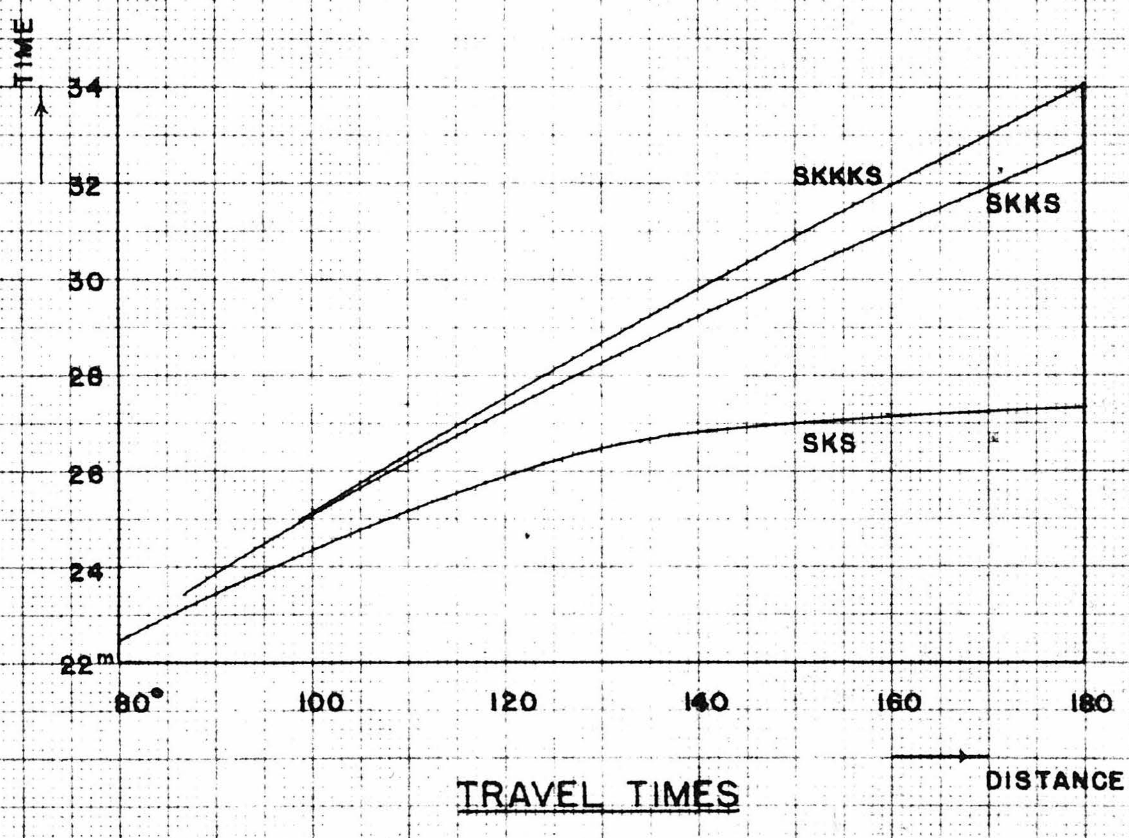

TIME
34
32
30
28
26
24
22m
SKKKS
SKKS
SKS
80°
100
120
140
160
180
DISTANCE
TRAVEL TIMES

FIGURE 1

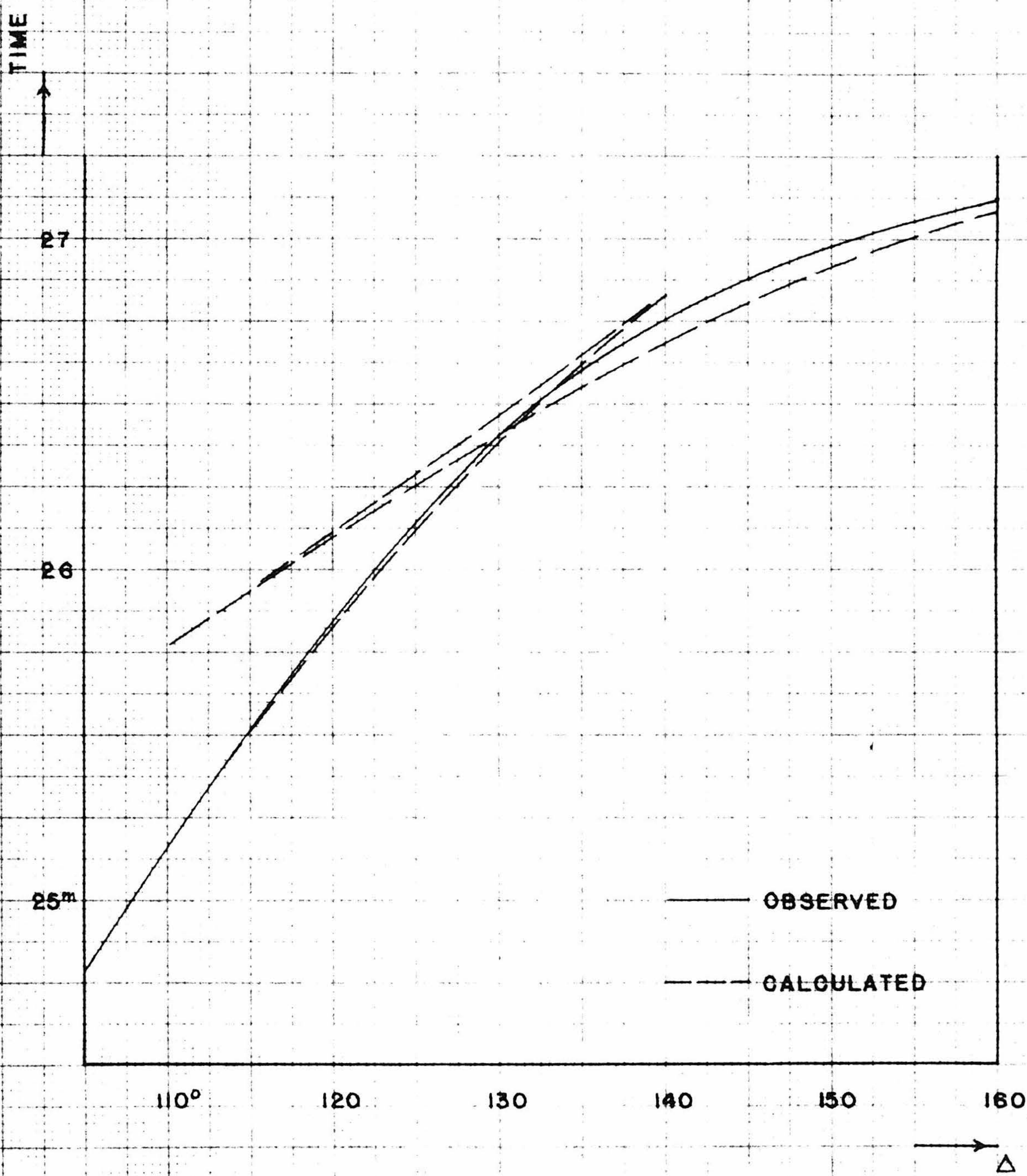

OBSERVED AND CALCULATED SKS
TRAVEL TIMES

FIGURE 2

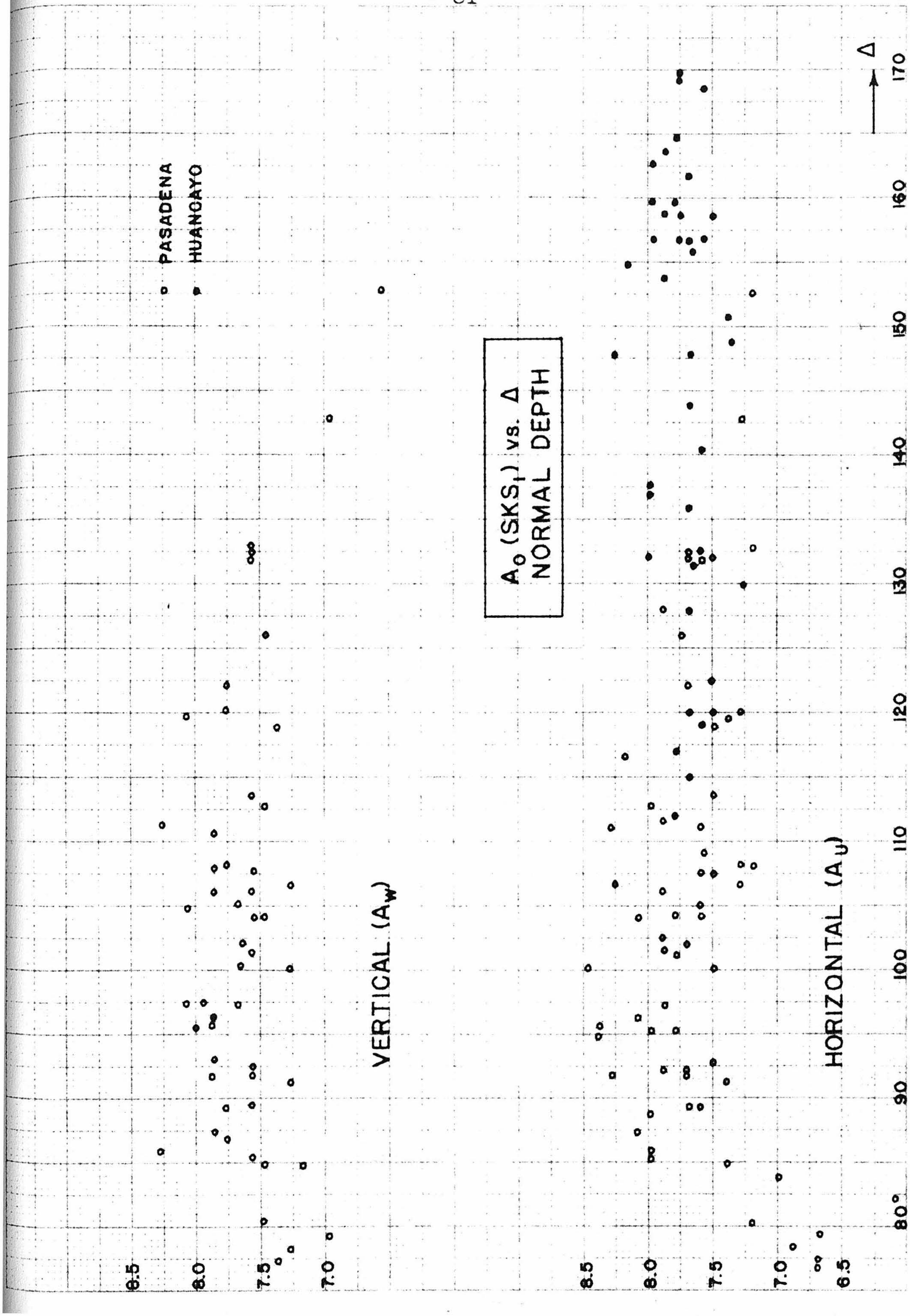

PASADENA
HUANCAYO
A_0 (SKS$_1$) vs. Δ
NORMAL DEPTH
VERTICAL (A_W)
HORIZONTAL (A_U)
8.5
8.0
7.5
7.0
6.5
80°
90
100
110
120
130
140
150
160
170
Δ

FIGURE 3

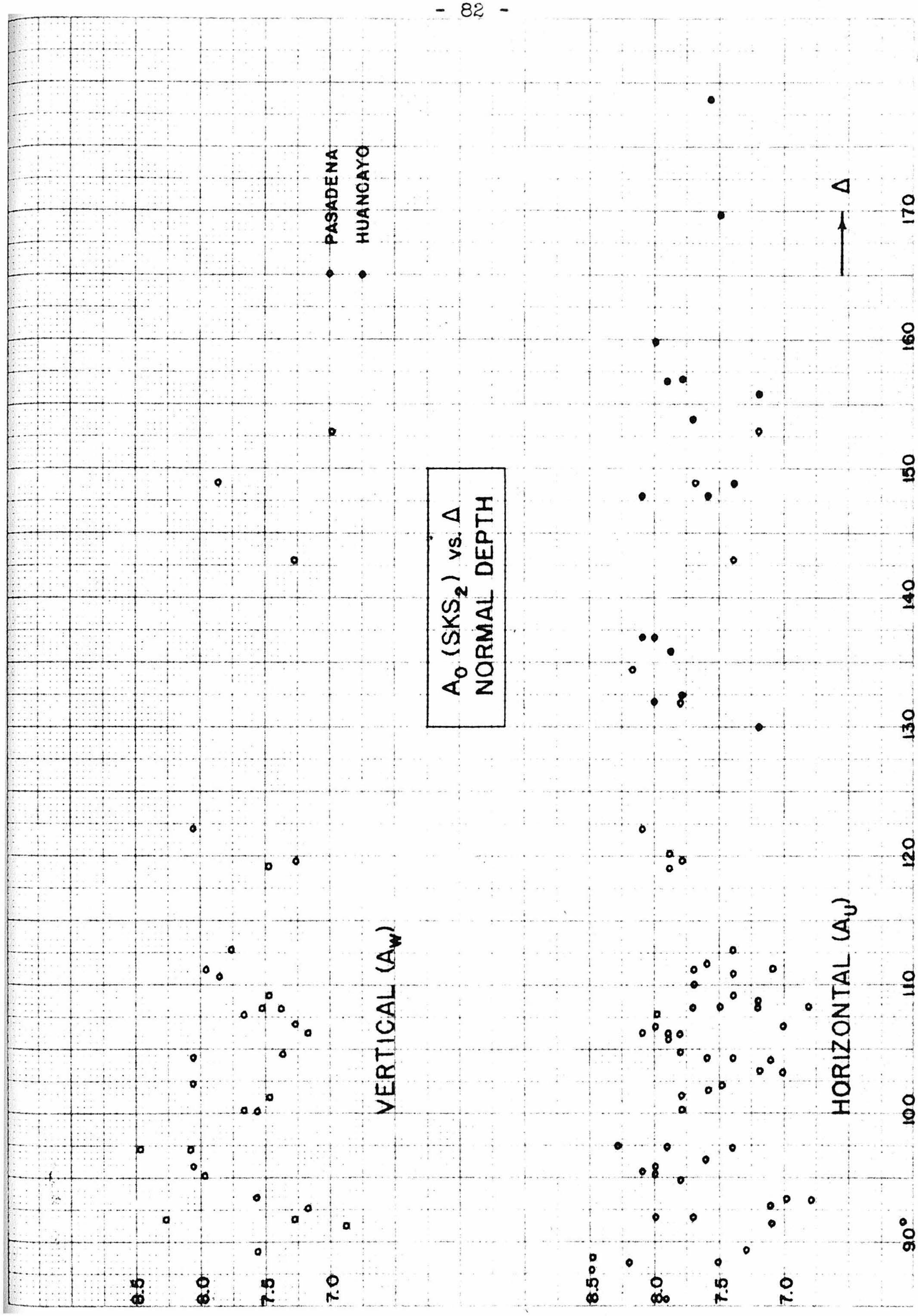

PASADENA
HUANCAYO
A_0 (SKS$_2$) vs. Δ
NORMAL DEPTH
VERTICAL (A_W)
HORIZONTAL (A_U)
8.5
8.0
7.5
7.0
90°
100
110
120
130
140
150
160
170
Δ

FIGURE 4

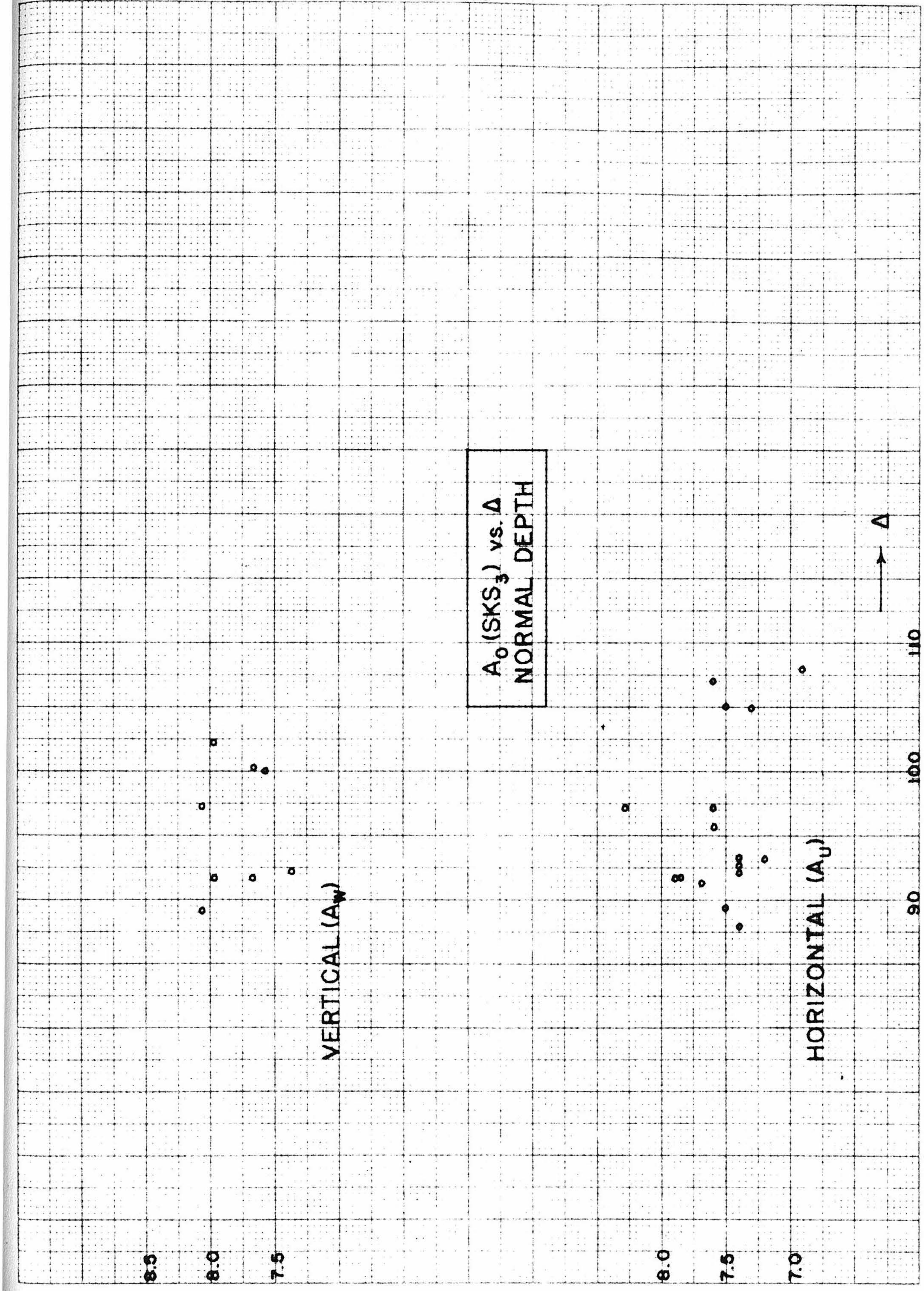

A0 (SKS3) vs. Δ
NORMAL DEPTH
VERTICAL (AW)
HORIZONTAL (AU)
8.5
8.0
7.5
8.0
7.5
7.0
90
100
110
→ Δ

FIGURE 5

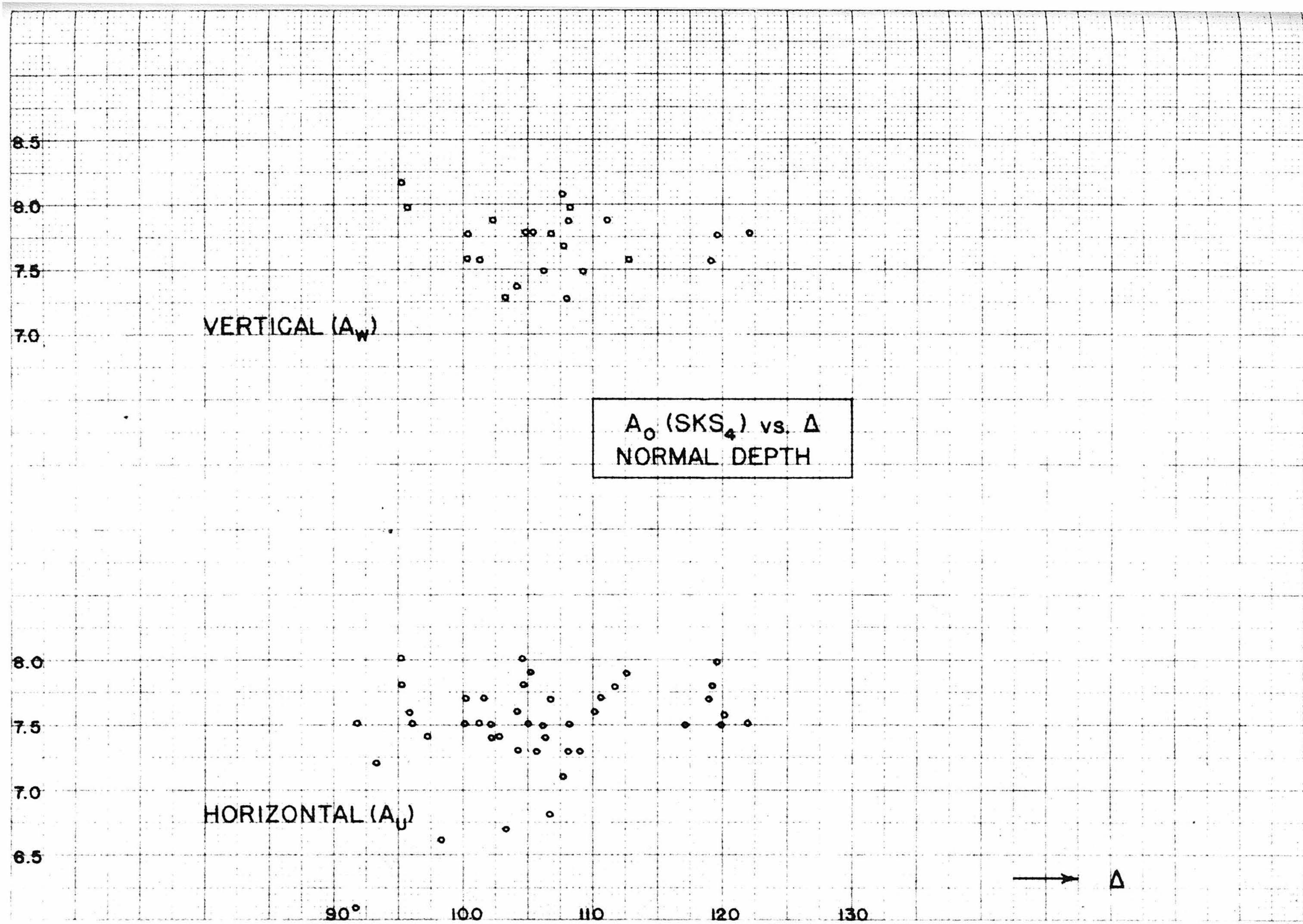
A_o (SKS$_4$) vs. Δ
NORMAL DEPTH
VERTICAL (A_W)
HORIZONTAL (A_U)
8.5
8.0
7.5
7.0
8.0
7.5
7.0
6.5
90°
100
110
120
130
Δ

FIGURE 6

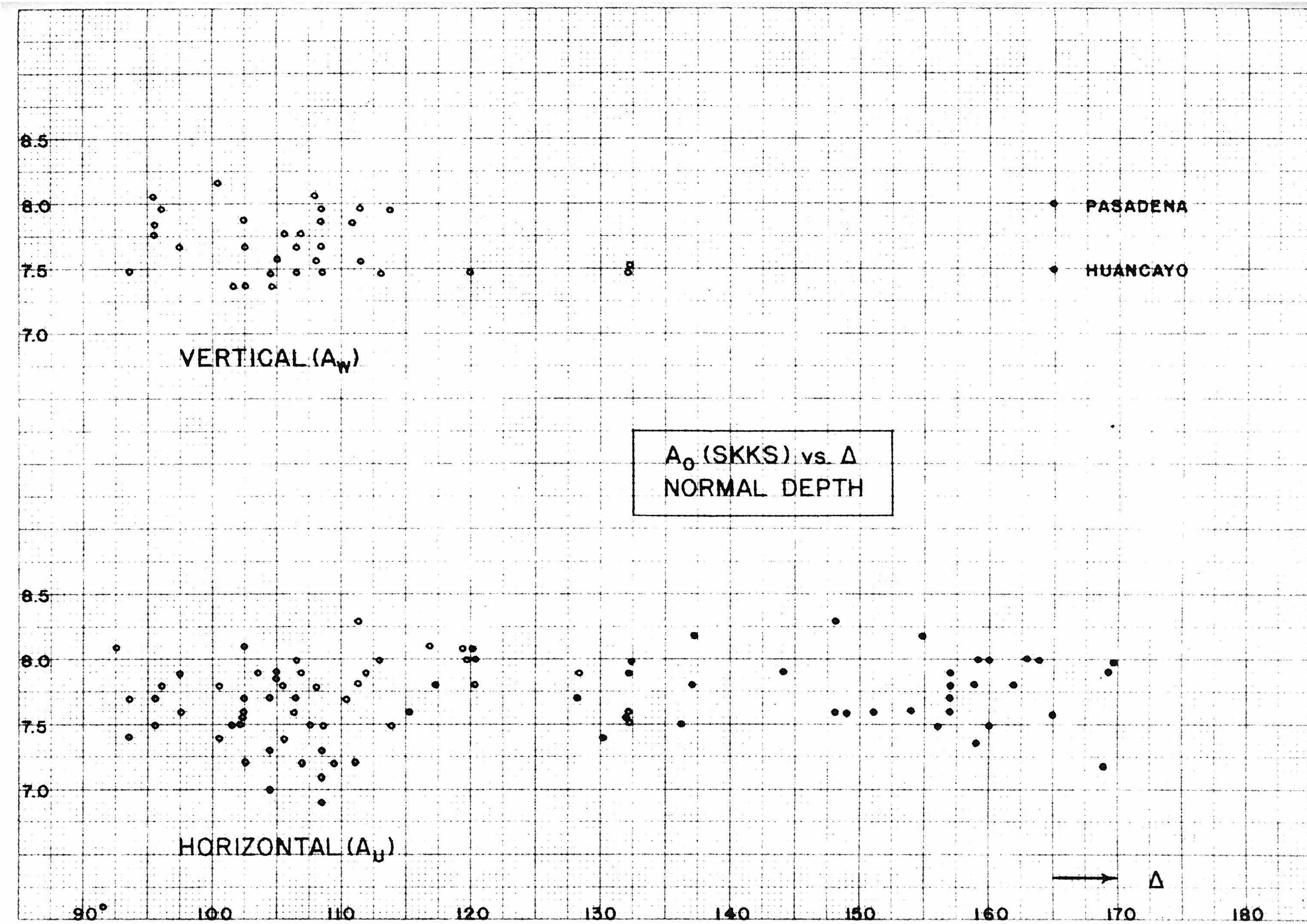
8.5
8.0
7.5
7.0
PASADENA
HUANCAYO
VERTICAL (A_w)
A_o (SKKS) vs. Δ
NORMAL DEPTH
8.5
8.0
7.5
7.0
HORIZONTAL (A_u)
Δ
90°
100
110
120
130
140
150
160
170
180

FIGURE 7

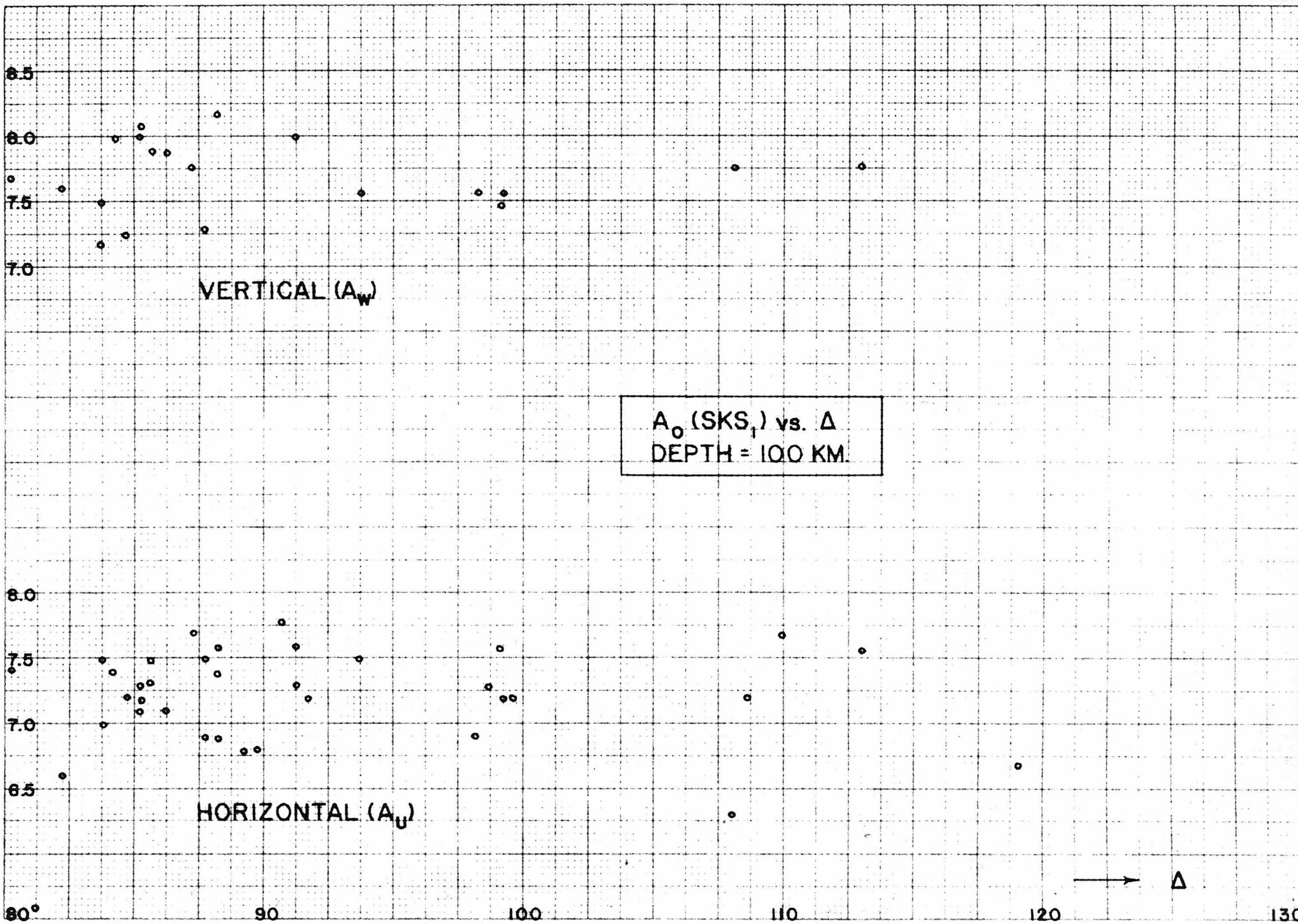
8.5
8.0
7.5
7.0
VERTICAL (A_W)
A_O (SKS_1) vs. Δ
DEPTH = 100 KM.
8.0
7.5
7.0
6.5
HORIZONTAL (A_U)
→ Δ
80°
90
100
110
120
130

FIGURE 8

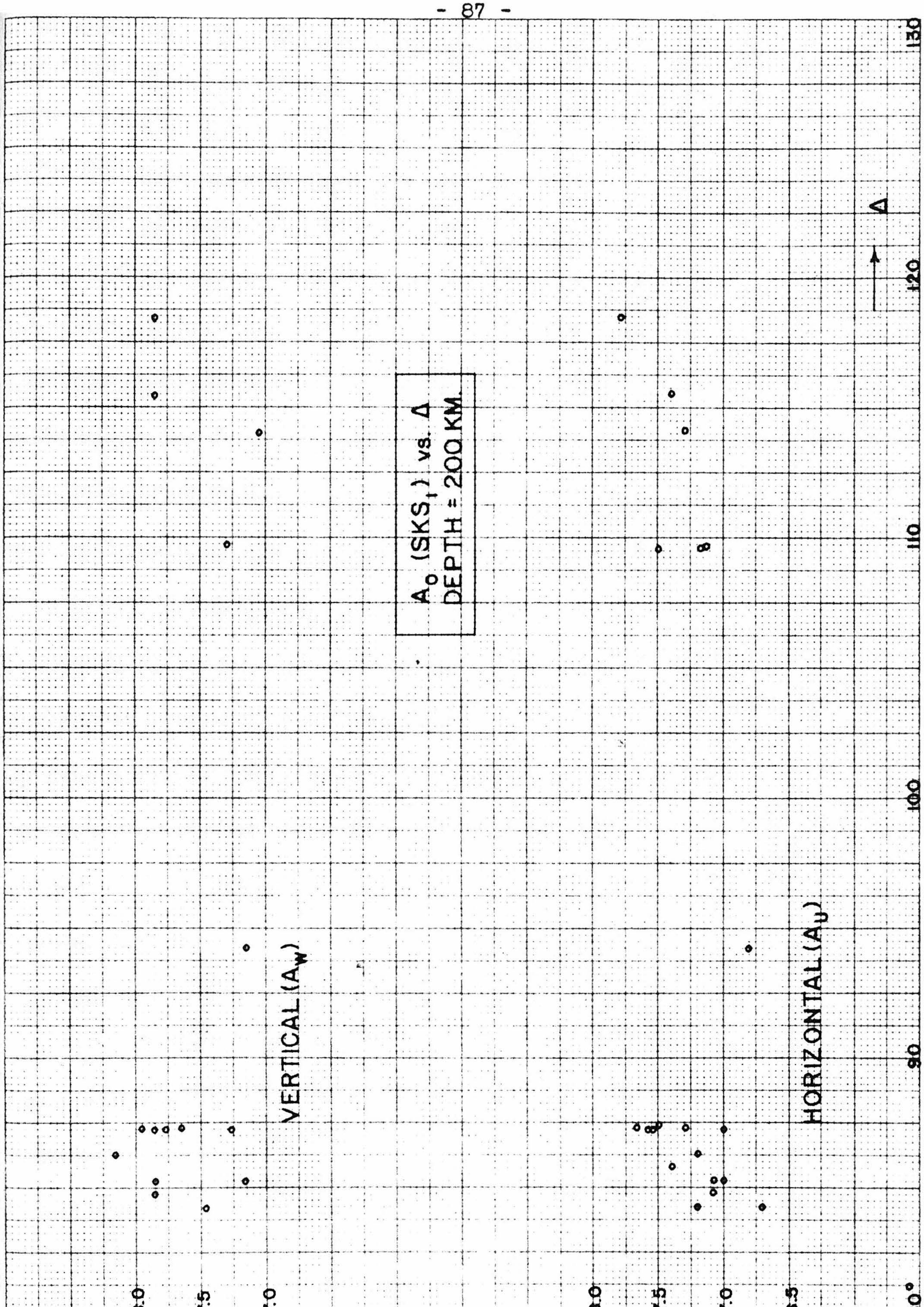
A$_o$ (SKS$_1$) vs. Δ
DEPTH = 200 KM.
VERTICAL (A$_W$)
HORIZONTAL (A$_U$)
8.0
7.5
7.0
8.0
7.5
7.0
6.5
80°
90
100
110
120
130
Δ

FIGURE 9

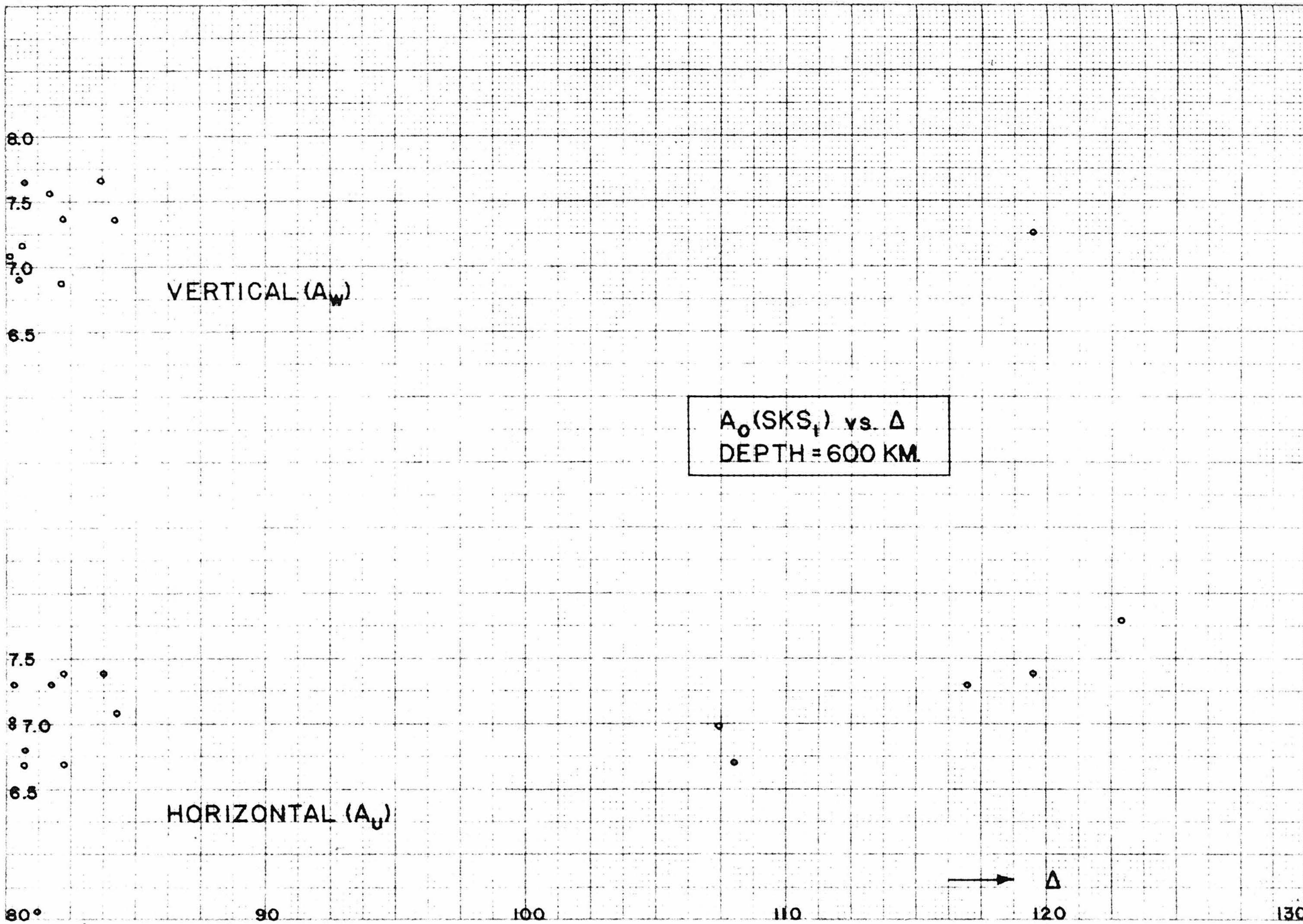
$A_o(SKS_t)$ vs. Δ
DEPTH = 600 KM.
VERTICAL (A_w)
HORIZONTAL (A_u)
8.0
7.5
7.0
6.5
7.5
7.0
6.5
80°
90
100
110
120
130
Δ

FIGURE 10

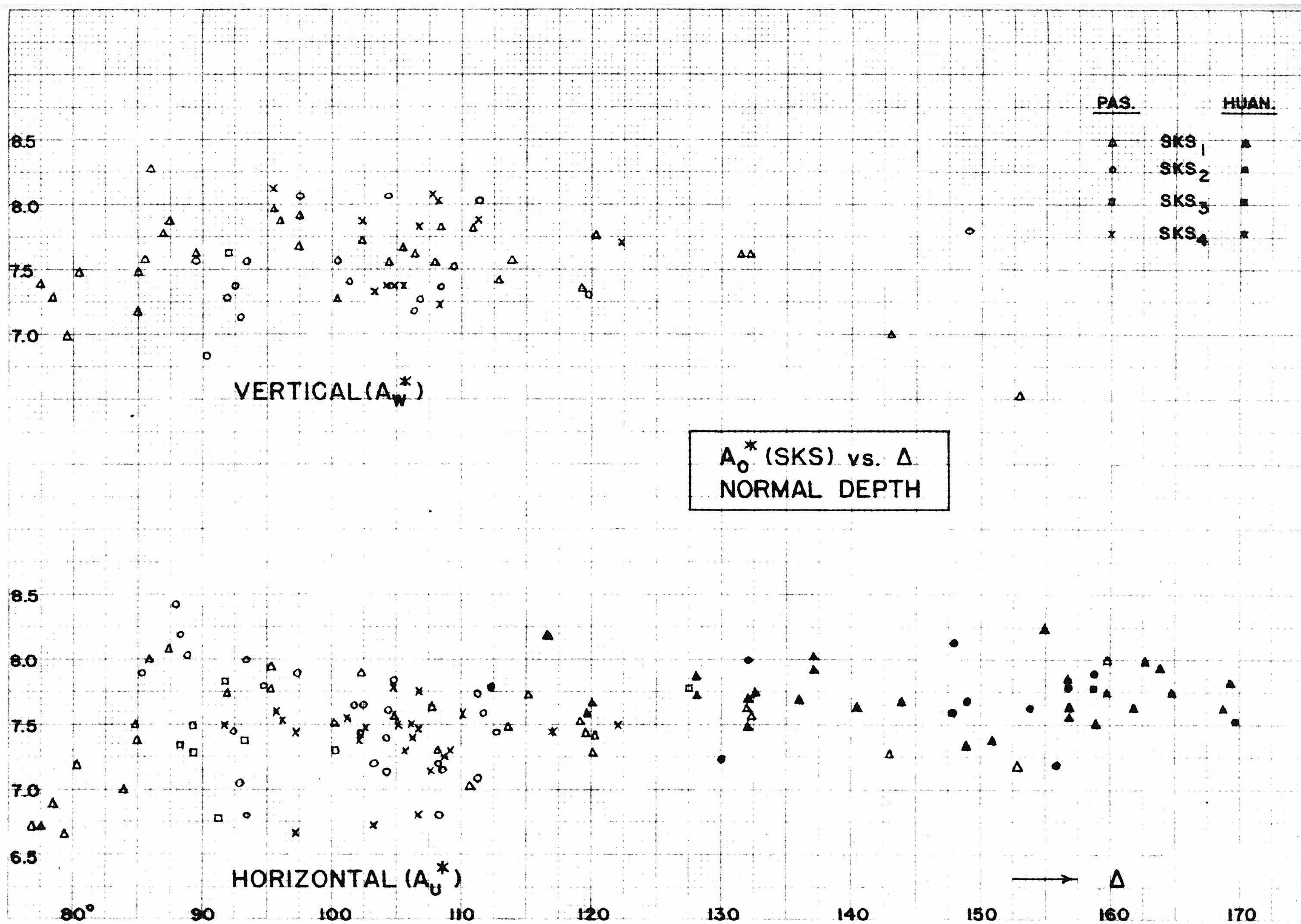
PAS.
HUAN.
SKS1
SKS2
SKS3
SKS4
8.5
8.0
7.5
7.0
VERTICAL(A*w)
A*o (SKS) vs. Δ
NORMAL DEPTH
8.5
8.0
7.5
7.0
6.5
HORIZONTAL (A*u)
Δ
80°
90
100
110
120
130
140
150
160
170

FIGURE 11

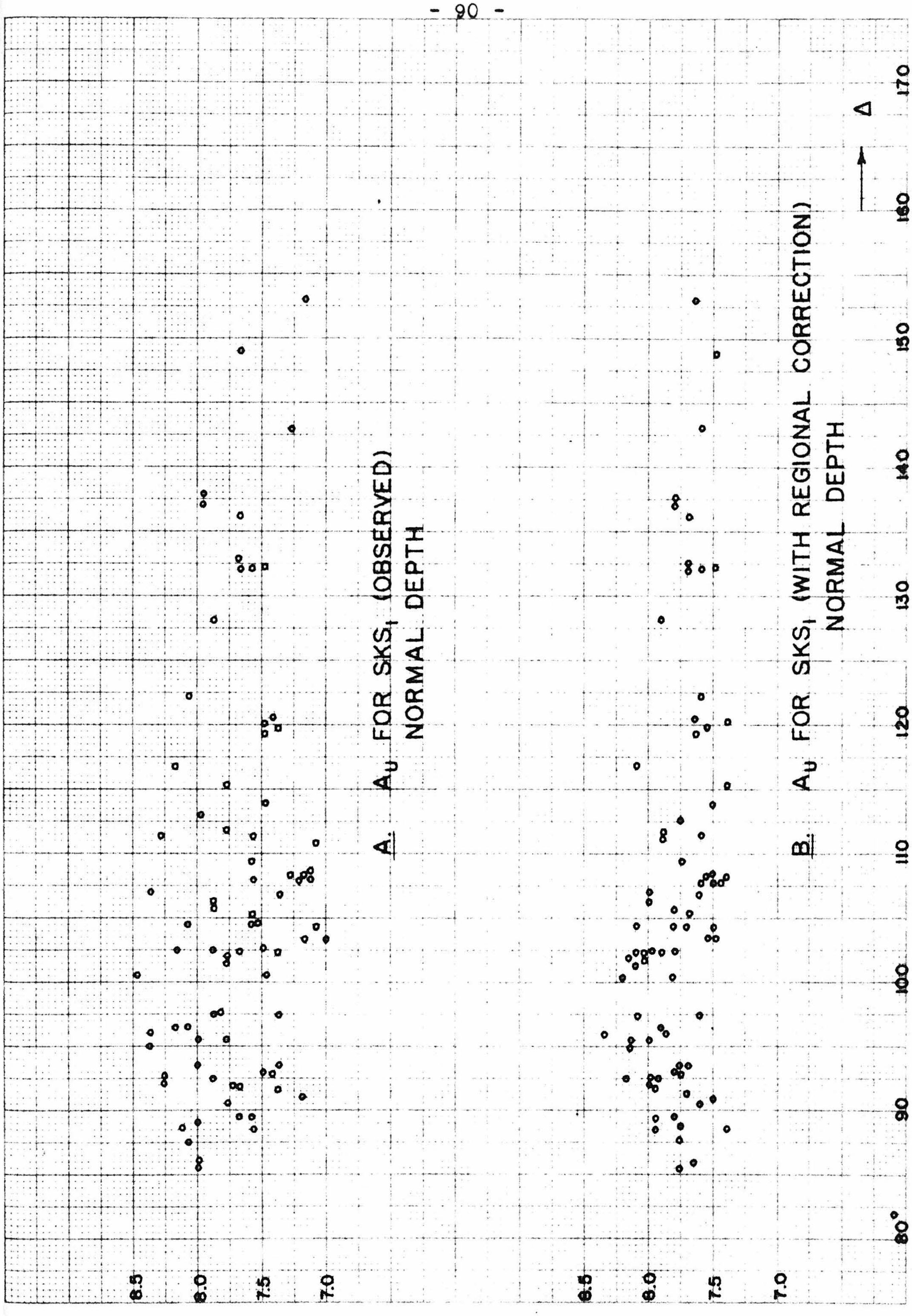
A. A_U FOR SKS_1 (OBSERVED)
NORMAL DEPTH
B. A_U FOR SKS_1 (WITH REGIONAL CORRECTION)
NORMAL DEPTH
8.5
8.0
7.5
7.0
80°
90
100
110
120
130
140
150
160
170
Δ

FIGURE 12

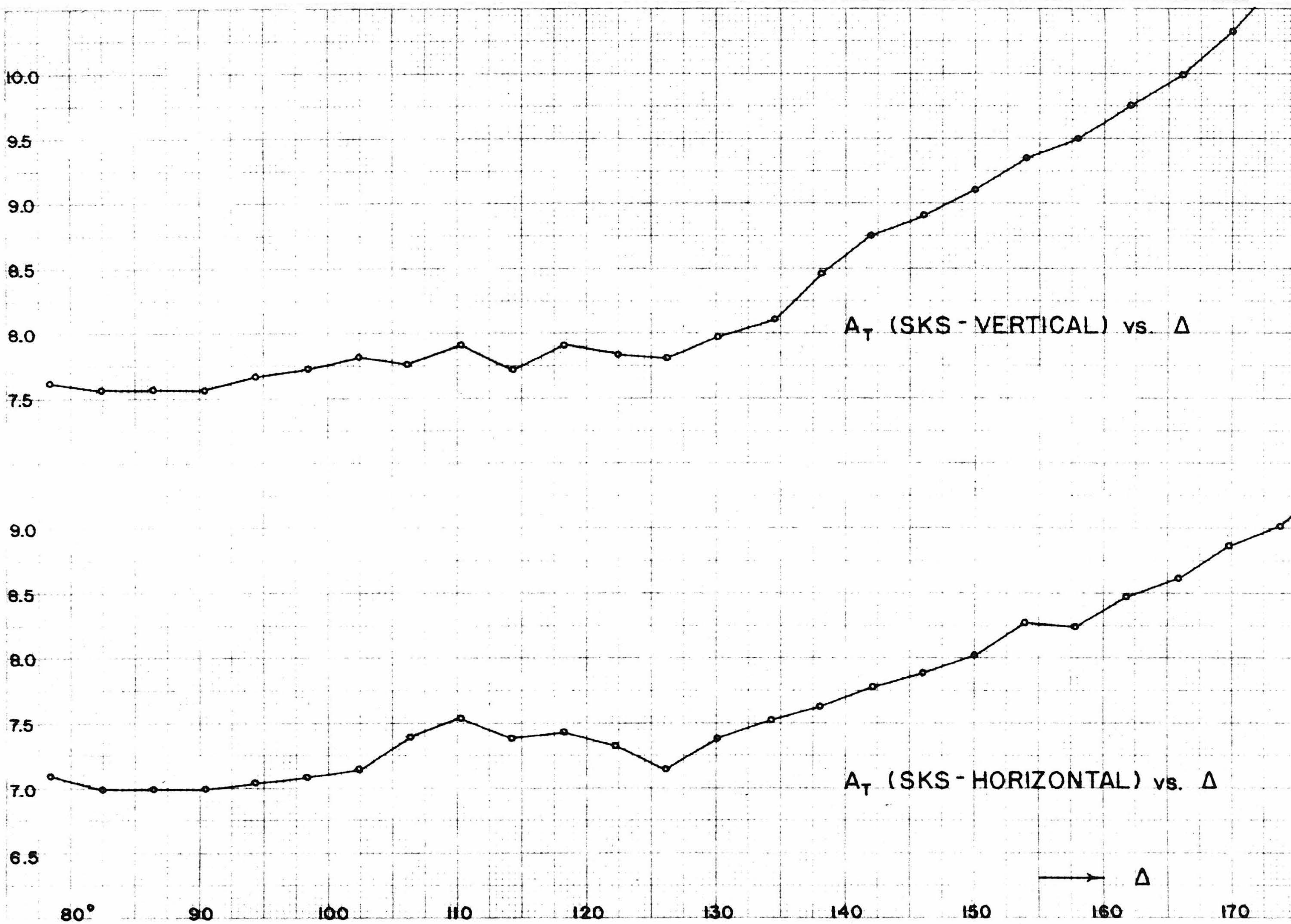
10.0
9.5
9.0
8.5
8.0
7.5
A_T (SKS - VERTICAL) vs. Δ
9.0
8.5
8.0
7.5
7.0
6.5
A_T (SKS - HORIZONTAL) vs. Δ
Δ
80°
90
100
110
120
130
140
150
160
170

FIGURE 13

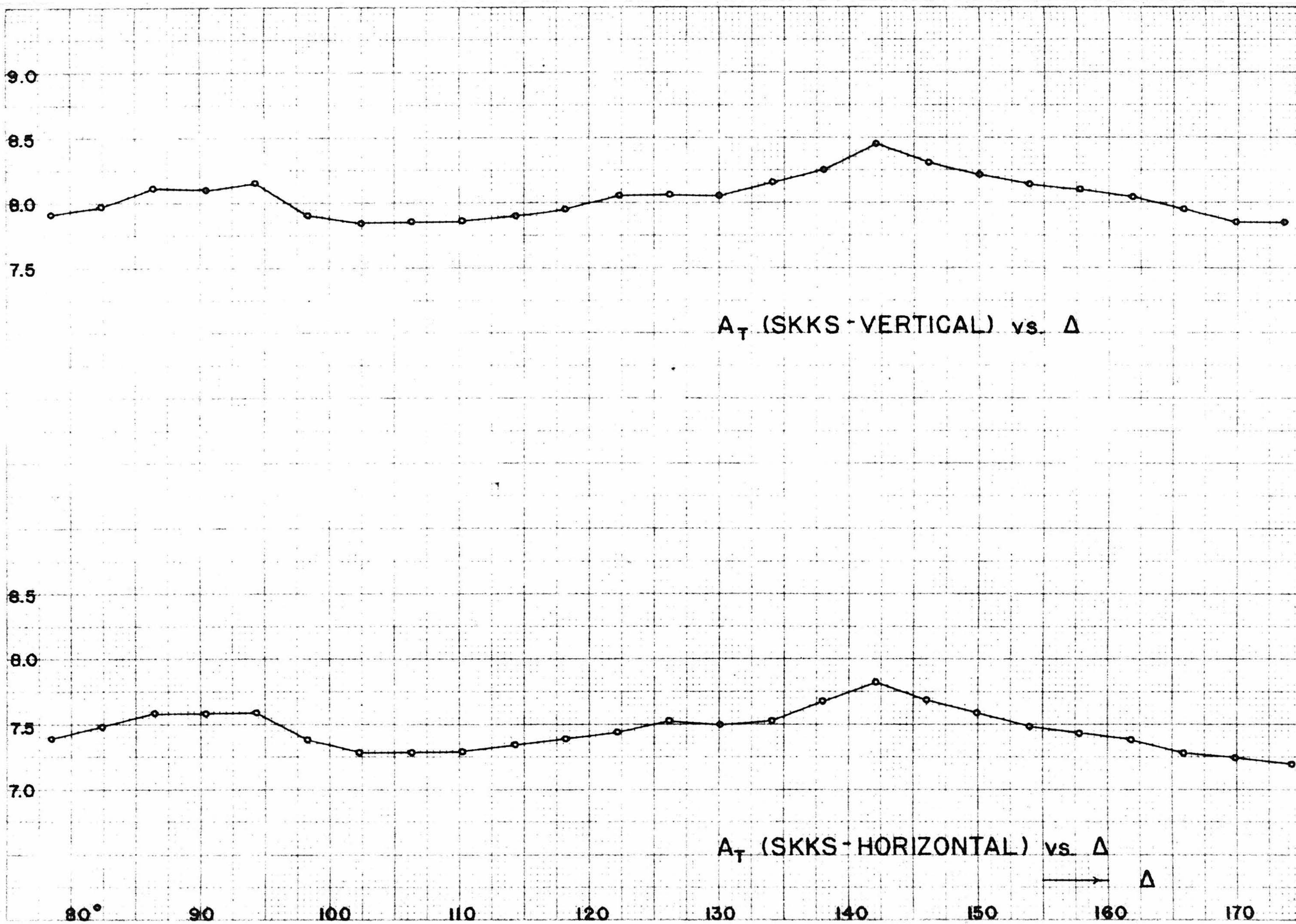
9.0
8.5
8.0
7.5
A_T (SKKS - VERTICAL) vs. Δ
8.5
8.0
7.5
7.0
A_T (SKKS - HORIZONTAL) vs. Δ
Δ
80°
90
100
110
120
130
140
150
160
170

FIGURE 14

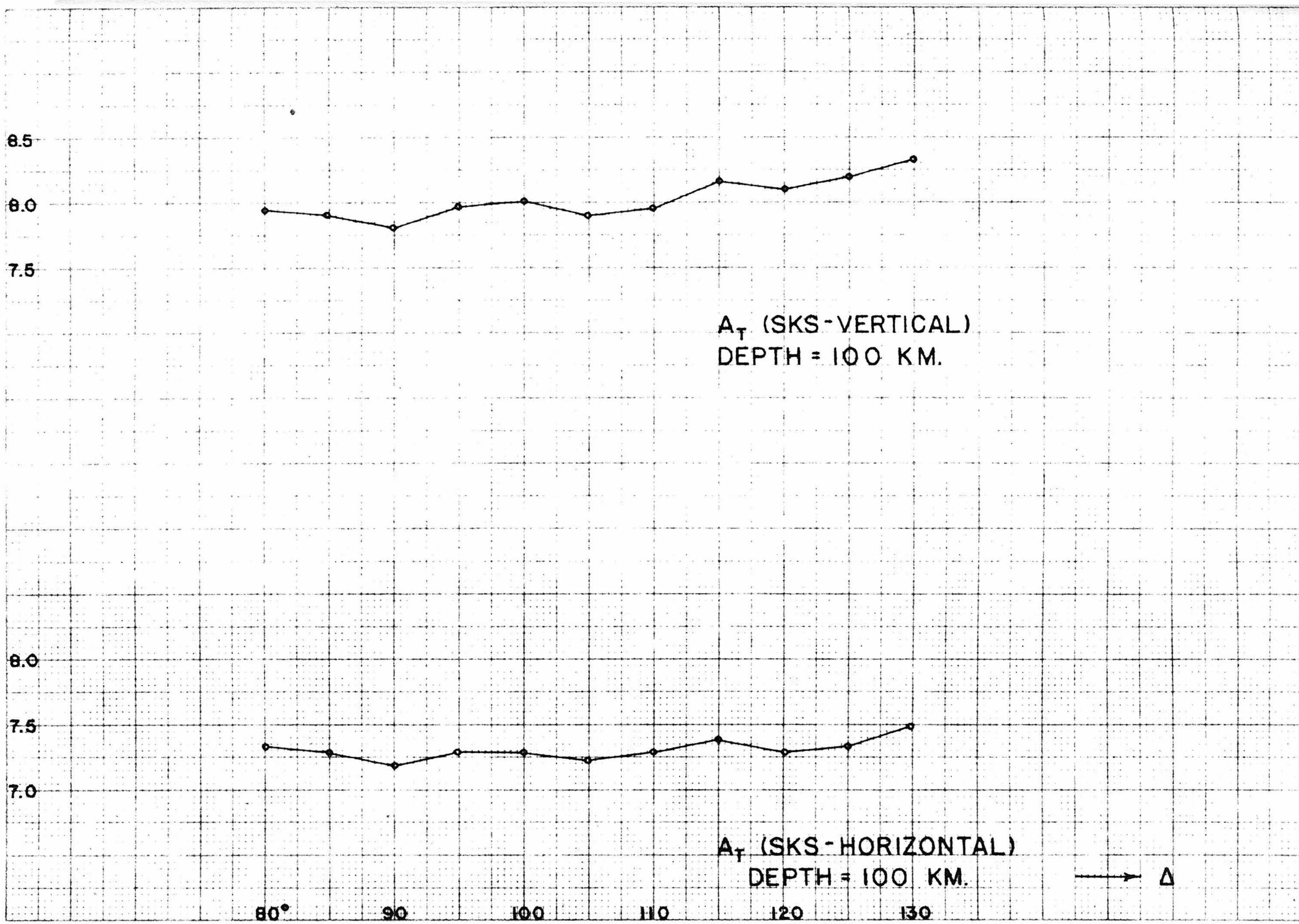
8.5
8.0
7.5
A_T (SKS-VERTICAL)
DEPTH = 100 KM.
8.0
7.5
7.0
A_T (SKS-HORIZONTAL)
DEPTH = 100 KM.
Δ
80°
90
100
110
120
130

FIGURE 15

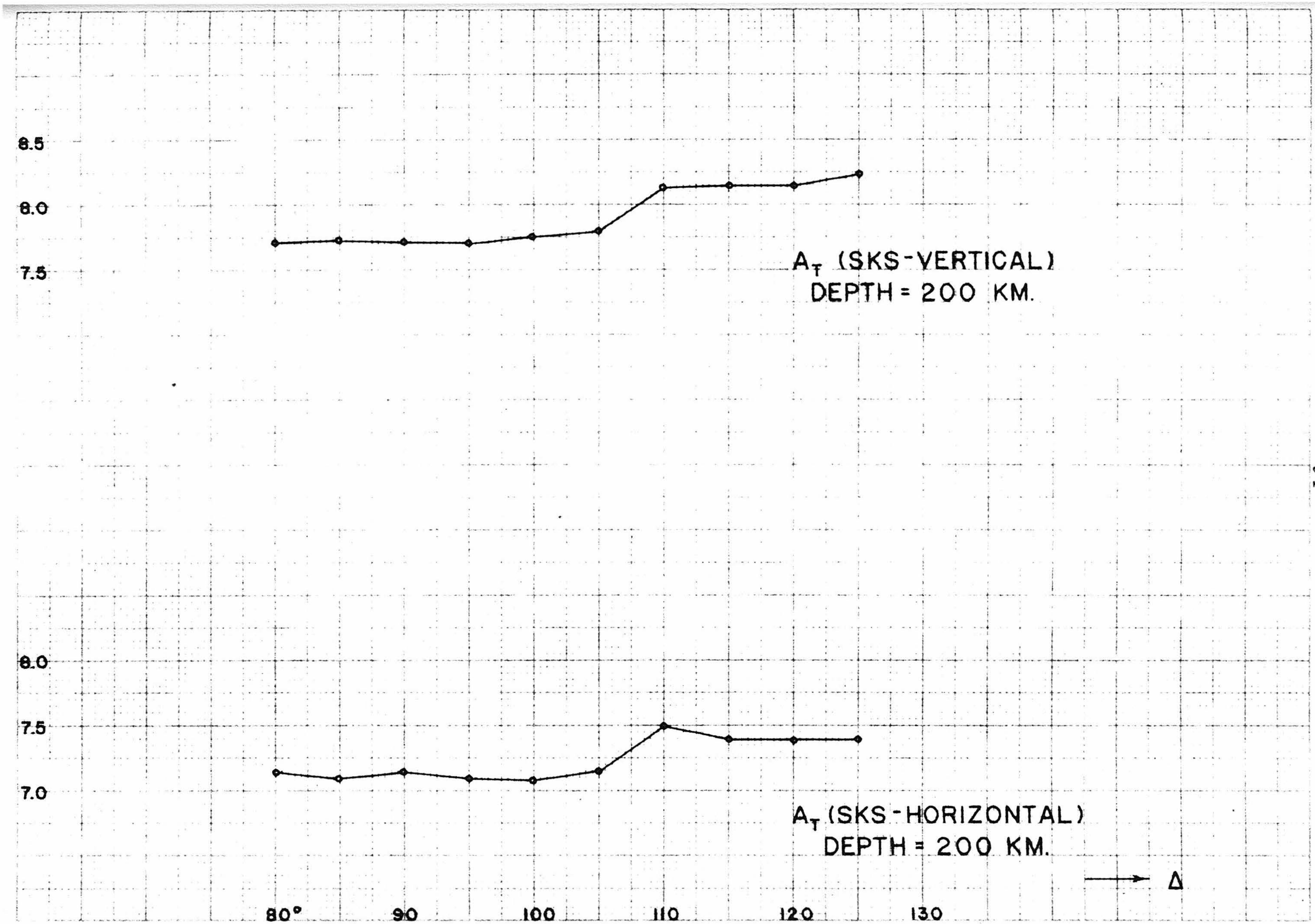
8.5
8.0
7.5
A_T (SKS-VERTICAL)
DEPTH = 200 KM.
8.0
7.5
7.0
A_T (SKS-HORIZONTAL)
DEPTH = 200 KM.
Δ
80°
90
100
110
120
130

FIGURE 16

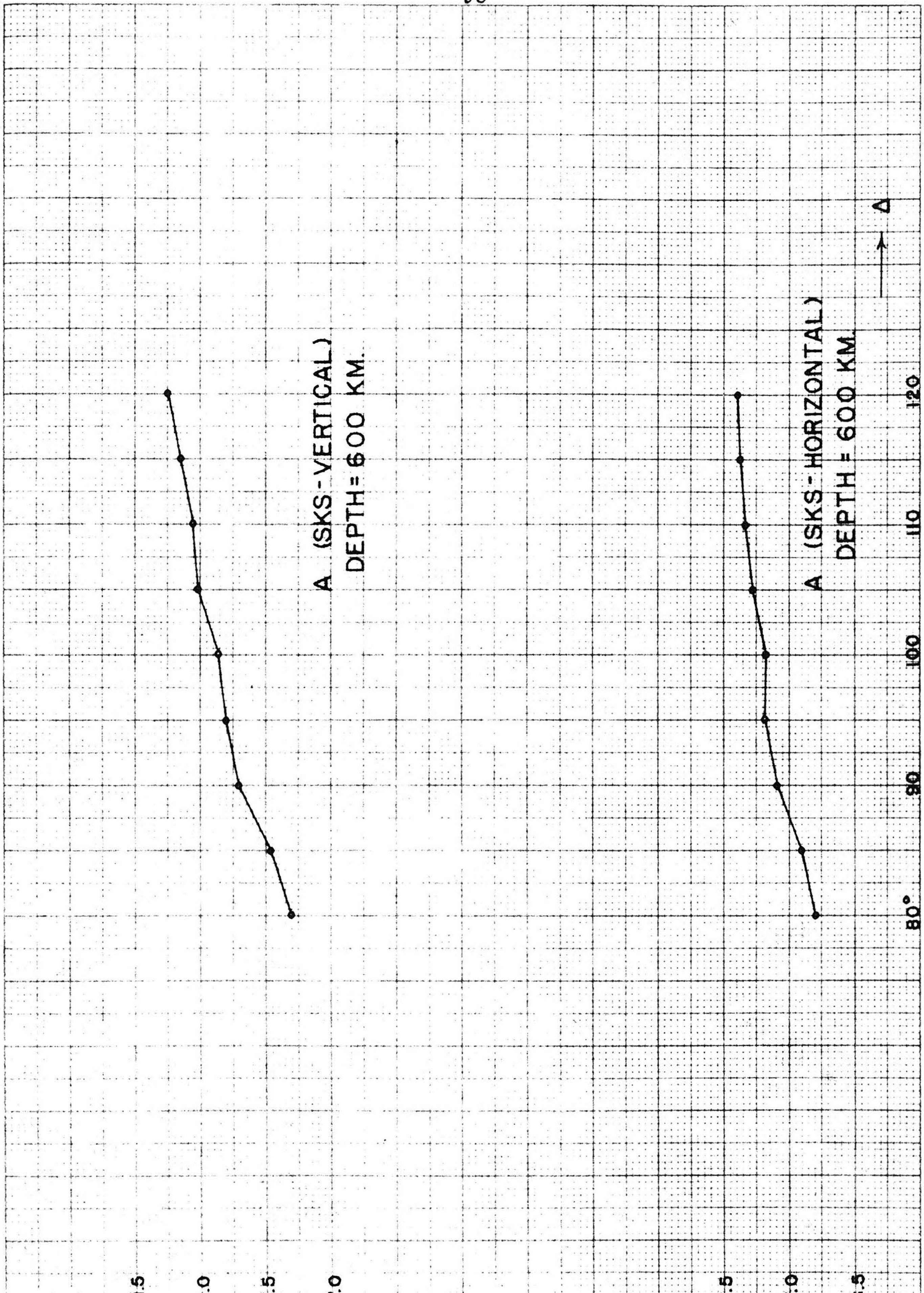
A (SKS-VERTICAL)
DEPTH = 600 KM.
A (SKS-HORIZONTAL)
DEPTH = 600 KM.
8.5
8.0
7.5
7.0
7.5
7.0
6.5
80°
90
100
110
120
Δ

FIGURE 17

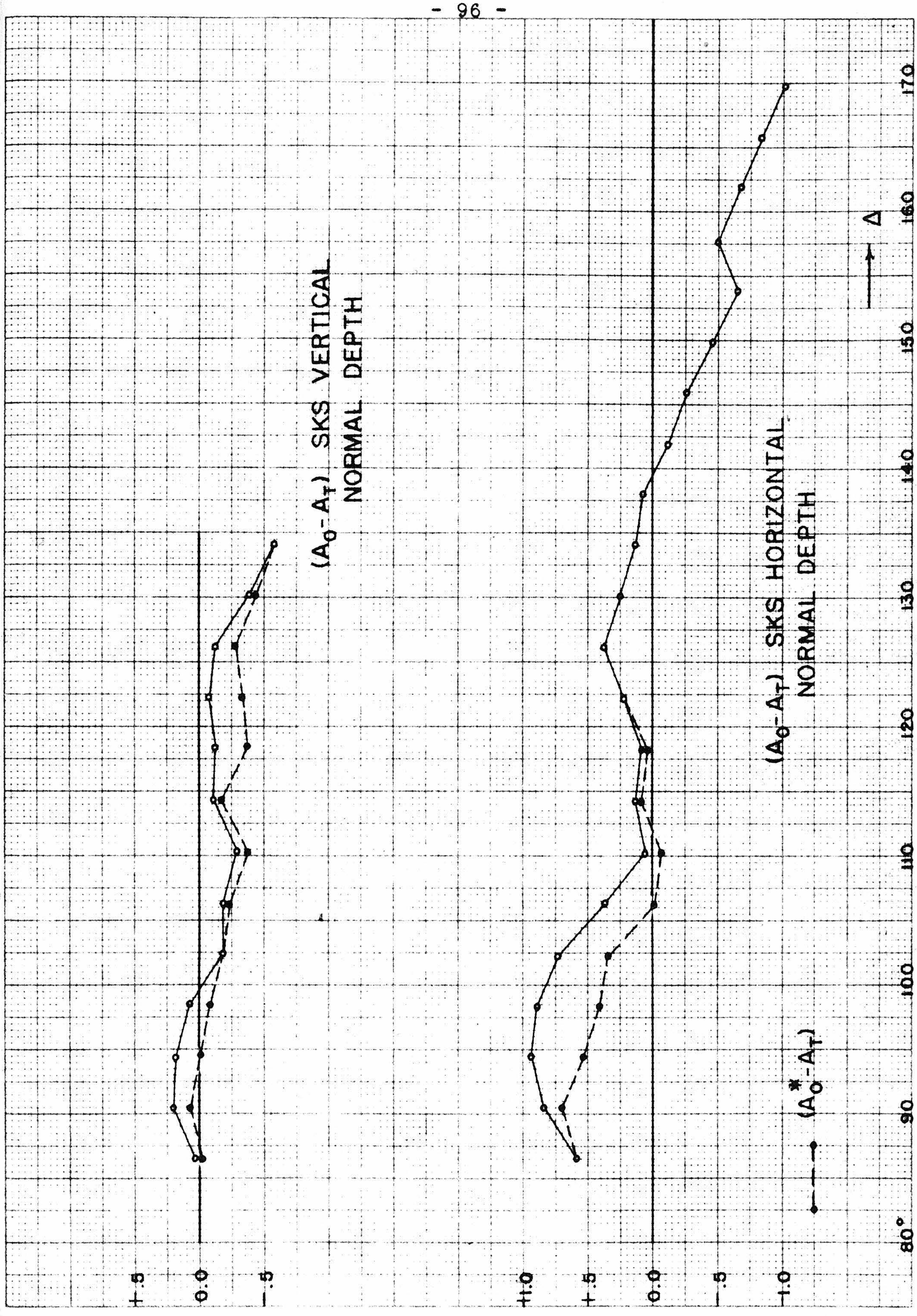
(A0-AT) SKS VERTICAL
NORMAL DEPTH
(A0-AT) SKS HORIZONTAL
NORMAL DEPTH
(A0*-AT)
Δ
80°
90
100
110
120
130
140
150
160
170
+.5
0.0
-.5
+1.0
+.5
0.0
-.5
-1.0

FIGURE 18

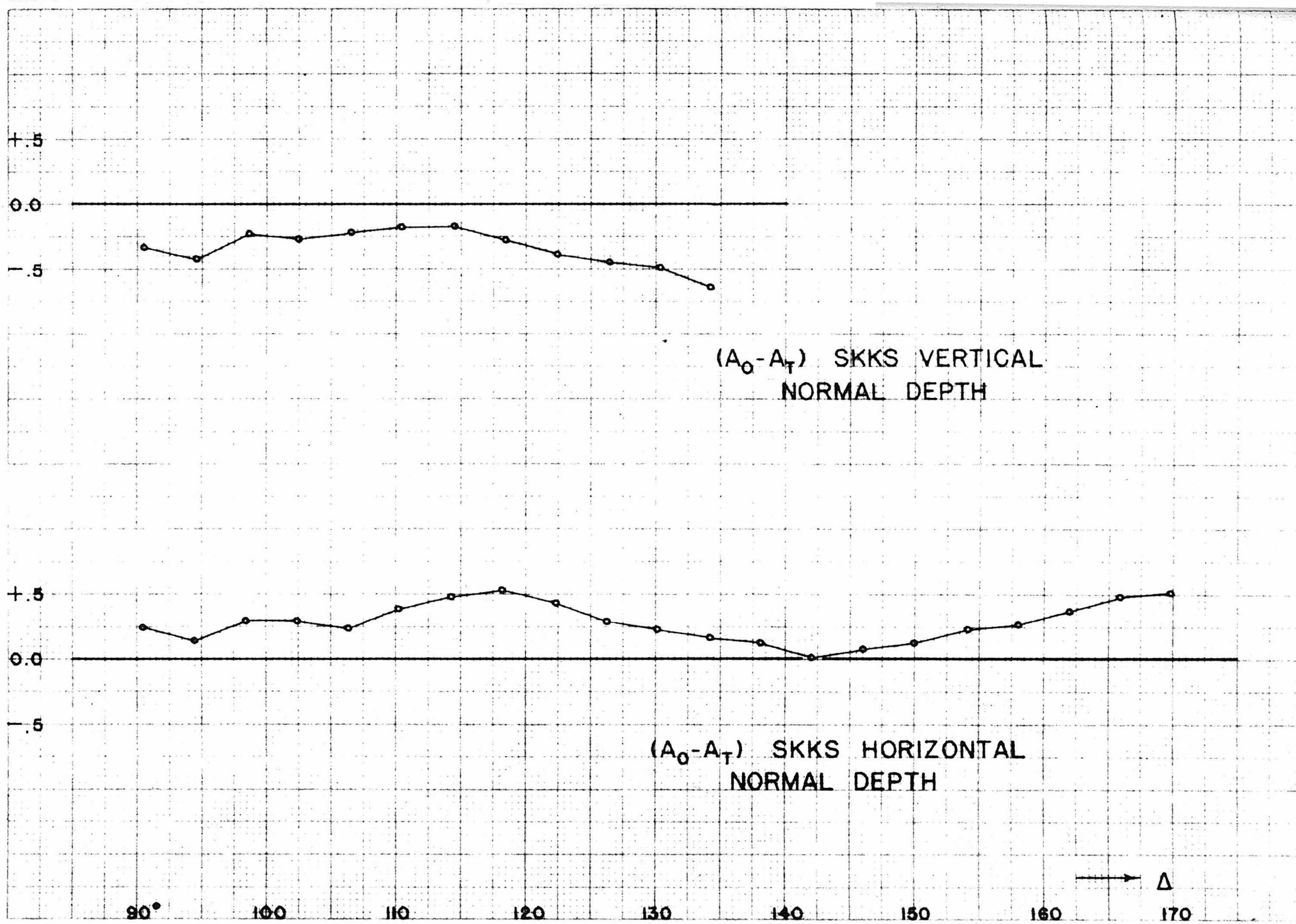
+.5
0.0
-.5
$(A_0 - A_T)$ SKKS VERTICAL
NORMAL DEPTH
+.5
0.0
-.5
$(A_0 - A_T)$ SKKS HORIZONTAL
NORMAL DEPTH
→ Δ
90°
100
110
120
130
140
150
160
170

FIGURE 19

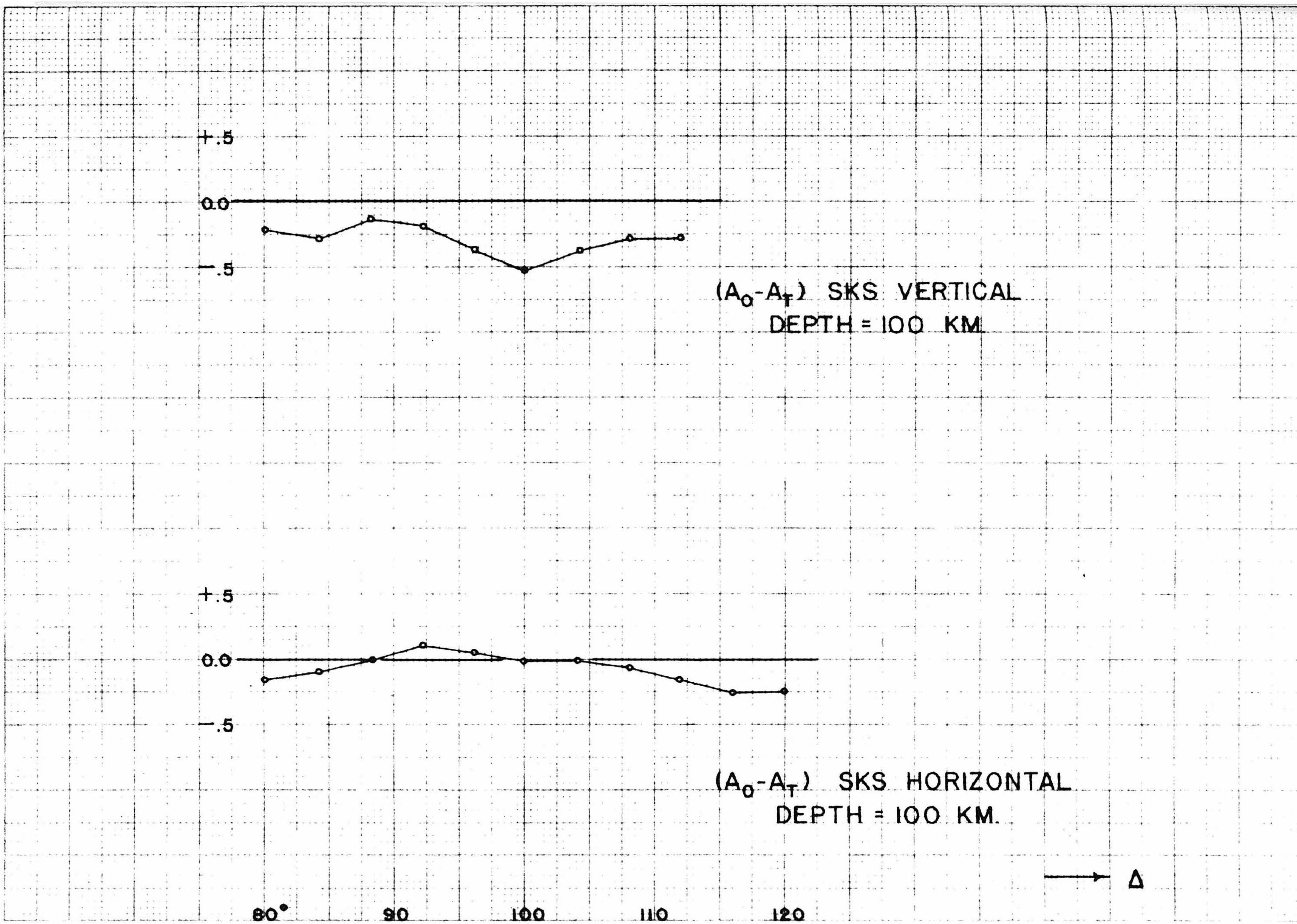
+.5
0.0
-.5
$(A_0 - A_T)$ SKS VERTICAL
DEPTH = 100 KM
+.5
0.0
-.5
$(A_0 - A_T)$ SKS HORIZONTAL
DEPTH = 100 KM.
Δ
80°
90
100
110
120

FIGURE 20

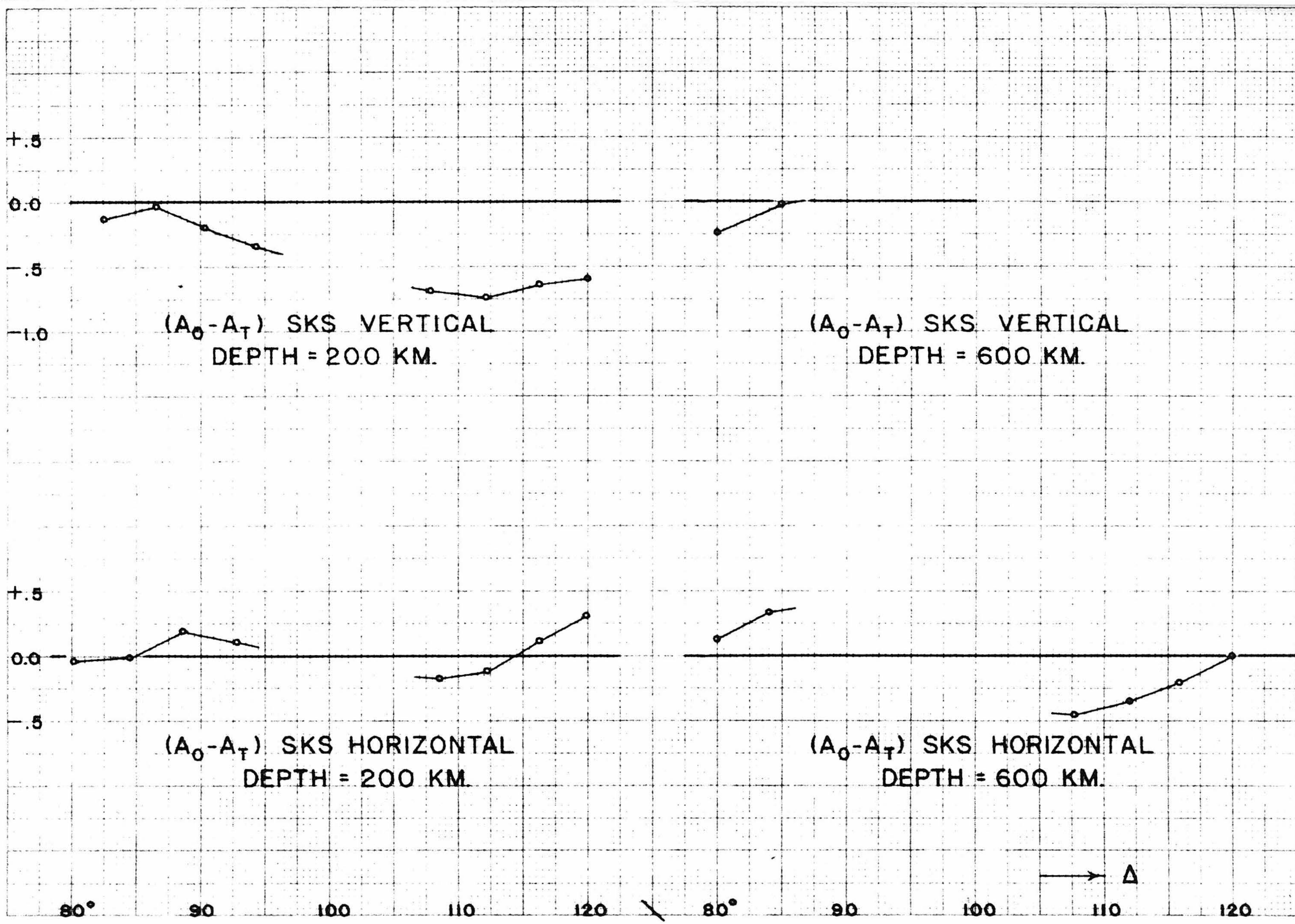
+.5
0.0
-.5
-1.0
$(A_O - A_T)$ SKS VERTICAL
DEPTH = 200 KM.
$(A_O - A_T)$ SKS VERTICAL
DEPTH = 600 KM.
+.5
0.0
-.5
$(A_O - A_T)$ SKS HORIZONTAL
DEPTH = 200 KM.
$(A_O - A_T)$ SKS HORIZONTAL
DEPTH = 600 KM.
Δ
80°
90
100
110
120
80°
90
100
110
120

FIGURE 21

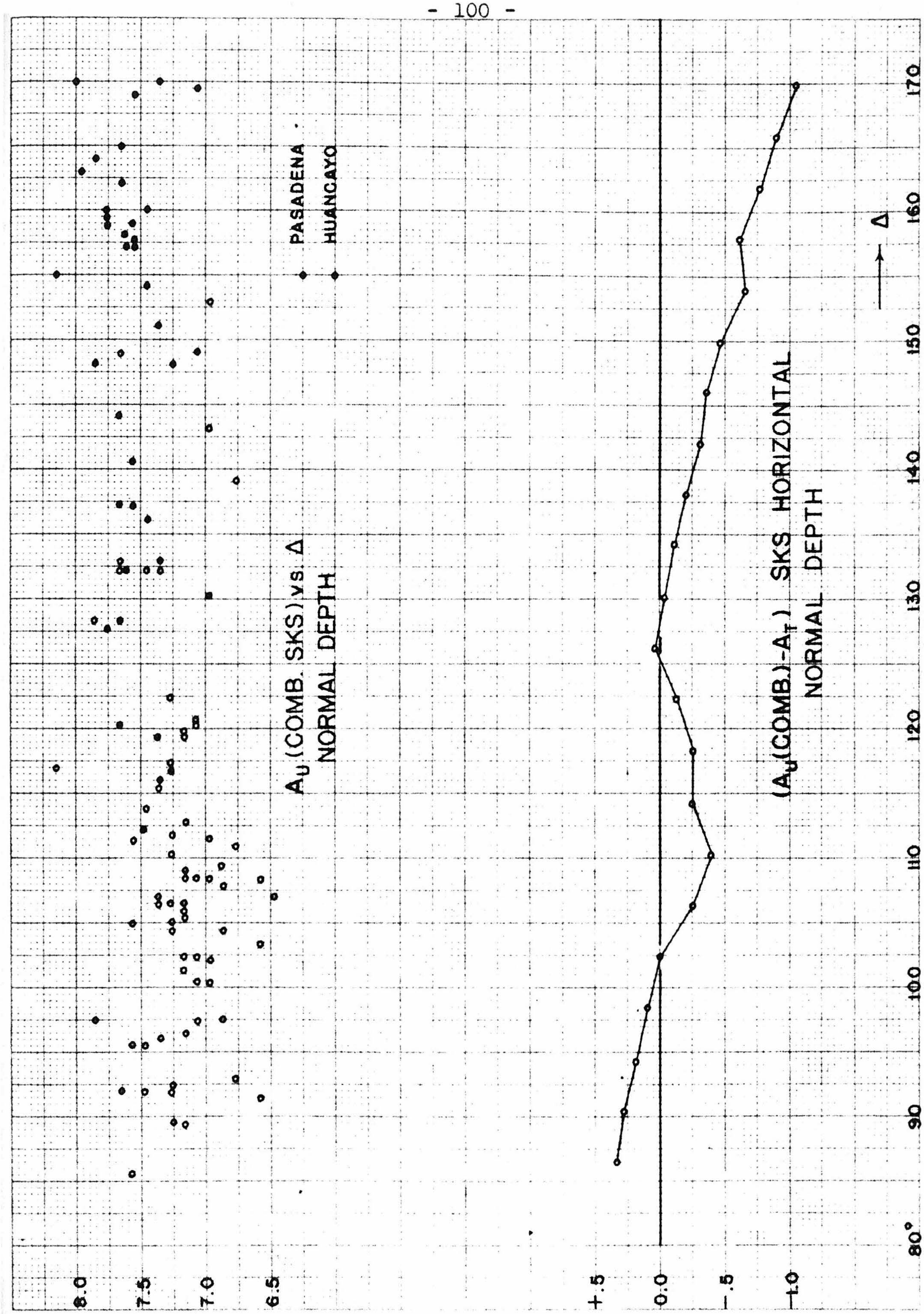

A_U(COMB. SKS) vs. Δ
NORMAL DEPTH
PASADENA
HUANCAYO
(A_U(COMB.)-A_T) SKS HORIZONTAL
NORMAL DEPTH
Δ
80°
90
100
110
120
130
140
150
160
170
8.0
7.5
7.0
6.5
+.5
0.0
-.5
-1.0

FIGURE 22

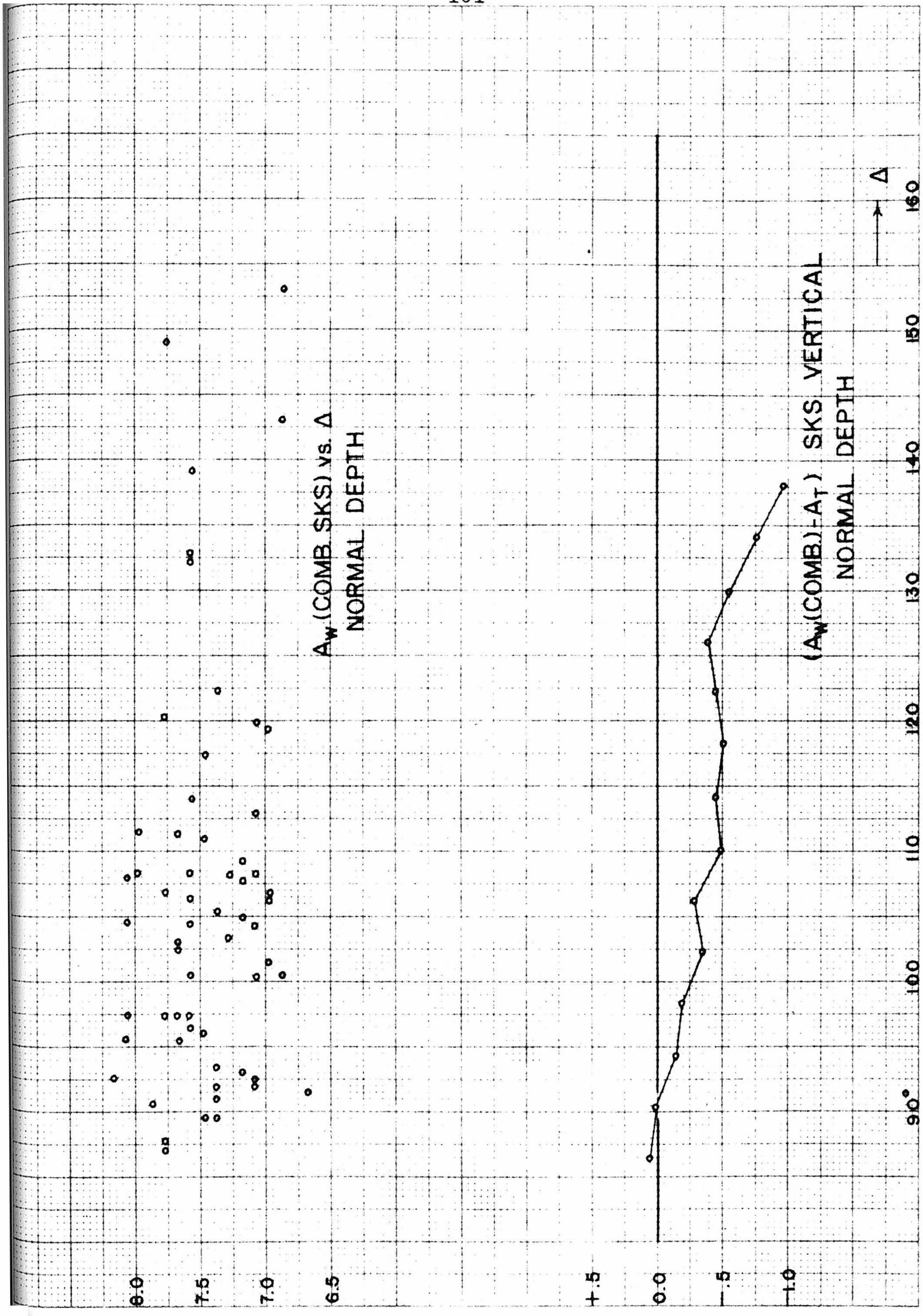
A_W (COMB SKS) vs. Δ
NORMAL DEPTH
(A_W(COMB)-A_T) SKS VERTICAL
NORMAL DEPTH
8.0
7.5
7.0
6.5
+.5
0.0
-.5
-1.0
90°
100
110
120
130
140
150
160
Δ

FIGURE 23

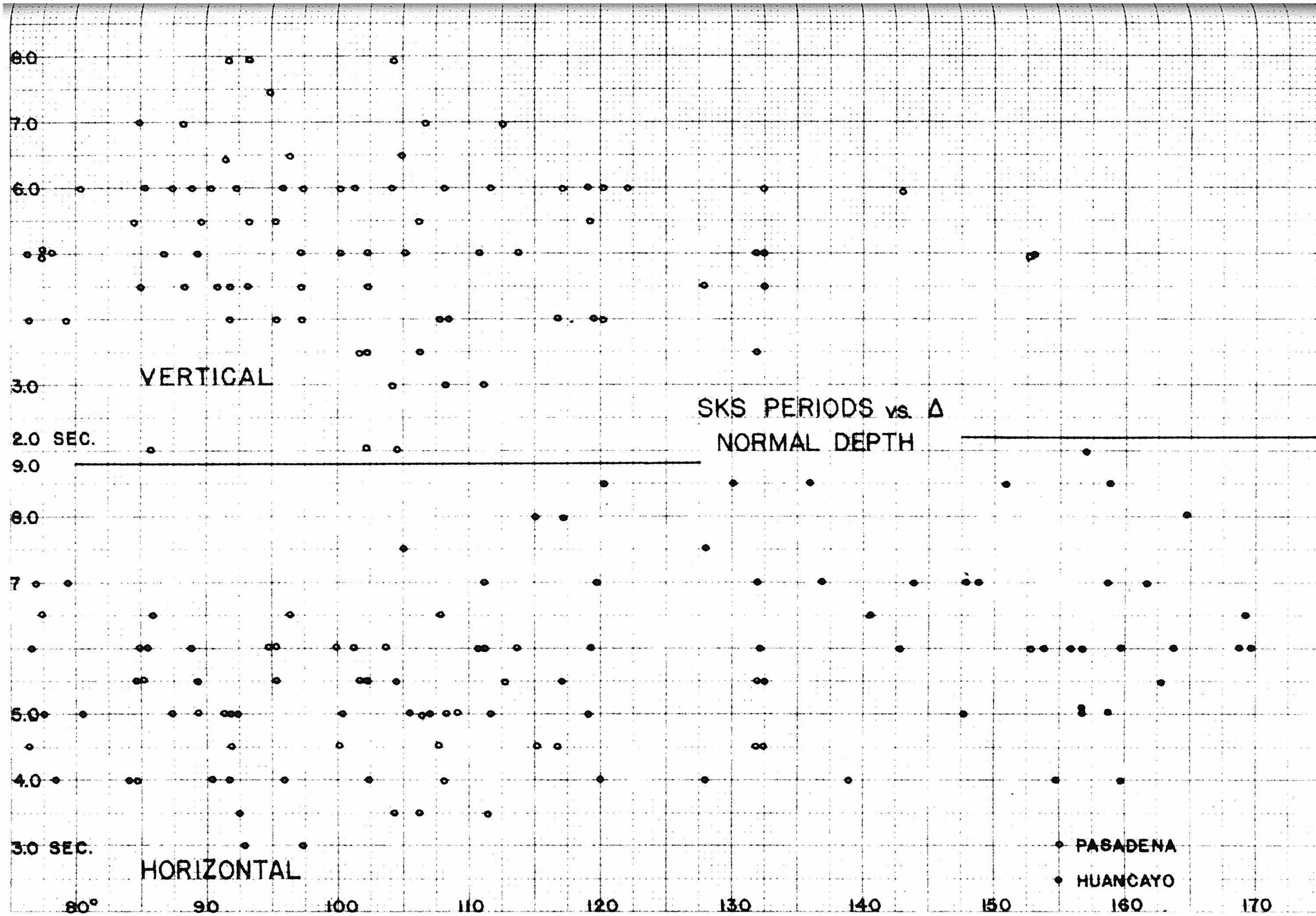
SKS PERIODS vs. Δ
NORMAL DEPTH
VERTICAL
HORIZONTAL
8.0
7.0
6.0
3.0
2.0 SEC.
9.0
8.0
7
5.0
4.0
3.0 SEC.
80°
90
100
110
120
130
140
150
160
170
PASADENA
HUANCAYO

FIGURE 24

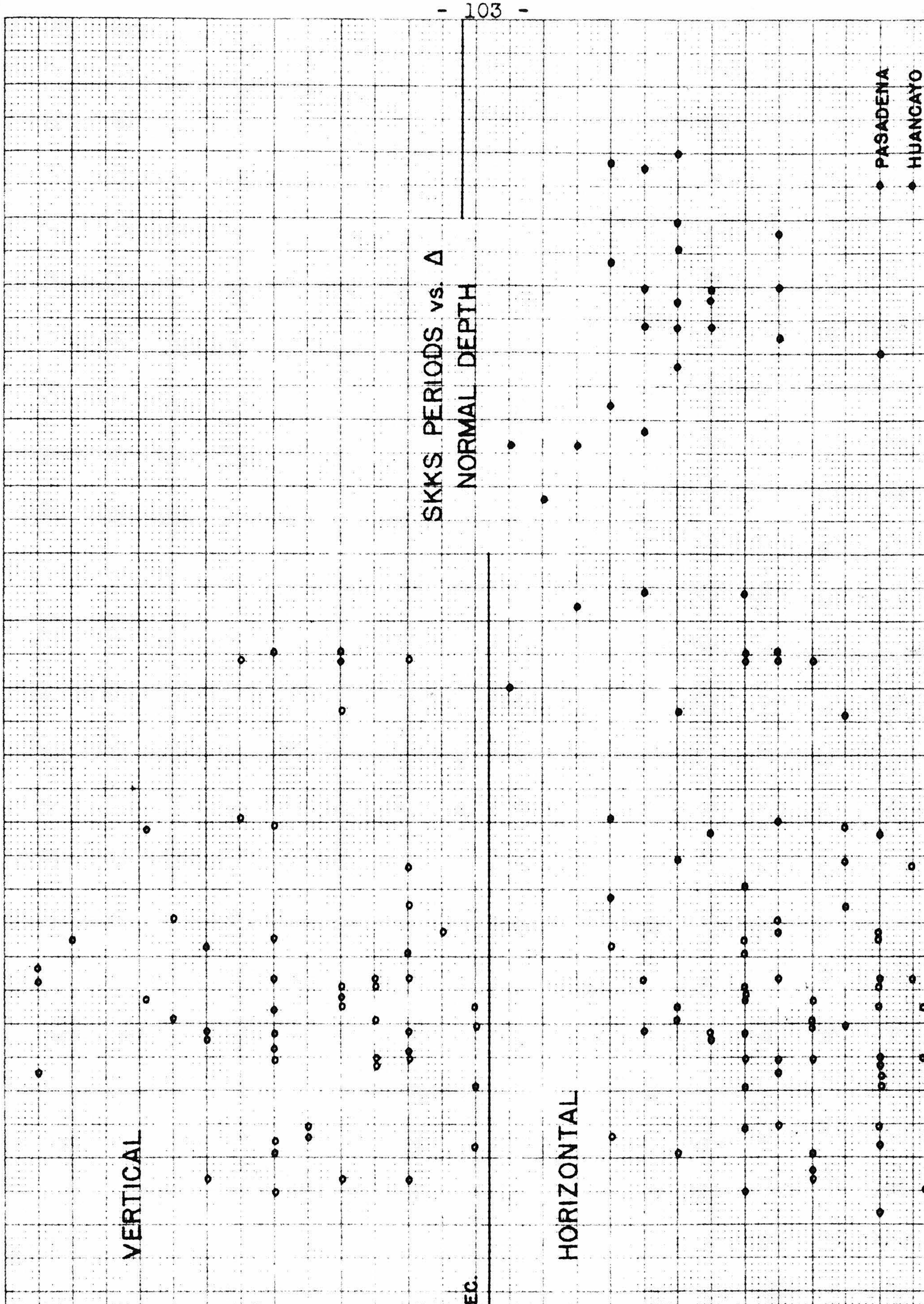
SKKS PERIODS vs. Δ
NORMAL DEPTH
VERTICAL
HORIZONTAL
PASADENA
HUANCAYO
3.0 SEC.
4.0
5.0
6.0
7.0
8.0
9.0
90°
100
110
120
130
140
150
160
170

FIGURE 25

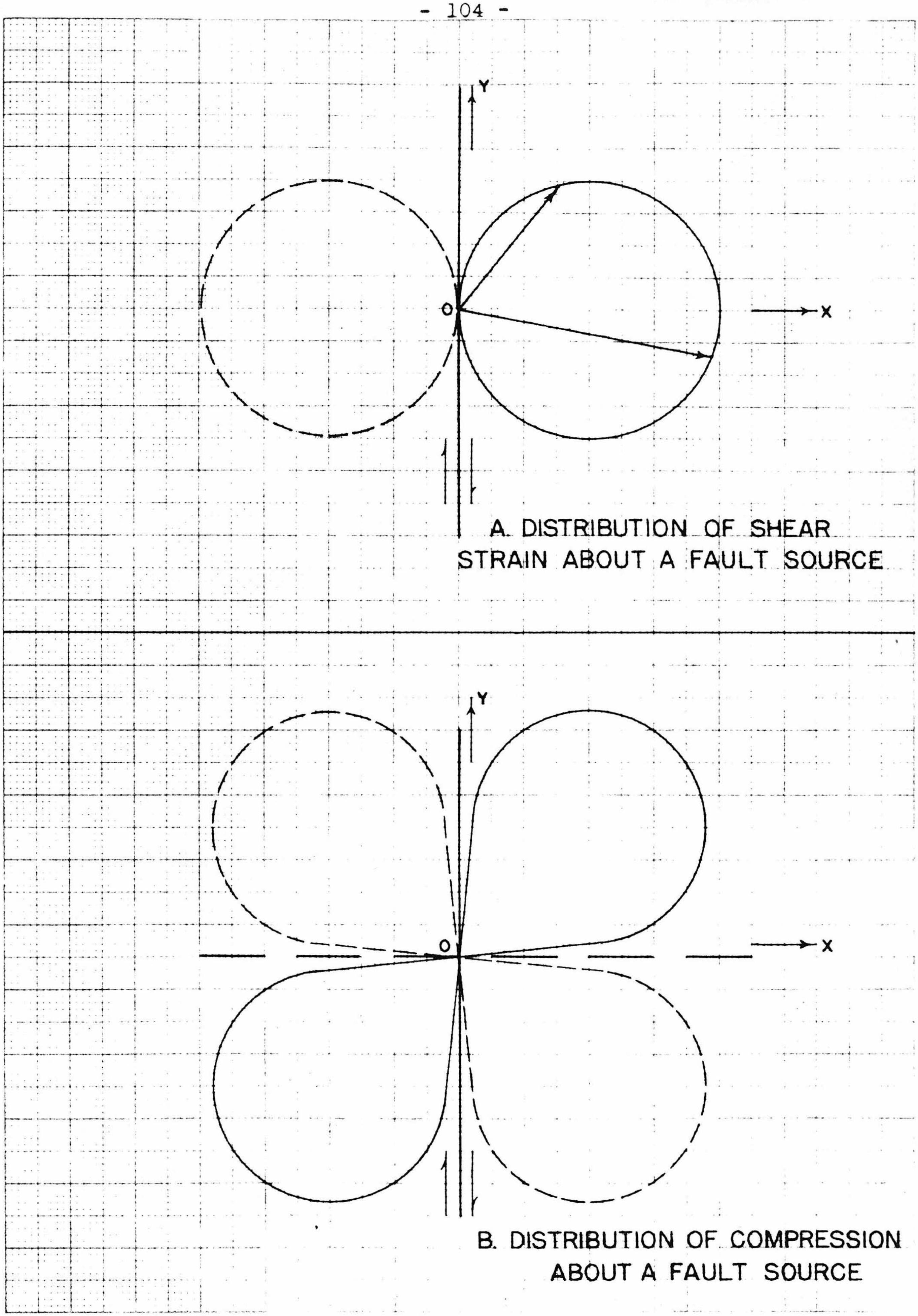

A. DISTRIBUTION OF SHEAR STRAIN ABOUT A FAULT SOURCE

B. DISTRIBUTION OF COMPRESSION ABOUT A FAULT SOURCE

FIGURE 26

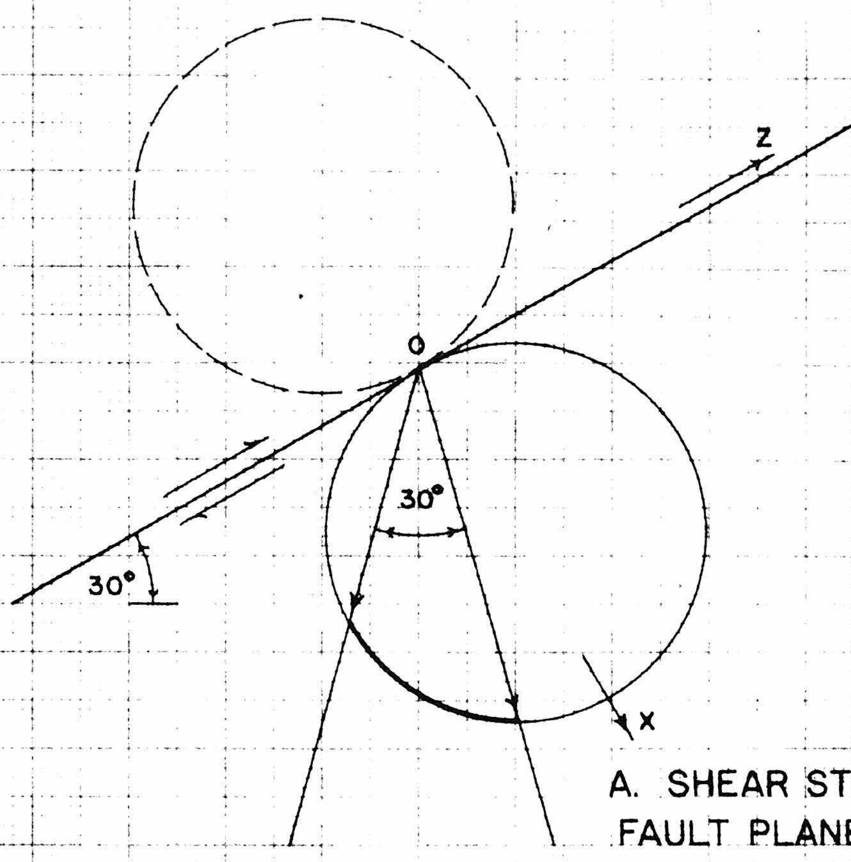

A. SHEAR STRAIN ABOUT FAULT PLANE WITH 30° DIP (DIP-SLIP MOTION)

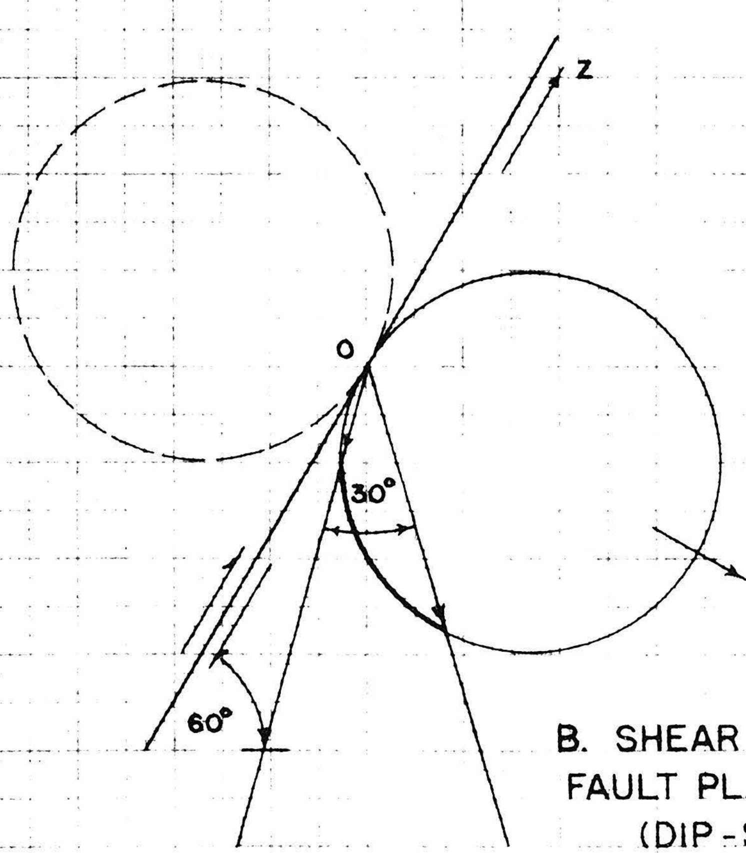

B. SHEAR STRAIN ABOUT FAULT PLANE WITH 60° DIP (DIP-SLIP MOTION)

FIGURE 27

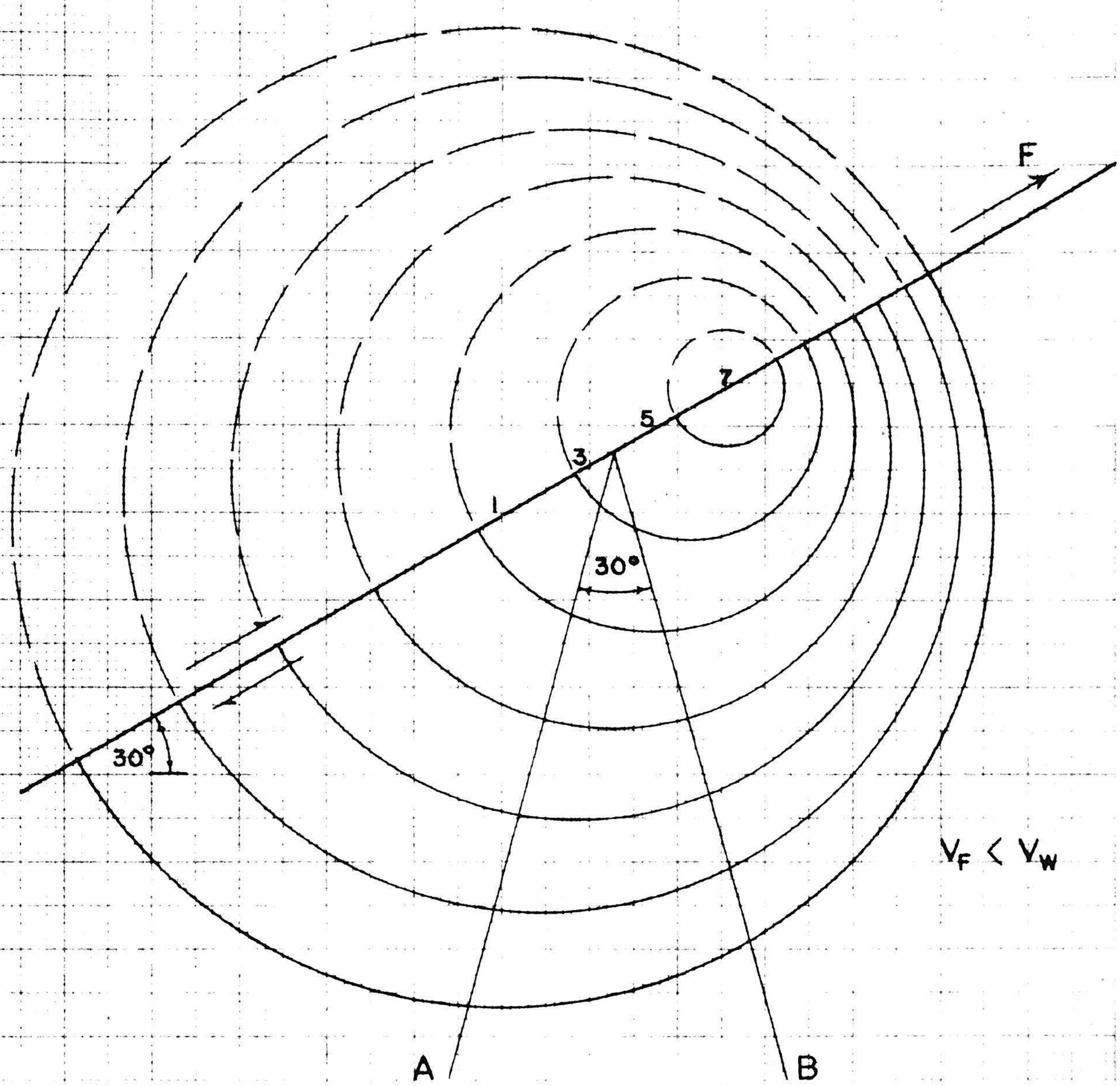

FIGURE 28

WAVE FRONTS GENERATED BY
PROGRESSIVE RUPTURE ALONG A
GENTLY DIPPING FAULT PLANE

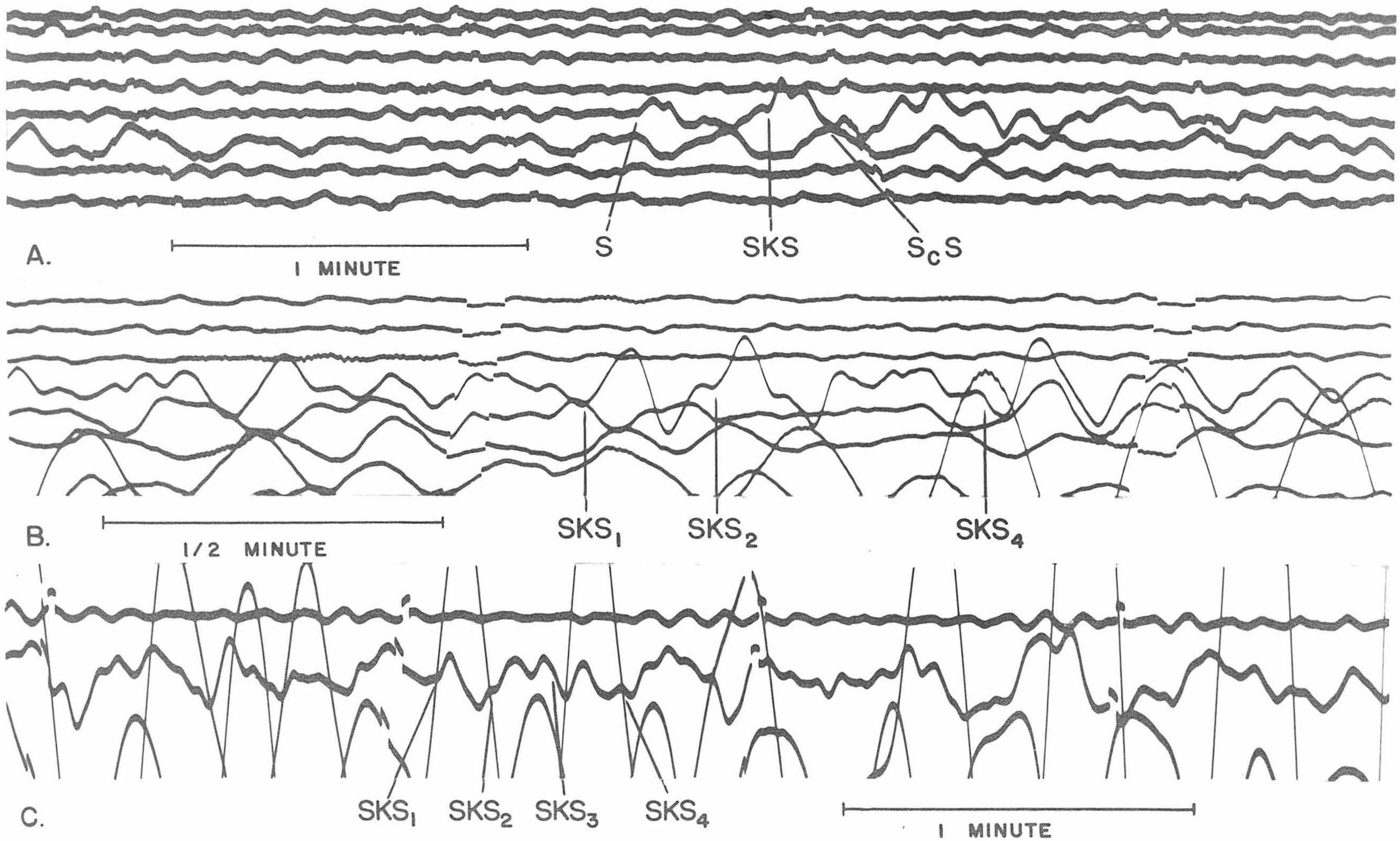

A. Earthquake of Nov. 15, 1942; $\Delta = 78^o$; Normal depth: Showing SKS following S.
B. Earthquake of Aug. 28, 1933; $\Delta = 120^o$; Normal depth: Showing SKS multiplicity.
C. Earthquake of Feb. 1, 1944; $\Delta = 100^o$; Normal depth: Showing SKS multiplicity.

PLATE I

REFERENCES

Benioff, H. (1949) "Seismic Evidence for the Fault Origin of Oceanic Deeps," Geol. Soc. Am., Bull., 60:1837-1856.

Byerly, P. (1926) "The Montana Earthquake of June 28, 1925, G.M.C.T., "Bull. Seism. Soc. Am., 16:209-265.

______ (1938) "The Earthquake of July 6, 1934: Amplitudes and First Motion," Bull. Seism. Soc. Am., 28:1-13.

______ (1942) "Seismology," Prentice-Hall Inc., New York.

Dana, S. W. (1944) "The Partition of Energy among Seismic Waves Reflected and Refracted at the Earth's Core," Bull. Seism. Soc. Am., 34:189-197.

Denson, M. E., Jr. (in press) "Longitudinal Waves Through the Earth's Core," Bull. Seism. Soc. Am., in press.

Ergin, K. (in press a) "Amplitudes of PcP, PcS, ScS, and ScP in Deep-Focus Earthquakes," Bull. Seism. Soc. Am., in press.

______ (in press b) "Observations on the Recorded Ground Motion due to P, PcP, S, and ScS," Bull. Seism. Soc. Am., in press.

Gutenberg, B. (1944) "Energy Ratio of Reflected and Refracted Seismic Waves," Bull. Seism. Soc. Am., 34:85-102.

______ (1945 a) "Amplitudes of P, PP, and S and Magnitude of Shallow Earthquakes," Bull. Seism. Soc. Am., 35: 57-69.

______ (1945 b) "Magnitude Determination for Deep-Focus Earthquakes," Bull. Seism. Soc. Am., 35:117-129.

______ (1949) "Unexplained Phases in Seismograms," Bull. Seism. Soc. Am., 39:79-92.

______ (1951) "PKKP, P'P', and the Earth's Core," Trans. Am. Geophys. Union, 32:373-390.

Gutenberg, B. and C. F. Richter (1934) "On Seismic Waves" (first paper), Gerlands Beitr. z. Geophysik, 43: 56-133.

______(1936) "On Seismic Waves" (third paper), Gerlands Beitr. z. Geophysik, 47:73-131.

______ (1939) "On Seismic Waves" (fourth paper), Gerlands Beitr. z. Geophysik, 54:94-136.

______ (1949) "Seismicity of the Earth and Associated Phenomena," Princeton University Press, Princeton, New Jersey.

Jeffreys, H. (1926) "The Viscosity of the Earth," Mon. Not. Roy. Astronom. Soc., Geophys. Sup., 1:412-424.

______ (1931) "Damping in Bodily Seismic Waves," Mon. Not. Roy. Astronom. Soc., Geophys. Sup., 2:318-323.

Jeffreys, H. (1939) "The Times of the Core Waves" (second paper), Mon. Not. Roy. Acad. Sci., Geophys. Sup., 4:594-615.

Macelwane, J. B. (1923) "A study of the Relation between the Periods of Elastic Waves and the Distance Travelled by them, Based upon the Seismograph Records of the California Earthquake, January 31, 1922," Bull. Seism. Soc. Am., 13:13-16.

Martner, S. T. (1950) "Observations on Seismic Waves Reflected at the Core Boundary of the Earth," Bull. Seism. Soc. Am., 40:95-109.

Mooney, H. M. (1951) "A Study of the Energy Content of the Seismic Waves P and pP," Bull. Seism. Soc. Am., 41:13-29.

Munk, W. H. (1947) "Increase in Period of Waves Travelling over Large Distances; with Application to Tsunamis, Swell, and Seismic Surface Waves," Trans. Am Geophys. Union, 28:198-217.

______ (1949) "Note on Period Increase of Waves," Bull. Seism. Soc. Am., 39:41-45.

Nakano, H. (1923) "Notes on the Nature of Forces Which Give Rise to Earthquake Motions," Seism. Bull. Centr. Meteorol. Observ. of Jap., 1:92-120.

Richter, C. F. (1935) "An Instrumental Earthquake Magnitude Scale," Bull. Seism. Soc. Am., 25:1-32.

Richter, C. F. (1943) "Mathematical Questions in Seismology," Bull. Am. Math. Soc., 49:477-493.

Sezawa K. and K. Kanai (1938,1939) "Damping of Periodic Visco-Elastic Waves with Increasing Focal Distance I, II," Bull. Earthquake Res. Instit., Tokyo Imp. Univ., 16:491-502 and 17:9-26.

Sommer, H. (1931) "On the Question of Dispersion in the First Preliminary Seismic Waves," Bull. Seism. Soc. Am., 21:87-158.

Stoneley, R. (1949) "The Seismological Implications of Aeolotropy in Continental Structures," Mon. Not. Roy. Acad. Sci., Geophys. Sup., 5:343-353.

Wadati, K., and K. Masuda (1934) "On the Travel Time of Earthquake Waves, pt. 6," Geophys. Mag., Tokyo, 8:187-194.

Wenner, F. (1929) "A New Seismometer Equipped for Electromagnetic Damping and Electromagnetic and Optical Magnification (Theory, General Design, and Preliminary Results)," Bur. Standards Jour. Res., 2:963-999.

Wilson, J. T. (1948) "Increase in Period of Earthquake Surface Waves with Distance Travelled," Bull. Seism. Soc. Am., 38:89-93.

Zoeppritz, K., L. Geiger, and B. Gutenberg (1912) "Über Erdbebenwellen. V," Nachr, K. Ges. d. Wiss. z. Göttingen, math.-phys. Kl., pp. 121-206.

NORMAL SHOCKS - PASADENA

No.	Date	Time	Location	Δ	Mag.
1	Nov. 2,1942	23:59:36	19S-173W	75	6.9
2	Oct. 10,1939	18 31 59	$38\frac{1}{2}$N-143E	76	7.4
3	June 18,1933	21 37 29	$38\frac{1}{2}$N-143E	76	7.3
4	Sept. 8,1948	15 09 11	21S-174W	76.5	7.8
5	Dec. 26,1949	06 23 52	$15\frac{1}{2}$S-180W	77	6.9
6	Nov. 2,1936	20 45 56	$38\frac{1}{4}$N-$142\frac{1}{4}$E	77	7.3
7	Nov. 15,1942	17 12 00	37N-$141\frac{1}{2}$E	78	7.0
8	Nov. 28,1942	10 38 45	$7\frac{1}{2}$N-36W	79	7.1
9	Dec. 19,1942	23 10 40	$31\frac{1}{2}$N-$142\frac{1}{2}$E	80	7.0
10	June 15,1948	11 44 33	$33\frac{3}{4}$N-$135\frac{1}{2}$E	83.5	6.9
11	Feb. 24,1934	06 23 40	$22\frac{1}{2}$N-144E	84	7.3
12	Aug. 13,1931	22 09 15	$29\frac{1}{2}$S-$175\frac{1}{2}$W	84.5	6.9
13	May 17,1941	02 24 50	10S-$166\frac{1}{4}$E	84.5	7.4
14	Aug. 2,1941	11 41 26	$28\frac{1}{2}$S-178W	84.5	7.1
15	May 17,1939	18 30 34	$22\frac{3}{4}$N-$143\frac{1}{2}$E	84.5	6.9
16	July 18,1934	19 40 15	$11\frac{3}{4}$S-$166\frac{1}{2}$E	85	8.2
17	July 21,1934	06 18 18	11S-$165\frac{3}{4}$E	85	7.3
18	Nov. 16,1944	12 10 58	$12\frac{1}{2}$S-167E	85	7.3
19	Aug. 7,1934	03 40 0	12S-166E	85.5	6.9
20	Dec. 20,1946	19 19 05	$32\frac{1}{2}$N-$134\frac{1}{2}$E	85.5	8.2
21	Mar. 11,1931	12 26 44	$23\frac{1}{4}$N-146E	86	6.9
22	Nov. 13,1943	18 43 57	19S-170E	86.5	7.2
23	Nov. 18,1941	16 46 22	32N-132E	87	7.8

Normal Shocks - Pasadena (cont.)

24	Nov. 2,1931	10:02:59	32N-131$\frac{1}{2}$E	87.5	7.6
25	Mar. 13,1934	13 12 02	10$\frac{3}{4}$S-162$\frac{1}{4}$E	88	6.9
26	Mar. 24,1934	12 04 36	10S-161$\frac{1}{2}$E	88	7.0
27	Oct. 10,1931	00 19 53	10S-161E	88	7.7
28	Oct. 3,1931	19 13 13	10$\frac{1}{2}$S-161$\frac{3}{4}$E	88.5	7.9
29	Mar. 14,1943	17 11 00	22S-169$\frac{1}{2}$E	89	7.1
30	Mar. 15,1943	02 24 29	22S-169$\frac{1}{2}$E	89	6.9
31	Jan. 20,1940	09 58 00	55S-133W	90	6.7
32	Feb. 3,1939	05 26 20	10$\frac{1}{2}$S-159E	90	7.1
33	Apr. 24,1931	17 22 15	6$\frac{1}{2}$S-156E	90.5	6.9
34	Jan. 30,1939	02 18 27	6$\frac{1}{2}$S-155$\frac{1}{2}$E	90.5	7.8
35	May 25,1944	12 58 05	2$\frac{1}{2}$S-152$\frac{3}{4}$E	91	7.5
36	Jan. 29,1932	13 41 10	6S-155E	91.5	7.0
37	Sept.29,1946	03 01 55	4$\frac{1}{2}$S-153$\frac{1}{2}$E	91.5	7.75
38	Sept. 3,1944	19 11 29	57S-122W	91.5	7.0
39	May 3, 1946	22 23 40	5S-153E	92	7.4
40	June 16,1938	02 15 15	27$\frac{1}{2}$N-129$\frac{1}{2}$E	92	7.4
41	Jan. 13,1941	16 27 38	4$\frac{1}{2}$S-152$\frac{1}{2}$E	92.5	7.0
42	Mar. 25,1947	20 32 14	38$\frac{1}{2}$S-178$\frac{1}{2}$E	93	7.0
43	Nov. 22,1933	12 42 19	5$\frac{3}{4}$S-151$\frac{1}{2}$E	93	6.9
44	Feb. 3, 1934	14 33 10	6S-151E	93	6.9
45	Feb. 2, 1931	22 46 42	39$\frac{1}{2}$S-177E	94.5	7.75
46	Feb. 13,1931	01 27 16	39$\frac{1}{2}$S-177E	95	7.1
47	Dec. 8, 1945	01 04 02	6$\frac{1}{2}$S-151E	95	7.1

Normal Shocks - Pasadena (cont.)

48	Mar. 21,1943	20:35:43	$5\frac{3}{4}$S-$152\frac{1}{4}$E	95	7.3
49	Dec. 28,1945	17 48 45	6S-150E	95.5	7.8
50	Mar. 5,1934	11 46 15	$40\frac{1}{2}$S-$175\frac{1}{2}$E	96	7.5
51	June 10,1938	09 53 39	$25\frac{1}{2}$N-125E	96	7.7
52	Dec. 17,1949	06 53 30	54S-71W	97	7.75
53	Dec. 17,1949	15 07 55	54S-71W	97	7.75
54	May 6,1947	20 30 32	$6\frac{1}{2}$S-$148\frac{1}{2}$E	97	7.6
55	May 12,1938	05 38 57	6S-$147\frac{3}{4}$E	97	7.5
56	Mar. 9,1944	22 12 58	44N-84E	100	7.2
57	Sept. 7,1938	04 03 18	$23\frac{3}{4}$N-$121\frac{1}{2}$E	100	7.0
58	Feb. 1,1944	03 22 36	$41\frac{1}{2}$N-$32\frac{1}{2}$E	100	7.4
59	Nov. 26,1943	22 20 36	41N-34E	101	7.6
60	Sept.20,1935	01 46 33	$3\frac{1}{2}$S-$141\frac{3}{4}$E	101.5	7.9
61	Aug. 7,1931	02 11 30	4S-142E	102	7.1
62	Apr. 19,1935	15 23 22	$31\frac{1}{2}$N-$15\frac{1}{4}$E	102	7.1
63	Feb. 23,1949	16 08 08	41N-$83\frac{1}{2}$E	102	7.3
64	Apr. 11,1946	01 52 20	1S-$14\frac{1}{2}$W	102	7.2
65	Dec. 20,1942	14 03 08	$40\frac{1}{2}$N-$36\frac{1}{2}$E	102	7.3
66	Apr. 2,1947	05 39 11	$1\frac{1}{2}$S-138E	103	7.4
67	May 28,1940	09 40 41	$2\frac{1}{2}$S-139E	103	6.9
68	Dec. 26,1939	23 57 21	$39\frac{1}{2}$N-$38\frac{1}{2}$E	103.5	8.0
69	Aug. 25,1933	07 50 25	$31\frac{3}{4}$N-$103\frac{1}{2}$E	104	7.4
70	Dec. 29,1949	03 03 54	18N-121E	104	7.2
71	Mar. 3,1948	09 09 54	$18\frac{1}{2}$N-119E	104	7.2

Normal Shocks - Pasadena (cont.)

72	May 3,1943	01:59:12	$12\frac{1}{2}$N-$125\frac{1}{2}$E	104	7.4
73	May 27,1947	05 58 54	$1\frac{1}{2}$S-$135\frac{1}{4}$E	104.5	7.25
74	Nov. 2,1946	18 28 25	$41\frac{1}{2}$N-$72\frac{1}{2}$E	104.5	7.6
75	Feb. 14,1934	03 59 34	$17\frac{1}{2}$N-119E	105	7.6
76	May 25,1943	23 07 36	$7\frac{1}{2}$N-128E	105	7.9
77	Sept. 1,1945	22 44 10	$46\frac{1}{2}$S-$165\frac{1}{2}$E	105.5	7.2
78	Apr. 15,1934	22 15 13	$7\frac{3}{4}$N-127E	106	7.3
79	Nov. 4,1946	21 47 47	$39\frac{3}{4}$N-$54\frac{1}{2}$E	106	7.5
80	Sept.12,1941	07 02 04	$\frac{1}{2}$S-$132\frac{1}{2}$E	106	7.0
81	Jan. 27,1942	13 29 08	$4\frac{1}{2}$S-135E	106.5	7.1
82	Apr. 3,1942	15 40 24	$13\frac{1}{2}$N-121E	106.5	7.7
83	Jan. 24,1938	10 31 44	61S-38W	106.5	7.1
84	May 25,1948	07 11 21	$29\frac{1}{2}$N-$100\frac{1}{2}$E	107.5	7.3
85	Nov. 15,1944	20 47 01	$4\frac{1}{2}$N-$127\frac{1}{2}$E	107.5	7.2
86	Mar. 18,1931	20 13 34	$5\frac{3}{4}$N-$126\frac{1}{4}$E	108	7.0
87	Mar. 27,1949	06 34 05	$3\frac{1}{2}$N-$127\frac{1}{2}$E	108	7.0
88	Jan. 24,1948	17 46 30	$10\frac{1}{2}$N-122E	108	8.2
89	Oct. 5,1948	20 12 05	$37\frac{1}{2}$N-58E	108	7.3
90	Nov. 6,1943	08 31 37	6S-$134\frac{1}{2}$E	108	7.6
91	Oct. 20,1942	23 21 44	$8\frac{1}{2}$N-$122\frac{1}{2}$E	109	7.3
92	Oct. 10,1938	20 48 05	$2\frac{1}{4}$N-$126\frac{3}{4}$E	110	7.3
93	July 29,1942	22 49 15	2S-$128\frac{1}{2}$E	110.5	7.0
94	July 29,1947	13 43 22	$28\frac{1}{2}$N-94E	111	7.5
95	Sept.12,1946	15 17 15	$23\frac{1}{2}$N-96E	111	7.5

Normal Shocks - Pasadena (cont.)

96	Feb. 1,1938	19:04:18	5¼S-130½E	111	8.2
97	May 14,1932	13 11 00	½N-126E	111.5	8.0
98	Sept. 6,1943	03 41 30	53S-159E	112.5	7.8
99	Oct. 23,1943	17 23 16	26N-93E	113.5	7.2
100	Aug. 16,1938	04 27 50	23½N-94¼E	115	7.2
101	May 30,1935	21 32 46	29½N-66¾E	116.5	7.5
102	May 19,1938	17 08 21	1S-120E	117	7.6
103	June 13,1934	22 10 23	27¾N-62½E	119	6.9
104	Nov. 2,1943	18 08 22	57S-26W	119	7.2
105	Mar. 9,1943	09 48 55	60S-27W	119.5	7.3
106	Aug. 28,1933	22 19 40	59½S-25W	120	7.5
107	Aug. 5,1947	14 24 17	26½N-63E	120	7.1
108	Nov. 27,1945	21 56 50	24½N-63E	122	8.25
109	Dec. 28,1935	02 35 22	0-98¼E	128	7.9
110	June 24,1933	21 54 46	5½S-104[illegible]E	132	7.5
111	May 8,1946	05 20 22	0-99½E	132	7.1
112	Apr. 1,1943	14 18 08	6½S-105½E	132	7.0
113	Feb. 10,1931	06 34 25	5¼S-102½E	132.5	7.1
114	Sept.25,1931	05 59 44	5S-102¾E	132.5	7.4
115	Mar. 21,1939	01 11 09	1½S-89½E	139	7.2
116	Feb. 29,1944	16 28 07	½N-76E	143	7.2
117	Aug. 1,1942	14 30 05	48S-99E	149	7.0
118	Nov. 10,1942	11 41 27	49½S-32E	153	7.9

NORMAL SHOCKS - HUANCAYO

No.	Date	- Time	Location	Δ	Mag.
201	Feb. 22,1935	17:06:12	52N-175E	111	6.9
202	Sept. 8,1939	12 04 45	51N-175E	112	
203	Apr. 16,1940	06 07 43	52N-173½E	112	7.1
204	Aug. 7,1934	03 40 07	12S-167E	114	
205	July 21,1934	06 18 18	11S-165¾E	115	7.3
206	Mar. 13,1934	13 11 50	12S-164E	117	6.75
207	Nov. 13,1936	12 31 27	55½N-163E	117	7.2
208	Mar. 24,1934	12 04 26	10S-161½E	119	7.1
209	June 30,1936	15 06 38	50½N-160E	120	7.4
210	May 20,1936	03 05 12	9S-160E	121	
211	Sept.23,1937	13 06 00	6S-154E	128	7.4
212	Dec. 12,1933	14 11 16	4S-153E	129.5	6.75
213	Feb. 21,1937	07 02 35	44½N-149½E	130	7.4
214	Feb. 3,1934	14 33 05	6S-152E	130	6.75
215	Jan. 13,1941	16 27 38	4½S-152½E	130	7.0
216	Feb. 28,1934	14 21 42	5S-150E	132	7.2
217	Sept.11,1935	14 04 02	43N-146½E	132	7.6
218	June 9,1934	12 58 43	4S-148E	134	
219	Aug. 1,1940	15 08 21	44½N-139E	136	7.7
220	Mar. 2,1933	17 31 00	39½N-143½E	136	
221	Nov. 2,1936	20 45 56	38¼N-142¼E	137	7.3
222	June 18,1933	21 37 29	38½N-143E	137	7.3
223	June 13,1934	22 10 23	29½N-63½E	138.5	

Normal Shocks - Huancayo (cont.)

224	Sept.23,1935	09:18:19	4S-143E	139	
225	Feb. 24,1934	06 23 40	22½N-144E	140.5	7.3
226	Oct. 18,1935	11 05 23	12½N-141½E	144	7.1
227	Jan. 27,1942	13 29 08	4½S-135E	146	7.1
228	Apr. 12,1936	20 51 00	8N-137½E	148	6.8
229	Feb. 15,1936	12 46 57	4½S-133E	148	7.3
230	Nov. 18,1941	16 46 22	32N-132E	148	7.8
231	Apr. 5,1937	06 56 41	1S-133E	149	6.9
232	Dec. 25,1932	02 04 24	39¼N-96½E	151	7.6
233	May 27,1936	06 19 19	28½N-83½E	154	7.0
234	Jan. 7,1937	13 20 35	35½N-98E	155	7.6
235	Oct. 5,1936	09 44 24	1½N-126¾E	156	7.1
236	Nov. 27,1934	06 14 16	2N-127E	156	6.75
237	Apr. 1,1936	02 09 15	4½N-126½E	157	7.7
238	Apr. 15,1934	22 15 13	7¾N-127E	157	7.3
239	Oct. 10,1938	20 48 05	2¼N-126¾E	157	7.3
240	Sept.27,1937	08 55 10	9½S-111E	157	7.2
241	Sept.17,1941	06 48 00	0°S-122E	158	
242	May 24,1935	05 36 31	12N-125E	159	6.8
243	Aug. 25,1933	07 50 25	31¾N-103½E	159	7.4
244	May 3,1943	01 59 12	12½N-125½E	159	7.4
245	Dec. 16,1941	19 19 39	21½N-120½E	160	7.1
246	Oct. 20,1942	23 21 44	8½N-122½E	160	7.3
247	Aug. 22,1936	06 51 35	22¼N-120¾E	160	7.2

Normal Shocks - Huancayo (cont.)

248	Dec. 4,1932	08:11:12	$2\frac{1}{2}$N-$121\frac{1}{2}$E	160.5	7.1
249	June 24,1933	21 54 46	$5\frac{1}{2}$S-$104\frac{3}{4}$E	161	7.5
250	Aug. 20,1937	11 59 16	$14\frac{1}{2}$N-$121\frac{1}{2}$E	162	7.5
251	Aug. 16,1938	04 27 50	$23\frac{1}{2}$N-$94\frac{1}{4}$E	163	7.2
252	Apr. 8,1942	15 40 24	$13\frac{1}{2}$N-121E	164	7.7
253	Feb. 14,1934	03 59 34	$17\frac{1}{2}$N-119E	165	7.6
254	Dec. 28,1935	02 35 12	0S-98E	167	
255	Aug. 23,1936	21 12 13	5N-95E	169	7.3
256	Sept.19,1936	01 01 47	$3\frac{3}{4}$N-$97\frac{1}{2}$E	169.5	7.2
257	Aug. 3,1935	01 10 01	$4\frac{1}{2}$N-$96\frac{1}{4}$E	170	7.0

INTERMEDIATE SHOCKS - PASADENA

No.	Date	Time	Location	Δ	Mag.	Depth
301	Aug. 21,1946	18:00:18	24S-177W	80	7.0	100
302	July 21,1931	03 36 22	21S-170E	81	7.0	140
303	Apr. 20,1949	05 29 08	37S-74W	82	7.4	70
304	Jan. 17,1940	01 15 00	17N-148E	83.5	7.3	80
305	Dec. 29,1940	16 37 44	18N-147½E	83.5	7.3	80
306	Nov. 24,1941	21 46 23	28S-177½W	83.5	7.3	80
307	July 27,1940	15 11 42	29S-177W	84	7.1	70
308	Sept.20,1949	11 55 27	29½S-177½W	84		80
309	Apr. 9,1943	08 48 59	19N-146E	84	7.0	170
310	Dec. 10,1950	13 23 04	28S-178½W	84	7.25	250
311	July 15,1945	05 35 13	17½N-146½E	84.5	7.1	120
312	Nov. 22,1949	00 51 49	28½S-178½W	84.5	7.4	160
313	Sept.27,1943	22 03 44	30S-178W	85	7.1	90
314	Mar. 1,1934	21 45 25	40S-72½W	85	7.1	120
315	Oct. 17,1939	06 22 06	14S-167¾E	85	7.4	120
316	Jan. 1,1933	08 48 39	14¾S-168E	85	7.0	140
317	Nov. 21,1948	19 10 28	13½S-167E	85	7.0	180
318	Feb. 20,1940	02 18 20	13½S-167E	85	7.0	200
319	Dec. 15,1948	19 11 26	22N-142½E	85	7.0	240
320	June 24,1935	23 23 14	15¾S-167 E	85.5	7.1	140
321	Aug. 12,1939	02 07 27	17¼S-168½E	85.5	7.2	180
322	Sept.10,1950	15 16 08	15½S-167E	86	7.1	100
323	July 23,1949	10 26 45	18½S-170E	86	7.2	150
324	June 14,1942	03 09 45	15N-145E	87	7.0	80

Intermediate Shocks - Pasadena (cont.)

325	Oct. 5,1944	17:28:27	22½S-172E	87	7.5	120
326	Jan. 29,1942	09 23 44	19S-169E	87	7.1	130
327	Sept.14,1942	11 31 01	22S-171E	87	7.0	130
328	Nov. 24,1944	04 49 03	19S-169E	87	7.5	170
329	Nov. 29,1944	18 51 21	19S-169E	87	7.0	170
330	July 9,1946	13 13 50	19S-169E	87	7.0	170
331	Sept. 9,1931	20 38 26	19N-145½E	87	7.1	100
332	July 11,1943	02 10 25	32½S-178½W	87	7.0	180
333	Aug. 1,1943	16 18 41	20S-170E	87	7.0	230
334	May 30,1938	14 29 50	20½S-169½E	87.5	7.0	70
335	Jan. 6,1940	14 03 24	22S-171E	87.5	7.2	90
336	Sept. 1,1937	08 38 59	32S-180	87.5	7.0	120
337	Apr. 5,1939	16 42 40	19½S-168E	88	7.1	70
338	Sept.15,1937	12 27 32	10½S-161½E	88	7.3	80
339	Aug. 17,1935	01 44 42	22½S-171E	88	7.2	120
340	Sept.19,1940	18 19 48	24S-171E	89	7.0	80
341	May 25,1950	18 35 07	13N-143½E	89.5	7.0	90
342	Sept. 4,1941	10 21 44	4¾S-154E	90.5	7.1	90
343	July 29,1950	23 49 02	6½S-155E	91	7.1	70
344	Dec. 29,1936	14 47 56	4½S-153½E	91	7.0	100
345	Dec. 4,1950	16 28 03	5S-153½E	91.5	7.2	110
346	Dec. 27,1944	15 25 49	6½S-152E	93.5	7.0	90
347	Nov. 10,1940	01 39 09	45¾N-26½E	94	7.4	150
348	Jan. 17,1946	09 39 35	7½S-147½E	98	7.2	100
349	Sept.26,1947	16 01 57	24¾N-123E	98	7.4	110

Intermediate Shocks - Pasadena (cont.)

350	Nov. 26,1948	05:36:37	5S-145E	98.5	7.0	70
351	Sept.23,1946	23 30 00	6S-145E	99	7.2	100
352	Dec. 1,1943	06 04 55	$4\frac{3}{4}$S-144E	99	7.2	120
353	Jan. 7,1944	02 49 20	$4\frac{1}{2}$S-$143\frac{1}{2}$E	99.5	7.1	120
354	May 23,1938	08 21 53	18N-$119\frac{1}{2}$E	104.5	7.0	80
355	Jan. 20,1936	16 56 19	6N-127E	107	7.1	80
356	Apr. 30,1949	01 23 32	$6\frac{1}{2}$N-125E	108	7.3	130
357	Oct. 7,1940	06 43 04	5N-126E	108.5	7.0	100
358	Feb. 28,1943	12 54 33	$36\frac{1}{2}$N-$70\frac{1}{2}$E	109.5	7.0	210
359	Mar. 4,1949	10 19 25	36N-$70\frac{1}{2}$E	109.5	7.5	230
360	Nov. 14,1937	10 58 12	$36\frac{1}{2}$N-$70\frac{1}{2}$E	109.5	7.2	240
361	Jan. 28,1948	03 47 21	$1\frac{1}{2}$N-$126\frac{1}{2}$E	110	7.2	80
362	Mar. 28,1931	12 38 37	7S-$129\frac{1}{2}$E	112.5	7.3	80
363	May 28,1942	01 01 48	0-124E	113	7.5	120
364	Dec. 21,1939	21 00 40	0-123E	114	8.0	150
365	Feb. 9,1948	14 54 22	0-$122\frac{1}{2}$E	114	7.2	160
366	Sept.17,1941	06 47 57	$\frac{1}{2}$S-$121\frac{1}{2}$E	115.5	7.1	190
367	June 13,1934	22 10 28	$27\frac{1}{2}$N-$62\frac{1}{2}$E	118	7.0	80
368	Sept. 8,1937	00 40 01	57S-27W	118	7.2	130
369	Mar. 22,1944	00 43 18	$8\frac{1}{2}$S-$123\frac{1}{2}$E	118.5	7.5	220
370	Nov. 15,1941	04 19 54	59S-$27\frac{1}{2}$W	119	7.0	80
371	Oct. 20,1938	02 19 27	9S-123E	119	7.3	90
372	July 23,1943	14 54 09	$9\frac{1}{2}$S-110E	130	7.75	90
373	May 1,1934	07 04 56	$3\frac{1}{2}$N-$97\frac{1}{2}$E	130	7.0	145
374	Nov. 26,1943	21 25 22	$2\frac{1}{2}$S-100E	133	7.1	130

DEEP SHOCKS - PASADENA

No.	Date	Time	Location	Δ	Mag.	Depth
401	July 10,1940	05:49:55	44N-131E	80	7.3	580
402	May 25,1944	01 06 37	21½S-179½W	80	7.2	640
403	Nov. 26,1945	05 13 10	21S-180	80	7.0	600
404	Sept. 6,1933	22 08 29	21½S-179¾W	80.5	7.1	600
405	July 20,1939	02 23 00	22S-179½W	80.5	7.0	650
406	Jan. 11,1946	01 33 29	44N-129½E	81.5	7.2	580
407	Oct. 10,1934	15 42 06	23½S-180	82	7.3	540
408	Dec. 15,1934	19 14 26	23½S-179½W	82	6.9	530
409	Apr. 5,1949	09 27 06	41N-131E	82	6.9	580
410	Sept.26,1946	10 53 15	25S-179E	82.5	7.0	600
411	Oct. 18,1931	04 30 33	26S-180	83.5	6.75	500
412	May 26,1932	16 09 40	25½S-179¼E	84	7.75	600
413	July 23,1931	14 20 56	6½S-155E	91	6.75	400
414	Feb. 4,1941	14 03 12	9N-124E	107.5	6.9	600
415	Sept.22,1940	22 51 56	8N-124E	108	6.75	680
416	June 29,1934	08 25 17	6¾S-123¾E	117	6.9	720
417	Nov. 27,1941	08 37 43	7½S-121½E	119.5	6.75	600
418	Aug. 11,1937	00 55 54	6¼S-116½E	123	7.2	610